A Mechanistic Investigation of T Cell Receptor-Mediated HIV Control

by

Gursev Anmole

B. Sc, Simon Fraser University, 2012

Thesis Submitted in Partial Fulfillment of the
Requirements for the Degree of
Doctor of Philosophy

in the
Department of Molecular Biology and Biochemistry
Faculty of Science

SIMON FRASER UNIVERSITY
Fall 2019

Approval

Name:	**Gursev Anmole**
Degree:	**Doctor of Philosophy**
Title:	**A Mechanistic Investigation of T Cell Receptor-Mediated HIV Control**
Examining Committee:	**Chair:** **Lynne Quarmby** Professor
	Mark Brockman Senior Supervisor Associate Professor
	Robert Holt Supervisor Professor
	Jonathan Choy Supervisor Associate Professor
	Lisa Craig Internal Examiner Professor
	Paul Goepfert External Examiner Professor Medicine and Microbiology The University of Alabama at Birmingham
Date Defended/Approved:	September 24th, 2019

Ethics Statement

The author, whose name appears on the title page of this work, has obtained, for the research described in this work, either:

a. human research ethics approval from the Simon Fraser University Office of Research Ethics

or

b. advance approval of the animal care protocol from the University Animal Care Committee of Simon Fraser University

or has conducted the research

c. as a co-investigator, collaborator, or research assistant in a research project approved in advance.

A copy of the approval letter has been filed with the Theses Office of the University Library at the time of submission of this thesis or project.

The original application for approval and letter of approval are filed with the relevant offices. Inquiries may be directed to those authorities.

Simon Fraser University Library
Burnaby, British Columbia, Canada

Update Spring 2016

Abstract

HIV remains a global pandemic. No vaccine or cure exists. Most infected individuals progress to AIDS in the absence of antiretroviral therapy, but a rare group of elite controllers (<0.5% of the infected population) suppresses viremia to an undetectable level. HIV control is often associated with a robust host immune response, mediated by selected HLA alleles that elicit T cells against more conserved HIV peptide epitopes. T cell recognition of an infected cell is determined by its unique T cell receptor (TCR), which binds a virus-derived peptide presented on the cell surface by an HLA protein. An individual's repertoire of TCR clones is large, but finite, and varies even among those who express the same HLA alleles. TCR sequence differences between controllers and non-controllers have been associated with variation in the antiviral activity of T cells, but few studies have explored this question comprehensively.

My thesis project aims to identify TCR features that contribute to HIV control. To do this, I examined CD8+ T cell responses against the immunodominant HIV Gag TL9 (TPQDLNTML) epitope. TL9 is presented by HLA-B*42 and B*81, but only B*81 is associated with HIV control. I sequenced TCR from TL9-specific T cells, including dual-reactive cells associated with HIV control in B*42 individuals that recognized TL9 presented by both B*42 and B*81, and then conducted functional and structural assessments of selected TCR clones. TL9-specific TCR from B*81 individuals and dual-reactive TCR from B*42 individuals were highly enriched for *TRBV12-3* gene usage. Furthermore, dual-reactive TCR from B*42 individuals were dominated by shared (or public) clones. Comprehensive functional analyses revealed that TCR from B*81 individuals and dual-reactive TCR from B*42 individuals displayed greater capacity to recognize TL9 variants, including common HIV escape mutations. Structural analyses of two dual-reactive TCR clones demonstrated an unusual peptide binding conformation driven by *TRBV12-3* germline residues. My results demonstrate that clonal differences in the ability of TCR to recognize TL9 variants are associated with HIV control. Functional and structural data provide mechanistic insight into key features of more effective TL9-specific TCR. By highlighting the impact of TCR clonotype on HIV control, my results will inform development of new vaccine and therapeutic strategies.

Keywords: HIV; Viral control; CD8 T cell; T cell receptor; Vaccine; Human Leukocyte Antigen

Dedication

To my grandfather, Mohinder Singh Anmole. You have influenced me immensely. Your love, support and guidance will forever be with me.

Acknowledgements

My journey to PhD completion could not have been taken alone. I was fortunate to have the tremendous support of all the wonderful people around me who not only supported me scientifically, but contributed immensely in making me who I am today. First and foremost, I would like to sincerely thank my senior supervisor and mentor Dr. Mark Brockman for his guidance, motivation, and supervision throughout the years. His passion for science and pursuing scientific questions with creativity made for an excellent learning environment. I would like to also thank Dr. Zabrina Brumme for contributing greatly to my mentorship and supporting me throughout my degree. My committee members, Dr. Robert Holt and Dr. Jonathan Choy, thank you for your advice and constructive feedback.

I would like to thank the past and current members of the Brockman/ Brumme and Choy lab, my lab family. Specifically, Dr. Tallie Kuang, Anh Le, Natalie Kinloch, Steven Jin, Kevin Rey, Aniqa Shahid, Eric Martin, Dr. Anna Von Rossum, Dr. Philip Mwimanzi, Kyle Cobarrubias, Gisele Umviligihozo, Rachel Miller, Hanwei Sudderuddin, Ashani Montgomery, Shayda Swann, Sukh Manku, Rajan Cheema, Catherine Cheneval, Dr. Tristan Markle, Fredrick Omondi, Dr. Martin Lee, Dr. Francis Mwimanzi and Franklin Tam and Dr. Ian Tietjen. Thank you creating a loving, supportive, helpful and exciting work environment. You all contributed immensely to my work and life in the past 8 years, lifted me when I was down and raised me higher when things were good. I am truly grateful to have you all in my life as friends and colleagues. Thank you to Winnie Enns and Dr. Bemulu Baraki for all your help and hard work through the years to make sure that our labs are in smooth working order and in helping build community. Thank you Dr. Tim Heslip for your help in cell sorting. I thank Funsho Ogunshola and Dr. Zaza Ndhlovu for a productive collaboration and all their contributions to my scientific discoveries, you were a pleasure to work with.

Finally, I would like to express gratitude towards my family. Natalie Kinloch, my partner, thank you so much for always being there, words cannot express my gratitude for your unconditional love and support. My sister Gurjeet Anmole, Mom, Dad, Grandma and Grandpa, thank you for always being there, making me who I am today and

supporting me unconditionally, always. To the Kinloch family, for giving me the love and support of a second family. I love you all.

Table of Contents

List of Tables

List of Figures

List of Acronyms

Å	Angstrom
AIDS	Acquired immunodeficiency syndrome
APC	Antigen presenting cell
cART	Combination antiretroviral therapy
CCR5	Chemokine receptor type 5
CD3	Cluster of differentiation 3
CD4	Cluster differentiation 4
CD8	Cluster differentiation 8
CDR	Complimentary determining region
CRM1	Chromosomal maintenance 1
CTL	Cytotoxic T Lymphocytes
CTLA-4	Cytotoxic T lymphocyte associated protein 4
DC	Dendritic cells
DNA	Deoxyribonucleic acid
ER	Endoplasmic Reticulum
GWAS	Genome wide association study
HIV	Human immunodeficiency virus type
HLA	Human leukocyte antigen
ITAM	Immunoreceptor tyrosine-based activation motif
KK10	HLA-B*27 restricted p24 Gag epitope (KRWIILGLNK)
LAT	Linker for activation of T cells
Lck	Tyrosine-protein kinase Lck
LTR	Long terminal repeat
MHC	Major Histocompatibility Complex
NFAT	Nuclear factor of activated T-cells
NHEJ	non-homologous end joining
P-TEFb	Primarily positive transcription elongation complex
PD-1	Programmed cell death protein 1
RAG	Recombination activating genes
RNA	Ribonucleic acid
RRE	REV response element

SNP	Single nucleotide polymorphisms
TAR	Trans-activation response element
TCR	T-cell Receptor
TdT	Terminal deoxynucleotide transferase
TL9	HLA-B*81/B*42 restricted p24 Gag epitope (TPQDLNTML)
TRAV	TCR alpha variable
TRBV	TCR beta variable
TW10	HLA-B*57 restricted p24 Gag epitope (TSTLQEQIGW)
ZAP70	Zeta chain of TCR associated protein kinase 70

Chapter 1. Introduction

1.1. Introduction to HIV

Human immunodeficiency virus type 1 (HIV-1) is responsible for a global pandemic that continues to have a significant impact on population health. Over 36 million people are currently living with HIV and though the incidence of new infections is decreasing, ~2 million people acquire HIV every year. The largest burden of HIV remains in Sub-Saharan Africa, where ~1.2 million new infections occur annually [1] . In most cases, uncontrolled HIV infection results in Acquired Immuno-Deficiency Syndrome (AIDS), a condition where the immune system deteriorates. AIDS is primarily caused by the loss of helper T-cells that express CD4 (Cluster of Differentiation 4), resulting in death of the infected individual due to opportunistic infections and cancer [2-5]. Since the discovery of highly effective combination antiretroviral therapy (cART), the life expectancy of HIV infected individuals has increased dramatically and cases of AIDS have greatly diminished; however, this requires individuals to adhere to life-long therapy [5-7]. Where this scenario predominates, such as in higher-income countries, HIV has become a clinically manageable chronic disease [8]. However, the issues of cART availability and drug adherence still remain problematic in many resource-limited settings and lower-income countries, thus negatively influencing clinical outcomes [9, 10]. A drawback of cART is that it requires life-long adherence, since HIV integrates into the genetic material of its host and a reservoir of replication-competent virus is maintained that can rebound within weeks, if treatment is interrupted [11-13]. Thus, there is an ongoing need to develop new therapeutic strategies that can reduce or eliminate the latent viral reservoir in cART-treated individuals. To date, the only people who have achieved long term remission of HIV in the absence of cART have undergone life-saving bone marrow transplants, which replaced their immune system and presumably purged the viral reservoir [14, 15]. Life-long adherence to cART is also associated with increased risk of cardiovascular disease and renal disease, as well as the potential accumulation of drug resistance mutations [16-20]. These factors highlight the need for additional HIV prevention or cure strategies as components of a strategy to eradicate this infection globally.

1.2. HIV genome and replication cycle

HIV is a retrovirus with a ~9.7 kb genome that primarily infects CD4+ T cells. The virus has a positive-sense RNA genome that encodes 9 genes: *gag, pol, env, nef, vpu, vpr, vif, tat and rev* (**Figure 1**) [21]. Three essential genes, *gag, pol and env,* encode critical structural and enzymatic proteins that are found in all retroviruses. The remaining genes encode accessory and regulatory proteins that enhance viral gene expression and increase viral infectivity and replication *in vivo*, including various mechanisms to evade the host immune system, thereby promoting persistence of HIV [21].

The viral replication cycle is initiated when the HIV Envelope trimer, composed of three gp120/gp41 hetero-dimers, attaches to target cells via interaction with the primary surface receptor, CD4 [22-24]. This interaction results in a conformational change that allows Envelope to bind to a co-receptor, either C-C Chemokine Receptor 5 (CCR5) or C-X-C Chemokine Receptor 4 (CXCR4) depending on the tropism of the viral strain, which initiates fusion of the virion lipid membrane with the cellular plasma membrane and release of the viral core particle containing the viral RNA genome into the cytoplasm of the target cell. The viral RNA genome is then converted into a double-stranded DNA copy by the viral Reverse Transcriptase enzyme [25], which subsequently transits to the cell nucleus where it is ligated into the chromosomal DNA of the host cell by the viral Integrase enzyme [26]. Once integrated into the host cell genome, the viral genome is often referred to as the “provirus”. The 5’ Long Terminal Repeat (LTR) domain functions as a promoter element for viral gene expression, which relies on cellular transcription factors and the RNA Polymerase II (Pol II) holoenzyme [27]. Viral RNA transcripts are initiated spontaneously from the LTR, but most are truncated and thus do not result in viral protein expression. The viral Tat protein enhances the processivity of RNA Pol II by recruiting cellular factors, primarily positive transcription elongation complex (P-TEFb) [28, 29], to the trans-activation response element (TAR) present on these short transcripts, resulting in production of a primary 9 kb RNA transcript [30, 31]. This primary transcript undergoes various alternative splicing events to generate mRNA species that encode all viral genes. Early viral proteins, Tat, Nef, Rev and Vpr, are produced from multiply-spliced RNA transcripts that are efficiently exported to the cytoplasm and translated by cellular ribosomal complexes. Later viral proteins are produced from singly-spliced transcripts (Vif and Env) or the primary 9 kb transcript (Gag and Pol) [32-34].

These intron-containing transcripts are not efficiently exported to the cytoplasm in the absence of Rev, which binds the Rev response element (RRE) on the viral transcript and interacts with the CRM1 nuclear export pathway to mediate RNA export [35, 36]. The virus relies on host cellular machinery to produce viral proteins and cellular trafficking mechanisms to generate and release new virions at the plasma membrane, thus continuing the cycle of infection.

Because integration of the HIV genome into the host cell genome is a critical step in the viral replication cycle, and subsequent transcription of the provirus depends in large part on host cell factors, a subset of cells naturally harbor a transcriptionally silent (or latent) copy of HIV. It is now recognized that these latently infected cells can persist life-long, even in the presence of cART, and that they lead to recrudescent infection upon treatment interruption [11-13]. Thus, the presence of latent replication-competent viral reservoirs is the major barrier to developing potential curative strategies for HIV.

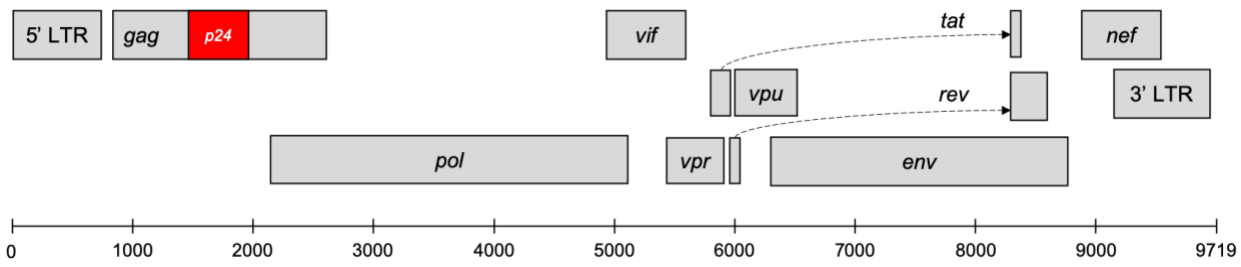

Figure 1-1. HIV genome and p24 Gag location.
The HIV genome is ~9.7 kb in size. It contains 9 genes, which encoding 15 proteins generated by a combination of alternative splicing and proteolytic cleavage events. The genome is flanked by long terminal repeat (LTR) regions at the 5' and 3' ends. Nucleotide positions (shown on the x-axis) represent those of the reference HXB2 strain. The p24 protein, located in *gag*, is highlighted in red. Gag p24 is the major component of the viral capsid, which is an important structural feature of the virion particle and also a crucial target of antiviral T cells. The immunodominant TL9 epitope (TPQDLNTML) is located in Gag p24 **(Appendix Figure 1-1)**.

1.3. Spontaneous control of HIV infection

In most cases, an HIV-infected individual progresses to AIDS in the absence of therapeutic intervention. However, a rare subset of infected individuals, referred to as HIV controllers, demonstrate the ability to spontaneously control viral replication for an extended duration of time [37, 38]. Representing less than 0.5% of all cases of HIV infection, “elite” controllers maintain very low plasma viral loads (below 50 copies of viral RNA per mL of blood) and typically display little or no loss of CD4 T cell counts over many years [39-42]. Another subset of individuals, referred to as viremic controllers, maintain partial suppression of viral replication (typically below 2000 copies of viral RNA per mL of blood) and often maintain normal CD4+ T cell counts in the periphery [43]. A combination of viral and host genetic factors are associated with the HIV controller phenotype. Thus, a better understanding of the interplay between the host and virus in cases of HIV control may aid in development of novel vaccine and therapeutic strategies.

1.3.1. Role of Viral Genetics in HIV Control

Viral genetics can contribute to HIV control, particularly when infection is established with a weakened strain that cannot replicate efficiently in the new host. The most prominent example of this mechanism of control is the Sydney blood bank cohort, where individuals with hemophilia were inadvertently transfused with a contaminated blood product that contained a *nef* deleted strain of HIV. A subset of these individuals exhibited spontaneous control of HIV and remained asymptomatic for more than 25 years [44-46], indicating that HIV replication capacity is an important determinant of viral pathogenesis and progression to AIDS [47]. Nef displays multiple activities, including the ability to downregulate cell surface Human Leukocyte Antigen (HLA) class I and CD4, and is also known to modify cell signaling events to enhance viral infection. These functions are lower in Nef clones derived from controllers compared to progressors [48, 49]. In addition to Nef, numerous studies have demonstrated that the *in vitro* replicative capacity of viruses derived from HIV controllers is lower due to mutations in *gag* and *pol* that attenuate the function of these proteins [50-52]. Understanding why certain HIV polymorphisms and sequence differences arise in individuals despite apparent impacts on viral fitness may provide important clues to augment natural host responses to

infection therapeutically. While transmission bottlenecks that result in infection by attenuated viral isolates may contribute in some cases, several lines of evidence suggest that most of the diversity observed in infected individuals is a result of viral adaptation to selective pressures mediated by the host immune response, specifically antibodies that target Envelope and T cells that target other viral protein (as discussed below).

1.3.2. Role of Host Genetics and Immuno-Genetics in HIV control

Several host genetic factors have been shown to contribute to HIV susceptibility and pathogenesis. The first major host genetic factor identified was a 32 bp deletion in the viral co-receptor CCR5 (referred to as the CCR5Δ32 mutation), which conferred resistance to infection by R5 tropic viruses [53, 54]. Approximately 10% of Caucasians of Northern European ancestry carry one copy of the CCR5Δ32 allele. Individuals who are homozygous for this mutation display a loss of CCR5 expression on their CD4+ T cells, thus preventing fusion by CCR5-tropic viral isolates while retaining sensitivity to CXCR4-tropic strains. A second major genetic determinant is the presence of 'protective' HLA class I alleles, especially alleles from the B locus such as B*27, B*57 and B*81, which are associated with enhanced control of infection [53, 55]. HLA genes are highly polymorphic as there are over 17000 known HLA class I alleles (IMGT-HLA http://hla.alleles.org/nomenclature/stats.html). HLA alleles cluster into "families" that show structural similarity and present common epitopes, therefore the diversity of HLA alleles contributing to peptide presentation is substantially less. Every individual possesses 6 HLA class I alleles and the composition of these alleles determines which epitopes can be presented to T cells. HLA molecules bind viral peptide epitopes in the endoplasmic reticulum and present them on the cell surface, where they can be recognized by T cells. HLA therefore serve as a immuno-genetic factor that mediates crucial aspects of the host immune response to infection. Population-based studies have demonstrated that HIV-infected individuals that express protective HLA alleles display lower plasma viral loads and delayed progression to AIDS (in the absence of therapy) compared to individuals that do not [56-58]. Protective HLA alleles are also over-represented among HIV controllers, further indicating that they, and the T cells that respond to them, are major contributors to viral pathogenesis.

Protective HLA alleles are more likely to present immunodominant peptides derived from more conserved regions of the HIV genome, such as the Gag protein [59, 60]. For example, three well-documented protective alleles, B*27, B*57 and B*81 present peptide epitopes derived from the Gag p24 protein **(Appendix Figure 1-1)** - KK10 (KRWILLGLNK) TW10 (TSTLQEQIGW) and TL9 (TPQDLNTML), respectively [61-66]. Gag p24 is the major component of the viral capsid, and its sequence is constrained due to important structural and functional elements. Thus, these peptide-HLA combinations drive CD8+ T-cell responses towards key sites where viral mutations are more likely to be detrimental to protein function and replication. An improved understanding of CD8+ T-cell responses associated with HIV control may define new immune mechanisms that can assist in the design of vaccines and therapeutics, including strategies to elicit more effective immune responses.

1.4. CD8+ T cell responses against HIV

1.4.1. Development of a T cell (receptor) repertoire

T cells arise from haematopoietic stem cells found in the bone marrow. Progenitor cells migrate from the bone marrow to the thymus, where they mature into thymocytes. Thymocytes undergo positive and negative selection in the thymus before they are released into the periphery as naïve T cells, each bearing a unique T cell receptor (TCR) that determines the antigen specificity of the cell [67]. The TCR is a heterodimeric cell surface molecule that is typically comprised of one alpha and one beta subunit **(Figure 1-2)** [68, 69]. Both TCR proteins are generated through a similar process of somatic recombination, mediated by recombination activating genes (RAG) 1 and 2, terminal deoxynucleotide transferase (TdT) and the non-homologous end joining (NHEJ) pathway for DNA repair, that together generate a tremendous amount of TCR diversity [70-74].

T cell progenitors first undergo recombination of the TCR beta gene locus. The new beta chain pairs with an invariant pre-TCR alpha chain to ensure that this recombination event is in-frame and productive. If successful, this triggers the thymocyte to adopt a CD4+CD8+ double-positive phenotype. Next, the TCR alpha gene locus is rearranged. If this event is productive, the new alpha chain pairs with the existing beta chain, and the double-positive cell will express a unique TCR alpha/beta receptor on its cell surface. In a minority of cases where the alpha chain rearrangement is non-

productive (i.e. the sequence is out of frame or contains a stop codon following recombination), the second alpha gene locus may undergo rearrangement to generate the TCR [75-77]. If the new TCR is activated by thymic antigen presenting cells (APC), through recognition of self-peptide bound to HLA, the thymocyte will receive survival signals (referred to as positive selection), otherwise it will die in the thymus due to neglect [78]. During positive selection, if the TCR interacts with peptide bound to HLA class I, the thymocyte adopts a CD8+ single-positive phenotype. Alternatively, if it interacts with peptide bound to HLA class II, it adopts a CD4+ single-positive phenotype [79, 80]. At this point during development, the single-positive T cells undergoes negative selection. If the TCR recognizes self-peptide/HLA antigens with high affinity, the thymocyte becomes hyperactivated, triggering cell death by apoptosis. This process of negative selection is also referred to as central tolerance [81]. Positive and negative selection ensures that mature single-positive T cells that emigrate from the thymus encode TCR sequences that are HLA-restricted (i.e. capable of recognizing foreign peptides bound to self-HLA molecules) and not overtly auto-reactive to self-peptides.

The antigen specificity of a TCR is determined by the presence of highly variable loops in the heterodimeric structure, referred to as Complementarity Determining Regions (CDR) (**Figure 1-2)**. Each TCR encodes a total of six CDRs, three in the alpha subunit and three in the beta subunit, which together form the primary points of contact with peptide/HLA antigens. Following recombination, each alpha chain gene is comprised of one Variable (V) region (of 47 possible genes), one Joining (J) region (of 61 possible) and a Constant (C) region. Each beta chain gene is comprised of one V region (of 54 possible), one Diversity (D) region (of two possible), one J region (of 14 possible) and one C region (of two possible) **(Figure 1-3)**. A standard nomenclature for TCR genes and allelic variants has been developed by the international ImMunoGeneTics (IMGT) consortium (http://www.imgt.org/), denoted as T cell Receptor Alpha Variable (TRAV), J (TRAJ) and C (TRAC), or T cell Receptor Beta Variable (TRBV), D (TRBD), J (TRBJ) and C (TRBC) followed by allelic variants (i.e. TRBV12-3*01). The V gene of each subunit encodes the CDR1 and CDR2 loops. These regions are germline encoded and typically interact with the HLA molecule. In contrast, the CDR3 loop of each subunit is formed at the site of V(D)J recombination. The CDR3 sequences are hypervariable, due to the stochastic nature of gene rearrangement as

well as the addition or deletion of nucleotides at this site during recombination, and typically interact with the peptide that is bound to HLA [82].

The population of unique TCR sequences present within an individual is often referred to as the “repertoire”. If all possible recombination events and alpha/beta pairings are taken into consideration, the potential TCR repertoire of humans consists of ~10^{18} unique clonotypes [83]. In reality, this never exists within an individual, since the number vastly exceeds the total number of T cells that are present in the body. Rather, it is estimated that the total number of unique TCR clonotypes present in an individual human is between 10^7 and 10^8 [84, 85]. While this number is still incredibly large, it pales in comparison to the number of foreign peptide antigens that an individual may encounter during a lifetime. This limitation is overcome, in part, by the ability of individual TCR clonotypes to recognize thousands (to tens of thousands) of different peptide sequences, which is variably referred to as being poly-reactive, cross-reactive, or “promiscuous” [86]. One study of a particularly highly poly-reactive autoimmune TCR clone suggested that it might recognize up to 1 million peptide variants [87]. Due to the complexity of TCR diversity and poly-reactivity, it is an enormous challenge to attempt to determine the antigen specificity of a TCR clone based only on its sequence; however, concerted efforts are underway in both the academic and commercial sectors to develop computational methods to do this using massive datasets of TCR sequences linked to antigen recognition profiles [88-91].

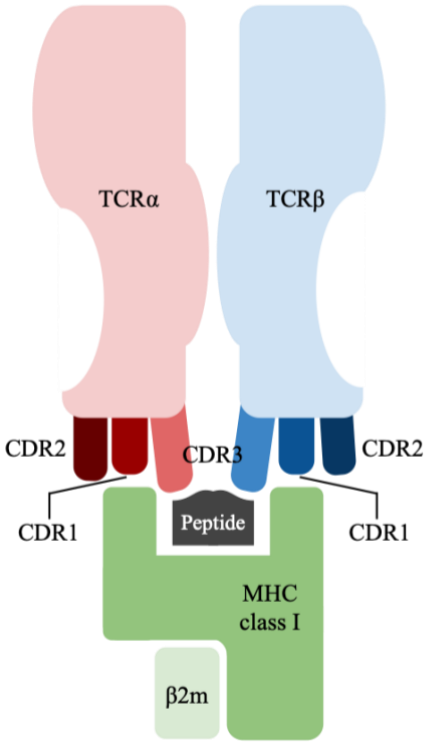

Figure 1-2. TCR interaction with peptide-MHC.
(A) Schematic showing the interaction of a TCR alpha and beta heterodimer with a MHC class one molecule bound to peptide. TCR alpha is shown in red and TCR beta is shown in blue. The CDR loops are color coded and show the classical interaction scheme where CDR3 loops are known to interact primarily with the peptide, and the CDR1 and CDR2 loops are known to interact with the MHC molecule.

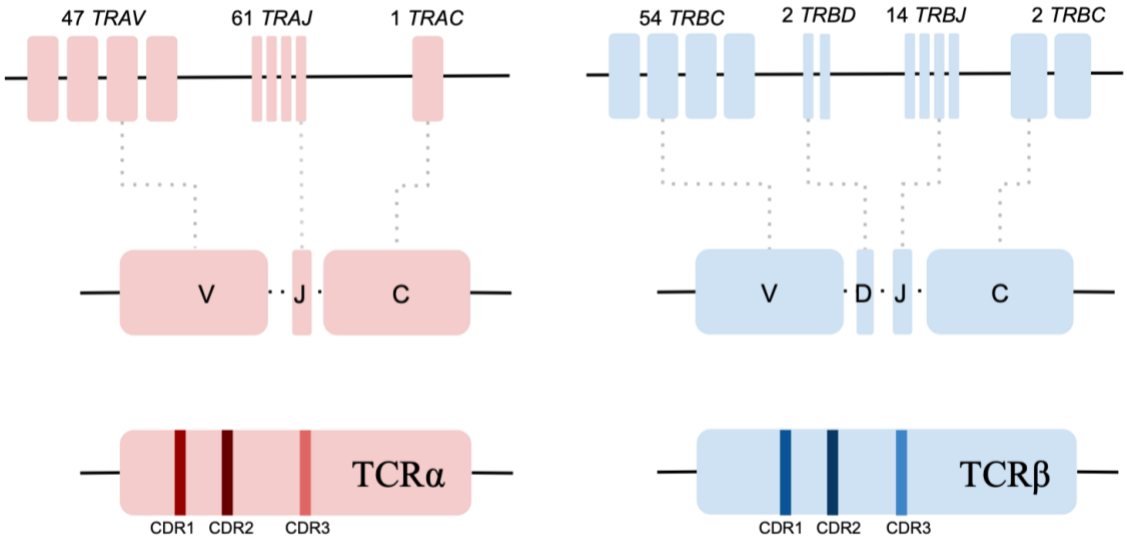

Figure 1-3. Somatic recombination of TCR genes.
This outlines V-(D)-J recombination in TCR alpha and TCR beta. The insertion of random nucleotides, that increase CDR3 variability, are shown by the dotted lines in-between the V-(D)-J regions. This recombination can yield a potential TCR repertoire containing ~10_{18} unique TCR clonotypes.

1.4.2. CD8+ T-cell activation and effector functions

Following emigration from the thymus, the diverse pool of resting naïve T cells expressing CD4+ or CD8+ circulate through the blood and lymphoid systems in search of cognate epitopes presented by APC [92]. For relevance to this thesis, I focus on CD8+ T cell activation in the context of HIV infection moving forward, though similar priming events occur in the case of CD4+ T cells and other pathogen infections.

CD8+ T cells recognize a foreign peptide epitopes presented on the surface of APCs in complex with HLA class I molecules. Antigenic peptides are generated by intracellular antigen processing, wherein host and pathogen proteins are degraded into short amino acid fragments by the proteasome in the cytosol [93]. These fragments are transported into the Endoplasmic Reticulum (ER) by the Transporter Associated with antigen Processing 1 (TAP1) or TAP2 protein and subsequently loaded onto nascent HLA class I molecules by the transmembrane glycoprotein Tapasin [94, 95]. The fragments are then trimmed at the N-terminus by ER-associated Aminopeptidases (ERAP) into 8-12 amino acid long peptides that display enhanced stability on the HLA molecule [96, 97]. Finally, the peptide/HLA complex is transported through the Golgi and vesicular protein

trafficking system to the extracellular surface, where it can be engaged by CD8+ T cells. This cytosolic antigen presentation pathway is active in all nucleated cells of the body. In addition, “professional” APC, such as Dendritic Cells (DC), support a process called cross-presentation that utilizes a proteasome-independent vacuolar pathway to generate antigenic peptides following endocytosis of extracellular products, allowing them to be processed and presented on HLA class I molecules in order to stimulate naïve CD8+ T cells, thus priming a *de novo* immune response [98, 99].

Three critical signals are necessary to prime naïve T cells and to initiate their differentiation into effector cells. First, the TCR expressed by the T cell must recognize a peptide/HLA antigen presented on the surface of a professional APC. DCs are among the first immune cells to encounter HIV following infection [100, 101] and they serve as a key APC to activate antiviral T cells [102]. This interaction is often referred to as Signal 1. TCR engagement results in activation of Lymphocyte-specific protein tyrosine kinase (or Lck), which is a 56 kD protein that is recruited to the TCR complex through interaction with the cytoplasmic tail of CD8 [103, 104]. Lck triggers a cascade of signaling events at the TCR, beginning with phosphorylation of CD3zeta and subsequent recruitment and phosphorylation of the signaling mediator Zeta-chain of T cell receptor Associated Protein kinase 70 (ZAP70) [105]. ZAP70-mediated phosphorylation of the membrane-associated scaffolding protein Linker of Activated T cells (LAT) provides docking sites to recruit multiple adaptor proteins and signaling molecules to the TCR complex via their Src-Homology 2 (SH2) domains, which act to amplify and diversify the downstream signaling cascade. Notably, TCR stimulation alone triggers Calcium flux and a predominantly NFAT-mediated signaling response that can lead to T cell anergy and inactivation [106], so a co-stimulatory signal (referred to as Signal 2) is required for efficient activation and differentiation of the T cell. This signal is typically mediated by the interaction of CD28 on the T cell with B7 family ligands (either CD80 or CD86) present on the surface of the APC [107, 108]. Together, Signal 1 and Signal 2 results in a more balanced signaling response that triggers proximal events at the TCR synapse (including actin remodeling [109, 110]) and also leads to the translocation of transcription factors NFAT, NFkB and AP-1 into the nucleus, which activate the expression of various genes required for cell growth and survival [111-113], including the cytokine IL-2 [114, 115]. For the reporter cell assays that form a central component of this thesis (described in **Chapter 2, 3 and 4**), I utilized NFAT-dependent gene expression to assess TCR antigen

recognition and to quantify TCR signaling strength. As shown in **Figure 1-4**, NFAT is translocated to the nucleus rapidly after TCR stimulation, driven by Calcium release from the ER. Finally, the CD8+ T-cell receives additional co-stimulatory signals (collectively referred to as Signal 3), provided by soluble pro-inflammatory cytokines IFNα and IL-12 that are produced by the activated APC. Together with various cytokines that signal through the common IL-2 receptor gamma chain (CD132) (i.e. IL-2, IL-7, IL-15, and IL-21), these factors promote expression of CD25 (the IL-2 receptor alpha chain) [116], stimulate T cell proliferation and development of key effector functions, including production of IFNγ, perforin and granzyme B, and trigger differentiation of naïve cells into effector and memory cell phenotypes [117-124].

Following their encounter with APC, primed CD8+ T cells exhibit critical effector characteristics and are often referred to as cytotoxic T lymphocytes (CTL). CTL display increased expression of cell surface LFA-1 that allows them to enter into peripheral tissues, as well as a reduced requirement for co-stimulatory signaling factors that allows them to trigger a cytolytic response following recognition of a target cell. Target cells are subsequently eliminated primarily through a perforin and granzyme-dependent lytic pathway. Delivery granzyme via perforin-formed pores in the target cell membrane results in the cleavage and activation of intracellular caspases, triggering cell death through apoptosis [125, 126].

1.4.3. CD8+ T cell effector functions associated with HIV control

Antiviral CD8+ T cells have been identified to be a major contributor to control of HIV viremia following infection. Indeed, in the absence of treatment, the generation and expansion of virus-specific CD8+ T-cell responses coincides with a profound reduction in plasma viral load during the acute stage of infection and the magnitude of antiviral CD8+ T cells is inversely correlated with set point viremia [127-129]. The importance of CD8+ T-cells was further confirmed using non-human primate models, wherein control of SIV infection was lost when CD8+ T-cells were depleted in animals [130, 131].

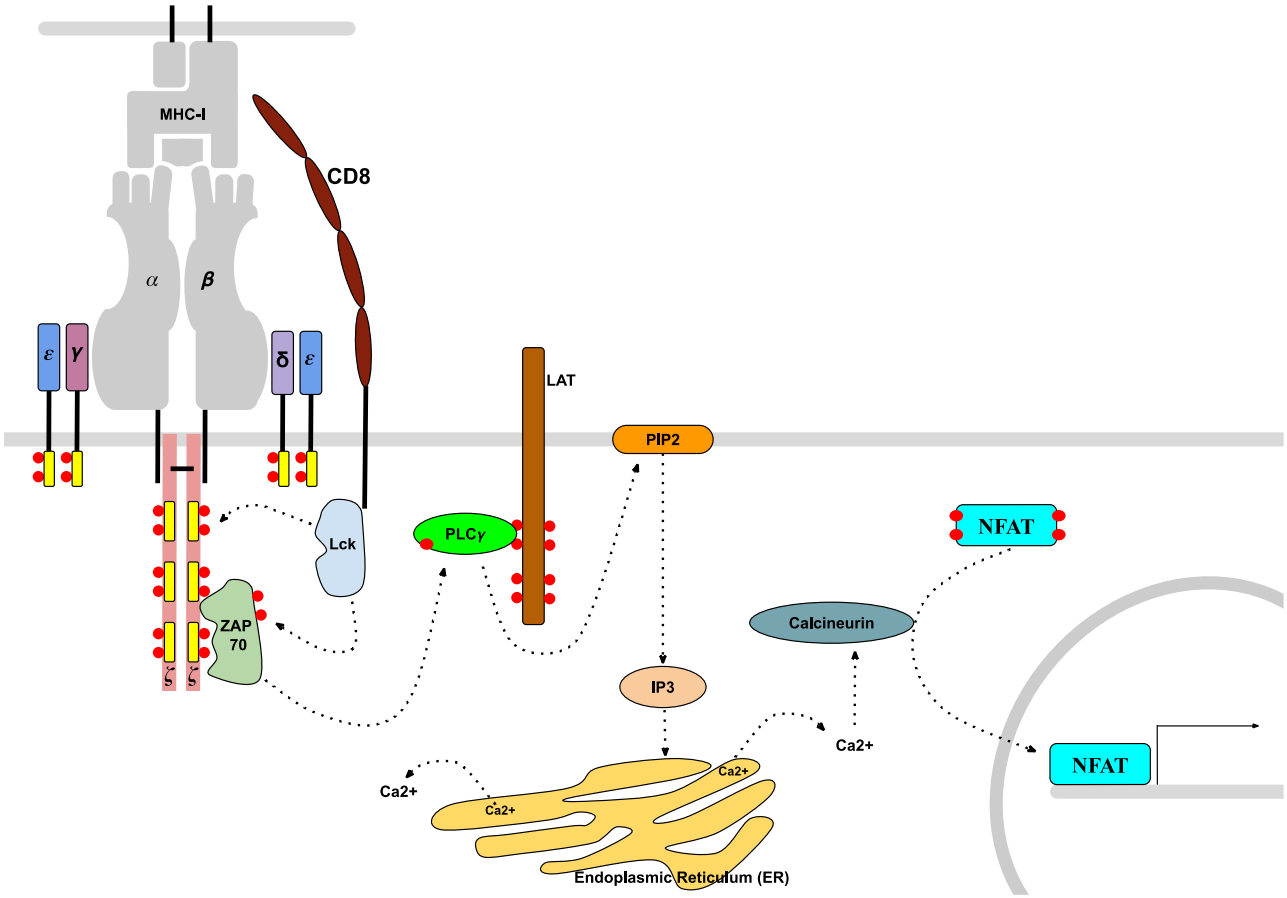

Figure 1-4. TCR stimulation and NFAT signalling.
Upon TCR engagement with peptide-MHC, the CD8 molecule recruits Lck to the site of TCR engagement. Lck phosphorylates ITAMs (Yellow) and this recruits ZAP70 which is then phosphorylated by Lck directly or upon ITAM engagement. Phosphorylation is shown by red dots in this figure. ZAP70 activates LAT and a signaling complex is formed, therefore activating PLCγ. This converts PIP2 to IP3, which induces a calcium flux from the Endoplasmic Reticulum (ER). The calcium binds calmodulin, which then induces dephosphorylation of NFAT and it's translocation to the nucleus resulting in expression of cell activation genes.

In addition, during chronic HIV infection, the breadth and magnitude of the CD8+T-cell response is inversely associated with clinical markers of disease progression (including plasma viral load and CD4 cell counts) [132], particularly for responses targeting the Gag protein [59]. Some studies have even suggested that specific features of the CD8+ T cell response are a better predictor of HIV control compared to HLA class I genotype [133, 134]. For example, T cell responses in HIV controllers tend to display higher polyfunctionality (assessed as the ability of cells to simultaneously produce multiple cytokines and/or effector functions, such as IFNγ, perforin and granzyme) [61, 135, 136], higher cytotoxicity towards infected cells [137, 138] and higher proliferative

responses when exposed to viral peptide antigens. The effector functions of a T cell can also be restrained by co-inhibitory receptors, primarily Programmed cell Death protein 1 (PD-1) and Cytotoxic T Lymphocyte Associated protein 4 (CTLA-4), which are upregulated on HIV-specific T cells following chronic antigen stimulation [139-142]. As such, the expression of co-inhibitory proteins is negatively associated with antiviral T cell activity. This process, which is often referred to as T cell exhaustion [143], also contributes to peripheral tolerance.

As mentioned previously, HIV control is frequently associated with CD8+ T-cell responses targeting the Gag p24 protein [144, 145] [146], which are immunodominant in individuals who express many protective HLA class I alleles, specifically HLA B*27, B*57 [147] and B*81 [148, 149]. This is likely due, in large part, to the high level of Gag expression by infected cells (resulting in efficient antigen processing) and the relative conservation of the p24 protein due to fitness constraints on the viral capsid (resulting in limited antigenic variability).

1.5. HIV adaptation and escape from the CD8+ T cell response

1.5.1. HLA-associated polymorphisms

During HIV replication, the low-fidelity viral reverse transcriptase enzyme incorporates random mutations into the viral genome. If a mutation is favorable to the fitness of the virus, it will be selected over time and subsequently predominate the viral quasi-species. CTL responses constitute a major selective pressure placed on HIV *in vivo*, and viral adaptation is frequently observed within peptide sequences targeted by CTL. Since viral peptide epitopes must be presented to CTL by a host HLA class I molecule, these mutations occur in an HLA-specific manner [150-152]. Therefore, they are variably referred to as either viral “escape” mutations (since they act to evade CTL) or as HLA-associated polymorphisms (reflecting their linkage to host immunogenetics). Such mutations help the virus to evade CTL responses by disrupting amino acid residues that are critical for either antigen processing [153], peptide binding to HLA [154], or recognition of the peptide by TCR [155].

While individuals who express protective HLA alleles can still lose control of HIV through selection of escape mutations within immunodominant epitope sequences [156, 157], these mutations often result in a fitness cost to the virus [50]. Examples of this are when escape occurs in Gag-derived epitopes such as B*27-KK10, B*57-TW10 and B*81-TL9. Escape mutations in KK10 (KRWILLGLNK) are frequently observed at position 2 (R264K) and position 6 (L268M). While L268M appears to be largely tolerated by the virus, the R264K mutation confers a substantial impact on viral replication capacity [62, 158]. Indeed, loss of HIV control in untreated B*27+ individuals is associated with a secondary mutation in Gag (S173A) that compensates for the reduced replicative capacity of R264K [63]. Reduced viral replicative capacity is also observed for the T242N mutation in TW10 (TSTLQEQIGW) [64, 159, 160] as well as the T186S mutation in TL9 (TLPQDNTML) [161]. Each of these epitopes are derived from the Gag p24 protein, suggesting that functional constraints on the viral capsid are likely to be important for long-term control of HIV in the context of these protective HLA alleles. Even though the mutational landscape of HIV is vast, it must maintain the integrity of key structural and functional regions to replicate.

1.5.2. Nef mediated HLA downregulation

A second strategy used by HIV to evade CTL responses is encoded by the viral accessory protein Nef. Nef is a ~27 kDa myristoylated protein that is expressed early and abundantly following infection [162]. Nef has many documented functions including the ability to modulate TCR-dependent cell signaling [49, 163] and to internalize CD4 [164, 165] and HLA class I [166] from the surface of virus-infected cells. It was recently discovered that Nef can also downregulate two Serine Incorporator (SERINC) family host restriction factors (SERINC3 and SERINC5), which contributes to Nef-mediated enhancement of viral infectivity [167-169]. The ability of Nef to downregulate HLA class I is most relevant to understanding viral evasion from CD8+ T cell responses. Nef is known to reduce the surface expression of both HLA-A and HLA-B molecules, thereby interfering with recognition and elimination of infected cells by host CTL [170, 171]. Nef isolates from HIV controllers and progressors displays substantial sequence and functional diversity [48], suggesting that differences in Nef may be clinically important. A better understanding of natural variation in Nef-mediated evasion of CTL immunity will

be important to design comprehensive strategies to eliminate HIV. The assay described in **Chapter 2** will help to support these efforts.

1.6. Contribution of TCR in CD8+ T cell-mediated HIV control

The composition of an individual's TCR repertoire is finite and highly variable, even among individuals who share the same HLA allele. Since TCR sequences dictate which HIV peptide/HLA antigens can be recognized by CD8+ T cells, it is plausible that differences in the TCR repertoire will contribute to variation in the antiviral activity of CTL that are necessary for HIV control; however, few studies have examined this question. Certain TCR clonotypes have been associated with enhanced control of HIV in the context of B*27-KK10 and B*57-TW10 [172, 173] responses, but detailed mechanistic analyses are lacking for most HIV epitopes. The potential impact of the TCR repertoire on HIV control hinges on two main facets. First, how TCR avidity for peptide/HLA contributes to antigen sensitivity of a CD8+ T cell. Second, how TCR poly-reactivity contributes to the ability of a CD8+ T-cell to recognize HIV escape variants [174]. More comprehensive studies of the sequence and functional variation present within antiviral TCR repertoires should improve our understanding of CD8+ T cell characteristics that contribute to HIV control, which may contribute to ongoing efforts to develop effective vaccines and interventions for HIV cure.

Antigen sensitivity is a crucial indicator of a high-quality CD8+ T-cell response against HIV [61, 175-177]. Antigen sensitivity is determined by multiple factors, including the affinity of the TCR to it's cognate peptide-MHC, the expression levels of TCR and CD8 on the T cell as well as the presence of co-stimulatory and co-inhibitory factors that can affect signaling upon engagement with the target cell. TCR avidity also correlates with the antigen sensitivity of T cells to their cognate antigen [155]. Thus, TCR sequence variability within an antigen-specific T cell population is likely to influence the antiviral activity of individual clones. In perhaps the best characterized example, B*27-KK10-responsive CD8+ T cell clones that displayed the highest antigen sensitivity were found to also have the greatest ability to suppress HIV replication *in vitro* [178]. Notably, the same highly functional TCR clone encoding the *TRBV4-3* gene was isolated from several unrelated individuals [155, 173, 175], illustrating the concept of a "public" TCR clonotype, which occurs unexpectedly often given the low probability. A link between

TCR avidity and antigen sensitivity has also been observed for other CD8+ T-cell responses, including epitopes presented by HLA-A*03 [179] and A*24 [180].

As described previously, CD8+ T cell responses can drive the selection of HIV escape mutations. Therefore, in addition to having higher avidity, a TCR repertoire that displays greater capacity to recognize emerging HIV variants is also expected to demonstrate better control of viremia. The presence of poly-reactive TCR clones has been associated with delayed progression to AIDS in some prior studies [172, 181]. Once again, in the well characterized example of B*27-KK10, the initial T cell response is typically dominated by clonotypes encoding *TRBV4-3* that display high avidity towards the wildtype KK10 epitope, but poor recognition of a viral mutation at position 6 (L268M; KRWIILG**M**NK). This allow HIV to evade the primary response by selecting L268M variants. In some individuals, a *de novo* response is generated that is dominated by TCR clonotypes encoding *TRBV6-5* that are cross-reactive to the L268M variant [173]. Individuals that elicit these cross-reactive TCR clones continue control the virus while those who fail to elicit this response tend to progress in disease. Thus, despite sharing the protective B*27 allele, clinical outcome appears to be associated with the interplay between TCR clonotypes and viral pathways of CTL escape.

1.7. Thesis Objectives

The objective of my thesis is to study HIV-specific TCR repertoires in individuals who show enhanced control of the virus to uncover mechanisms of CD8+ T-cell mediated control of HIV. My overarching hypothesis is that individuals who control HIV infection will contain HIV-specific TCR clonotypes in their repertoire that show enhanced antigen sensitivity and/or cross-reactivity towards viral escape mutations. By identifying and studying the features of TCR clones isolated from CD8+ T cells in HIV controllers, my results will inform HIV vaccine design and TCR-based therapeutics for HIV cure.

In the following chapters, I highlight the major results and observations of my PhD research studies. **Chapter 2** contains a published study (titled “A robust and scalable TCR-based reporter cell assay to measure HIV-1 Nef-mediated T cell immune evasion”) that describes an *in vitro* reporter cell assay that I have used to rapidly assess the functional characteristics of TCR signaling capacity and recognition of peptide variants. In **Chapter 3,** I utilize single cell TCR sequencing methods and this TCR reporter assay

to characterize TCR clones isolated from HIV Gag TL9-specific T cells that are associated with HIV control in HLA-B*81 and B*42 individuals. My results demonstrate that HIV control is linked with TCR cross-reactivity towards viral escape variants. In **Chapter 4**, I describe detailed follow-up studies of TL9-specific TCR clones from B*42 individuals to further examine mechanisms associated with TCR-mediated control of HIV. In addition to presenting data for an expanded panel of HLA-B*42 TL9-specific TCR clones, this chapter highlights my efforts to establish Illumina-based methods to sequence TCR as well as results from a new collaboration to analyze the structure of cross-reactive TCR clones bound to TL9/HLA ligands that illustrate critical features that may contribute to HIV control. Finally, the implications and significance of my thesis research are discussed in **Chapter 5.**

1.8. References

[1] UNIADS, "UNAIDS Data 2018," 2018. [Online]. Available: https://www.unaids.org/sites/default/files/media_asset/UNAIDS_FactSheet_en.pdf.

[2] A. E. Friedman-Kien, "Disseminated Kaposi's sarcoma syndrome in young homosexual men," (in eng), *J Am Acad Dermatol,* vol. 5, no. 4, pp. 468-71, Oct 1981, doi: 10.1016/s0190-9622(81)80010-2.

[3] M. S. Gottlieb *et al.*, "Pneumocystis carinii pneumonia and mucosal candidiasis in previously healthy homosexual men: evidence of a new acquired cellular immunodeficiency," (in eng), *The New England journal of medicine,* vol. 305, no. 24, pp. 1425-31, Dec 10 1981, doi: 10.1056/nejm198112103052401.

[4] K. B. Hymes *et al.*, "Kaposi's sarcoma in homosexual men-a report of eight cases," (in eng), *Lancet (London, England),* vol. 2, no. 8247, pp. 598-600, Sep 19 1981, doi: 10.1016/s0140-6736(81)92740-9.

[5] F. P. Siegal *et al.*, "Severe acquired immunodeficiency in male homosexuals, manifested by chronic perianal ulcerative herpes simplex lesions," (in eng), *The New England journal of medicine,* vol. 305, no. 24, pp. 1439-44, Dec 10 1981, doi: 10.1056/nejm198112103052403.

[6] R. T. D'Aquila *et al.*, "Nevirapine, zidovudine, and didanosine compared with zidovudine and didanosine in patients with HIV-1 infection. A randomized, double-blind, placebo-controlled trial. National Institute of Allergy and Infectious Diseases AIDS Clinical Trials Group Protocol 241 Investigators," (in eng), *Ann Intern Med,* vol. 124, no. 12, pp. 1019-30, Jun 15 1996, doi: 10.7326/0003-4819-124-12-199606150-00001.

[7] S. Staszewski *et al.*, "Virological and immunological analysis of a triple combination pilot study with loviride, lamivudine and zidovudine in HIV-1-infected patients," (in eng), *Aids,* vol. 10, no. 5, pp. F1-7, May 1996.

[8] H. Samji *et al.*, "Closing the gap: increases in life expectancy among treated HIV-positive individuals in the United States and Canada," *PLoS One,* Research Support, N.I.H., Extramural

Research Support, N.I.H., Intramural

Research Support, Non-U.S. Gov't

Research Support, U.S. Gov't, P.H.S. vol. 8, no. 12, p. e81355, 2013, doi: 10.1371/journal.pone.0081355.

[9] J. M. Costa, T. S. Torres, L. E. Coelho, and P. M. Luz, "Adherence to antiretroviral therapy for HIV/AIDS in Latin America and the Caribbean: Systematic review and meta-analysis," (in eng), *J Int AIDS Soc,* vol. 21, no. 1, Jan 2018, doi: 10.1002/jia2.25066.

[10] T. Minior *et al.*, "The Critical Role of Supply Chains in Preventing Human Immunodeficiency Virus Drug Resistance in Low- and Middle-Income Settings," (in eng), *The Journal of infectious diseases,* vol. 216, no. suppl_9, pp. S812-s815, Dec 1 2017, doi: 10.1093/infdis/jix403.

[11] T. W. Chun *et al.*, "Rebound of plasma viremia following cessation of antiretroviral therapy despite profoundly low levels of HIV reservoir: implications for eradication," (in eng), *Aids,* vol. 24, no. 18, pp. 2803-8, Nov 27 2010, doi: 10.1097/QAD.0b013e328340a239.

[12] R. T. Davey, Jr. *et al.*, "HIV-1 and T cell dynamics after interruption of highly active antiretroviral therapy (HAART) in patients with a history of sustained viral suppression," (in eng), *Proceedings of the National Academy of Sciences of the United States of America,* vol. 96, no. 26, pp. 15109-14, Dec 21 1999, doi: 10.1073/pnas.96.26.15109.

[13] J. D. Siliciano *et al.*, "Long-term follow-up studies confirm the stability of the latent reservoir for HIV-1 in resting CD4+ T cells," (in eng), *Nature medicine,* vol. 9, no. 6, pp. 727-8, Jun 2003, doi: 10.1038/nm880.

[14] G. Hutter *et al.*, "Long-term control of HIV by CCR5 Delta32/Delta32 stem-cell transplantation," (in eng), *The New England journal of medicine,* vol. 360, no. 7, pp. 692-8, Feb 12 2009, doi: 10.1056/NEJMoa0802905.

[15] R. K. Gupta *et al.*, "HIV-1 remission following CCR5Delta32/Delta32 haematopoietic stem-cell transplantation," (in eng), *Nature,* vol. 568, no. 7751, pp. 244-248, Apr 2019, doi: 10.1038/s41586-019-1027-4.

[16] V. C. Marconi *et al.*, "Prevalence of HIV-1 drug resistance after failure of a first highly active antiretroviral therapy regimen in KwaZulu Natal, South Africa," (in eng), *Clinical infectious diseases : an official publication of the Infectious*

Diseases Society of America, vol. 46, no. 10, pp. 1589-97, May 15 2008, doi: 10.1086/587109.

[17] A. Mocroft *et al.*, "Estimated glomerular filtration rate, chronic kidney disease and antiretroviral drug use in HIV-positive patients," (in eng), *Aids,* vol. 24, no. 11, pp. 1667-78, Jul 17 2010, doi: 10.1097/QAD.0b013e328339fe53.

[18] C. A. Sabin *et al.*, "Use of nucleoside reverse transcriptase inhibitors and risk of myocardial infarction in HIV-infected patients enrolled in the D:A:D study: a multi-cohort collaboration," (in eng), *Lancet (London, England),* vol. 371, no. 9622, pp. 1417-26, Apr 26 2008, doi: 10.1016/s0140-6736(08)60423-7.

[19] B. T. Tadesse *et al.*, "High Levels of Dual-Class Drug Resistance in HIV-Infected Children Failing First-Line Antiretroviral Therapy in Southern Ethiopia," (in eng), *Viruses,* vol. 10, no. 2, Feb 1 2018, doi: 10.3390/v10020060.

[20] J. Young *et al.*, "Renal function in patients with HIV starting therapy with tenofovir and either efavirenz, lopinavir or atazanavir," (in eng), *Aids,* vol. 26, no. 5, pp. 567-75, Mar 13 2012, doi: 10.1097/QAD.0b013e32834f337c.

[21] A. D. Frankel and J. A. Young, "HIV-1: fifteen proteins and an RNA," (in eng), *Annu Rev Biochem,* vol. 67, pp. 1-25, 1998, doi: 10.1146/annurev.biochem.67.1.1.

[22] H. Deng *et al.*, "Identification of a major co-receptor for primary isolates of HIV-1," (in eng), *Nature,* vol. 381, no. 6584, pp. 661-6, Jun 20 1996, doi: 10.1038/381661a0.

[23] T. Dragic *et al.*, "HIV-1 entry into CD4+ cells is mediated by the chemokine receptor CC-CKR-5," (in eng), *Nature,* vol. 381, no. 6584, pp. 667-73, Jun 20 1996, doi: 10.1038/381667a0.

[24] Y. Feng, C. C. Broder, P. E. Kennedy, and E. A. Berger, "HIV-1 entry cofactor: functional cDNA cloning of a seven-transmembrane, G protein-coupled receptor," (in eng), *Science,* vol. 272, no. 5263, pp. 872-7, May 10 1996, doi: 10.1126/science.272.5263.872.

[25] A. Jacobo-Molina and E. Arnold, "HIV reverse transcriptase structure-function relationships," *Biochemistry,* vol. 30, no. 26, pp. 6351-6361, 1991/07/02 1991, doi: 10.1021/bi00240a001.

[26] F. D. Bushman, T. Fujiwara, and R. Craigie, "Retroviral DNA integration directed by HIV integration protein in vitro," (in eng), *Science,* vol. 249, no. 4976, pp. 1555-8, Sep 28 1990, doi: 10.1126/science.2171144.

[27] K. A. Jones, "HIV trans-activation and transcription control mechanisms," (in eng), *New Biol,* vol. 1, no. 2, pp. 127-35, Nov 1989.

[28] T. H. Tahirov, N. D. Babayeva, K. Varzavand, J. J. Cooper, S. C. Sedore, and D. H. Price, "Crystal structure of HIV-1 Tat complexed with human P-TEFb," (in

eng), *Nature,* vol. 465, no. 7299, pp. 747-51, Jun 10 2010, doi: 10.1038/nature09131.

[29] C. Dingwall *et al.*, "Human immunodeficiency virus 1 tat protein binds trans-activation-responsive region (TAR) RNA in vitro," (in eng), *Proceedings of the National Academy of Sciences of the United States of America,* vol. 86, no. 18, pp. 6925-9, Sep 1989, doi: 10.1073/pnas.86.18.6925.

[30] G. Nabel and D. Baltimore, "An inducible transcription factor activates expression of human immunodeficiency virus in T cells," (in eng), *Nature,* vol. 326, no. 6114, pp. 711-3, Apr 16-22 1987, doi: 10.1038/326711a0.

[31] S. Roy, U. Delling, C. H. Chen, C. A. Rosen, and N. Sonenberg, "A bulge structure in HIV-1 TAR RNA is required for Tat binding and Tat-mediated trans-activation," (in eng), *Genes Dev,* vol. 4, no. 8, pp. 1365-73, Aug 1990, doi: 10.1101/gad.4.8.1365.

[32] S. Schwartz, B. K. Felber, D. M. Benko, E. M. Fenyö, and G. N. Pavlakis, "Cloning and functional analysis of multiply spliced mRNA species of human immunodeficiency virus type 1," *Journal of virology,* vol. 64, no. 6, pp. 2519-2529, 1990. [Online]. Available: https://jvi.asm.org/content/jvi/64/6/2519.full.pdf.

[33] D. F. Purcell and M. A. Martin, "Alternative splicing of human immunodeficiency virus type 1 mRNA modulates viral protein expression, replication, and infectivity," (in eng), *Journal of virology,* vol. 67, no. 11, pp. 6365-6378, 1993. [Online]. Available: https://www.ncbi.nlm.nih.gov/pubmed/8411338

https://www.ncbi.nlm.nih.gov/pmc/articles/PMC238071/.

[34] K. E. Ocwieja *et al.*, "Dynamic regulation of HIV-1 mRNA populations analyzed by single-molecule enrichment and long-read sequencing," *Nucleic Acids Research,* vol. 40, no. 20, pp. 10345-10355, 2012, doi: 10.1093/nar/gks753.

[35] P. Askjaer, T. H. Jensen, J. Nilsson, L. Englmeier, and J. Kjems, "The specificity of the CRM1-Rev nuclear export signal interaction is mediated by RanGTP," (in eng), *J Biol Chem,* vol. 273, no. 50, pp. 33414-22, Dec 11 1998, doi: 10.1074/jbc.273.50.33414.

[36] M. H. Malim, J. Hauber, S. Y. Le, J. V. Maizel, and B. R. Cullen, "The HIV-1 rev trans-activator acts through a structured target sequence to activate nuclear export of unspliced viral mRNA," (in eng), *Nature,* vol. 338, no. 6212, pp. 254-7, Mar 16 1989, doi: 10.1038/338254a0.

[37] S. G. Deeks and B. D. Walker, "Human immunodeficiency virus controllers: mechanisms of durable virus control in the absence of antiretroviral therapy," (in eng), *Immunity,* vol. 27, no. 3, pp. 406-16, Sep 2007, doi: 10.1016/j.immuni.2007.08.010.

[38] B. D. Walker and X. G. Yu, "Unravelling the mechanisms of durable control of HIV-1," (in eng), *Nature reviews. Immunology,* vol. 13, no. 7, pp. 487-98, Jul 2013, doi: 10.1038/nri3478.

[39] P. W. Hunt *et al.*, "Relationship between T cell activation and CD4+ T cell count in HIV-seropositive individuals with undetectable plasma HIV RNA levels in the absence of therapy," (in eng), *The Journal of infectious diseases,* vol. 197, no. 1, pp. 126-33, Jan 1 2008, doi: 10.1086/524143.

[40] J. B. Hubert *et al.*, "Natural history of serum HIV-1 RNA levels in 330 patients with a known date of infection. The SEROCO Study Group," (in eng), *Aids,* vol. 14, no. 2, pp. 123-31, Jan 28 2000.

[41] A. D. Olson *et al.*, "An evaluation of HIV elite controller definitions within a large seroconverter cohort collaboration," (in eng), *PloS one,* vol. 9, no. 1, p. e86719, 2014, doi: 10.1371/journal.pone.0086719.

[42] O. Lambotte *et al.*, "HIV controllers: a homogeneous group of HIV-1-infected patients with spontaneous control of viral replication," (in eng), *Clinical infectious diseases : an official publication of the Infectious Diseases Society of America,* vol. 41, no. 7, pp. 1053-6, Oct 1 2005, doi: 10.1086/433188.

[43] J. F. Okulicz *et al.*, "Clinical outcomes of elite controllers, viremic controllers, and long-term nonprogressors in the US Department of Defense HIV natural history study," (in eng), *The Journal of infectious diseases,* vol. 200, no. 11, pp. 1714-23, Dec 1 2009, doi: 10.1086/646609.

[44] N. J. Deacon *et al.*, "Genomic structure of an attenuated quasi species of HIV-1 from a blood transfusion donor and recipients," (in eng), *Science,* vol. 270, no. 5238, pp. 988-91, Nov 10 1995. [Online]. Available: https://science.sciencemag.org/content/270/5238/988.long.

[45] J. C. Learmont *et al.*, "Immunologic and virologic status after 14 to 18 years of infection with an attenuated strain of HIV-1. A report from the Sydney Blood Bank Cohort," (in eng), *The New England journal of medicine,* vol. 340, no. 22, pp. 1715-22, Jun 3 1999, doi: 10.1056/nejm199906033402203.

[46] J. Learmont *et al.*, "Long-term symptomless HIV-1 infection in recipients of blood products from a single donor," (in eng), *Lancet (London, England),* vol. 340, no. 8824, pp. 863-7, Oct 10 1992.

[47] F. Kirchhoff, T. C. Greenough, D. B. Brettler, J. L. Sullivan, and R. C. Desrosiers, "Brief report: absence of intact nef sequences in a long-term survivor with nonprogressive HIV-1 infection," (in eng), *The New England journal of medicine,* vol. 332, no. 4, pp. 228-32, Jan 26 1995, doi: 10.1056/nejm199501263320405.

[48] P. Mwimanzi *et al.*, "Attenuation of multiple Nef functions in HIV-1 elite controllers," *Retrovirology,* vol. 10, no. 1, p. 1, 2013/01/07 2013, doi: 10.1186/1742-4690-10-1.

[49] S. W. Jin *et al.*, "Modulation of TCR-dependent NFAT signaling is impaired in HIV-1 Nef isolates from elite controllers," (in eng), *Virology,* vol. 530, pp. 39-50, Apr 2019, doi: 10.1016/j.virol.2019.02.008.

[50] T. Miura *et al.*, "Impaired replication capacity of acute/early viruses in persons who become HIV controllers," (in eng), *Journal of virology,* vol. 84, no. 15, pp. 7581-91, Aug 2010, doi: 10.1128/jvi.00286-10.

[51] T. Miura *et al.*, "HLA-associated alterations in replication capacity of chimeric NL4-3 viruses carrying gag-protease from elite controllers of human immunodeficiency virus type 1," (in eng), *Journal of virology,* vol. 83, no. 1, pp. 140-9, Jan 2009, doi: 10.1128/jvi.01471-08.

[52] Z. L. Brumme *et al.*, "Reduced replication capacity of NL4-3 recombinant viruses encoding reverse transcriptase-integrase sequences from HIV-1 elite controllers," (in eng), *Journal of acquired immune deficiency syndromes (1999),* vol. 56, no. 2, pp. 100-8, Feb 1 2011, doi: 10.1097/QAI.0b013e3181fe9450.

[53] P. J. McLaren *et al.*, "Polymorphisms of large effect explain the majority of the host genetic contribution to variation of HIV-1 virus load," (in eng), *Proceedings of the National Academy of Sciences of the United States of America,* vol. 112, no. 47, pp. 14658-63, Nov 24 2015, doi: 10.1073/pnas.1514867112.

[54] M. Samson *et al.*, "Resistance to HIV-1 infection in caucasian individuals bearing mutant alleles of the CCR-5 chemokine receptor gene," (in eng), *Nature,* vol. 382, no. 6593, pp. 722-5, Aug 22 1996, doi: 10.1038/382722a0.

[55] F. Pereyra *et al.*, "The major genetic determinants of HIV-1 control affect HLA class I peptide presentation," (in eng), *Science,* vol. 330, no. 6010, pp. 1551-7, Dec 10 2010, doi: 10.1126/science.1195271.

[56] M. Carrington and S. J. O'Brien, "The influence of HLA genotype on AIDS," (in eng), *Annu Rev Med,* vol. 54, pp. 535-51, 2003, doi: 10.1146/annurev.med.54.101601.152346.

[57] J. Fellay *et al.*, "A whole-genome association study of major determinants for host control of HIV-1," (in eng), *Science,* vol. 317, no. 5840, pp. 944-7, Aug 17 2007, doi: 10.1126/science.1143767.

[58] A. Leslie *et al.*, "Additive contribution of HLA class I alleles in the immune control of HIV-1 infection," (in eng), *Journal of virology,* vol. 84, no. 19, pp. 9879-88, Oct 2010, doi: 10.1128/jvi.00320-10.

[59] P. Kiepiela *et al.*, "CD8+ T-cell responses to different HIV proteins have discordant associations with viral load," (in eng), *Nature medicine,* vol. 13, no. 1, pp. 46-53, Jan 2007, doi: 10.1038/nm1520.

[60] J. A. Borghans, A. Molgaard, R. J. de Boer, and C. Kesmir, "HLA alleles associated with slow progression to AIDS truly prefer to present HIV-1 p24," (in eng), *PloS one,* vol. 2, no. 9, p. e920, Sep 19 2007, doi: 10.1371/journal.pone.0000920.

[61] J. R. Almeida *et al.*, "Superior control of HIV-1 replication by CD8+ T cells is reflected by their avidity, polyfunctionality, and clonal turnover," (in eng), *The*

Journal of experimental medicine, vol. 204, no. 10, pp. 2473-85, Oct 1 2007, doi: 10.1084/jem.20070784.

[62] A. Schneidewind *et al.*, "Structural and Functional Constraints Limit Options for Cytotoxic T-Lymphocyte Escape in the Immunodominant HLA-B27-Restricted Epitope in Human Immunodeficiency Virus Type 1 Capsid," *Journal of virology,* vol. 82, no. 11, pp. 5594-5605, 2008, doi: 10.1128/jvi.02356-07.

[63] A. Schneidewind *et al.*, "Escape from the dominant HLA-B27-restricted cytotoxic T-lymphocyte response in Gag is associated with a dramatic reduction in human immunodeficiency virus type 1 replication," (in eng), *Journal of virology,* vol. 81, no. 22, pp. 12382-93, Nov 2007, doi: 10.1128/jvi.01543-07.

[64] M. A. Brockman *et al.*, "Escape and compensation from early HLA-B57-mediated cytotoxic T-lymphocyte pressure on human immunodeficiency virus type 1 Gag alter capsid interactions with cyclophilin A," (in eng), *Journal of virology,* vol. 81, no. 22, pp. 12608-18, Nov 2007, doi: 10.1128/jvi.01369-07.

[65] C. Geldmacher *et al.*, "CD8 T-cell recognition of multiple epitopes within specific Gag regions is associated with maintenance of a low steady-state viremia in human immunodeficiency virus type 1-seropositive patients," *Journal of virology,* vol. 81, no. 5, pp. 2440-8, Mar 2007, doi: 10.1128/JVI.01847-06.

[66] A. Leslie *et al.*, "Differential selection pressure exerted on HIV by CTL targeting identical epitopes but restricted by distinct HLA alleles from the same HLA supertype," (in eng), *J Immunol,* vol. 177, no. 7, pp. 4699-708, Oct 01 2006.

[67] N. Kurd and E. A. Robey, "T-cell selection in the thymus: a spatial and temporal perspective," (in eng), *Immunol Rev,* vol. 271, no. 1, pp. 114-126, 2016, doi: 10.1111/imr.12398.

[68] M. Attaf, M. Legut, D. K. Cole, and A. K. Sewell, "The T cell antigen receptor: the Swiss army knife of the immune system," (in eng), *Clin Exp Immunol,* vol. 181, no. 1, pp. 1-18, Jul 2015, doi: 10.1111/cei.12622.

[69] J. B. Huppa and M. M. Davis, "The interdisciplinary science of T-cell recognition," (in eng), *Adv Immunol,* vol. 119, pp. 1-50, 2013, doi: 10.1016/b978-0-12-407707-2.00001-1.

[70] M. A. Oettinger, D. G. Schatz, C. Gorka, and D. Baltimore, "RAG-1 and RAG-2, adjacent genes that synergistically activate V(D)J recombination," (in eng), *Science,* vol. 248, no. 4962, pp. 1517-23, Jun 22 1990, doi: 10.1126/science.2360047.

[71] T. Komori, A. Okada, V. Stewart, and F. W. Alt, "Lack of N regions in antigen receptor variable region genes of TdT-deficient lymphocytes," (in eng), *Science,* vol. 261, no. 5125, pp. 1171-5, Aug 27 1993, doi: 10.1126/science.8356451.

[72] S. Gilfillan, A. Dierich, M. Lemeur, C. Benoist, and D. Mathis, "Mice lacking TdT: mature animals with an immature lymphocyte repertoire," (in eng), *Science,* vol. 261, no. 5125, pp. 1175-8, Aug 27 1993, doi: 10.1126/science.8356452.

[73] G. E. Taccioli, G. Rathbun, E. Oltz, T. Stamato, P. A. Jeggo, and F. W. Alt, "Impairment of V(D)J Recombination in Double-Strand Break Repair Mutants," *Science,* vol. 260, no. 5105, pp. 207-210, 1993. [Online]. Available: http://www.jstor.org.proxy.lib.sfu.ca/stable/2881308.

[74] C. Boboila, F. W. Alt, and B. Schwer, "Classical and alternative end-joining pathways for repair of lymphocyte-specific and general DNA double-strand breaks," (in eng), *Adv Immunol,* vol. 116, pp. 1-49, 2012, doi: 10.1016/b978-0-12-394300-2.00001-6.

[75] F. Wang, C. Y. Huang, and O. Kanagawa, "Rapid deletion of rearranged T cell antigen receptor (TCR) Valpha-Jalpha segment by secondary rearrangement in the thymus: role of continuous rearrangement of TCR alpha chain gene and positive selection in the T cell repertoire formation," (in eng), *Proceedings of the National Academy of Sciences of the United States of America,* vol. 95, no. 20, pp. 11834-11839, 1998, doi: 10.1073/pnas.95.20.11834.

[76] F. R. Santori, I. Arsov, M. Lilic, and S. Vukmanovic, "Editing autoreactive TCR enables efficient positive selection," (in eng), *J Immunol,* vol. 169, no. 4, pp. 1729-34, Aug 15 2002, doi: 10.4049/jimmunol.169.4.1729.

[77] M. A. McGargill, J. M. Derbinski, and K. A. Hogquist, "Receptor editing in developing T cells," (in eng), *Nature immunology,* vol. 1, no. 4, pp. 336-41, Oct 2000, doi: 10.1038/79790.

[78] Z. Sun *et al.*, "Requirement for RORgamma in thymocyte survival and lymphoid organ development," (in eng), *Science,* vol. 288, no. 5475, pp. 2369-73, Jun 30 2000, doi: 10.1126/science.288.5475.2369.

[79] A. Singer, S. Adoro, and J. H. Park, "Lineage fate and intense debate: myths, models and mechanisms of CD4- versus CD8-lineage choice," (in eng), *Nature reviews. Immunology,* vol. 8, no. 10, pp. 788-801, Oct 2008, doi: 10.1038/nri2416.

[80] H. S. Teh *et al.*, "Thymic major histocompatibility complex antigens and the alpha beta T-cell receptor determine the CD4/CD8 phenotype of T cells," (in eng), *Nature,* vol. 335, no. 6187, pp. 229-33, Sep 15 1988, doi: 10.1038/335229a0.

[81] H. von Boehmer, H. S. Teh, and P. Kisielow, "The thymus selects the useful, neglects the useless and destroys the harmful," (in eng), *Immunol Today,* vol. 10, no. 2, pp. 57-61, Feb 1989, doi: 10.1016/0167-5699(89)90307-1.

[82] N. L. La Gruta, S. Gras, S. R. Daley, P. G. Thomas, and J. Rossjohn, "Understanding the drivers of MHC restriction of T cell receptors," (in eng), *Nature reviews. Immunology,* vol. 18, no. 7, pp. 467-478, Jul 2018, doi: 10.1038/s41577-018-0007-5.

[83] A. K. Sewell, "Why must T cells be cross-reactive?," (in eng), *Nature reviews. Immunology,* vol. 12, no. 9, pp. 669-77, Sep 2012, doi: 10.1038/nri3279.

[84] T. P. Arstila, A. Casrouge, V. Baron, J. Even, J. Kanellopoulos, and P. Kourilsky, "A direct estimate of the human alphabeta T cell receptor diversity," (in eng), *Science,* vol. 286, no. 5441, pp. 958-61, Oct 29 1999, doi: 10.1126/science.286.5441.958.

[85] J. J. Miles, D. C. Douek, and D. A. Price, "Bias in the alphabeta T-cell repertoire: implications for disease pathogenesis and vaccination," (in eng), *Immunology and cell biology,* vol. 89, no. 3, pp. 375-87, Mar 2011, doi: 10.1038/icb.2010.139.

[86] D. Mason, "A very high level of crossreactivity is an essential feature of the T-cell receptor," (in eng), *Immunol Today,* vol. 19, no. 9, pp. 395-404, Sep 1998.

[87] L. Wooldridge *et al.*, "A single autoimmune T cell receptor recognizes more than a million different peptides," (in eng), *J Biol Chem,* vol. 287, no. 2, pp. 1168-77, Jan 6 2012, doi: 10.1074/jbc.M111.289488.

[88] P. Dash *et al.*, "Quantifiable predictive features define epitope-specific T cell receptor repertoires," (in eng), *Nature,* vol. 547, no. 7661, pp. 89-93, Jul 6 2017, doi: 10.1038/nature22383.

[89] J. Glanville *et al.*, "Identifying specificity groups in the T cell receptor repertoire," (in eng), *Nature,* vol. 547, no. 7661, pp. 94-98, Jul 6 2017, doi: 10.1038/nature22976.

[90] M. E. Birnbaum *et al.*, "Deconstructing the peptide-MHC specificity of T cell recognition," (in eng), *Cell,* vol. 157, no. 5, pp. 1073-87, May 22 2014, doi: 10.1016/j.cell.2014.03.047.

[91] M. H. Gee *et al.*, "Antigen Identification for Orphan T Cell Receptors Expressed on Tumor-Infiltrating Lymphocytes," (in eng), *Cell,* vol. 172, no. 3, pp. 549-563.e16, 2018, doi: 10.1016/j.cell.2017.11.043.

[92] T. R. Mempel, S. E. Henrickson, and U. H. Von Andrian, "T-cell priming by dendritic cells in lymph nodes occurs in three distinct phases," (in eng), *Nature,* vol. 427, no. 6970, pp. 154-9, Jan 8 2004, doi: 10.1038/nature02238.

[93] P. Cascio, C. Hilton, A. F. Kisselev, K. L. Rock, and A. L. Goldberg, "26S proteasomes and immunoproteasomes produce mainly N-extended versions of an antigenic peptide," (in eng), *EMBO J,* vol. 20, no. 10, pp. 2357-2366, 2001, doi: 10.1093/emboj/20.10.2357.

[94] J. J. Neefjes, F. Momburg, and G. J. Hammerling, "Selective and ATP-dependent translocation of peptides by the MHC-encoded transporter," (in eng), *Science,* vol. 261, no. 5122, pp. 769-71, Aug 6 1993, doi: 10.1126/science.8342042.

[95] J. C. Shepherd *et al.*, "TAP1-dependent peptide translocation in vitro is ATP dependent and peptide selective," (in eng), *Cell,* vol. 74, no. 3, pp. 577-84, Aug 13 1993, doi: 10.1016/0092-8674(93)80058-m.

[96] T. Serwold, F. Gonzalez, J. Kim, R. Jacob, and N. Shastri, "ERAAP customizes peptides for MHC class I molecules in the endoplasmic reticulum," (in eng), *Nature,* vol. 419, no. 6906, pp. 480-3, Oct 3 2002, doi: 10.1038/nature01074.

[97] L. Saveanu *et al.*, "Concerted peptide trimming by human ERAP1 and ERAP2 aminopeptidase complexes in the endoplasmic reticulum," (in eng), *Nature immunology,* vol. 6, no. 7, pp. 689-97, Jul 2005, doi: 10.1038/ni1208.

[98] O. P. Joffre, E. Segura, A. Savina, and S. Amigorena, "Cross-presentation by dendritic cells," *Nature Reviews Immunology,* Review Article vol. 12, p. 557, 07/13/online 2012, doi: 10.1038/nri3254.

[99] J. F. Fonteneau *et al.*, "Characterization of the MHC class I cross-presentation pathway for cell-associated antigens by human dendritic cells," (in eng), *Blood,* vol. 102, no. 13, pp. 4448-55, Dec 15 2003, doi: 10.1182/blood-2003-06-1801.

[100] G. Zambruno *et al.*, "Detection of HIV-1 in epidermal Langerhans cells of HIV-infected patients using the polymerase chain reaction," (in eng), *J Invest Dermatol,* vol. 96, no. 6, pp. 979-82, Jun 1991.

[101] L. Bhoopat *et al.*, "In vivo identification of Langerhans and related dendritic cells infected with HIV-1 subtype E in vaginal mucosa of asymptomatic patients," (in eng), *Mod Pathol,* vol. 14, no. 12, pp. 1263-9, Dec 2001, doi: 10.1038/modpathol.3880472.

[102] M. L. Dustin and J. T. Groves, "Receptor signaling clusters in the immune synapse," (in eng), *Annu Rev Biophys,* vol. 41, pp. 543-56, 2012, doi: 10.1146/annurev-biophys-042910-155238.

[103] A. S. Shaw *et al.*, "Short related sequences in the cytoplasmic domains of CD4 and CD8 mediate binding to the amino-terminal domain of the p56lck tyrosine protein kinase," (in eng), *Mol Cell Biol,* vol. 10, no. 5, pp. 1853-62, May 1990, doi: 10.1128/mcb.10.5.1853.

[104] A. M. Norment, R. D. Salter, P. Parham, V. H. Engelhard, and D. R. Littman, "Cell-cell adhesion mediated by CD8 and MHC class I molecules," (in eng), *Nature,* vol. 336, no. 6194, pp. 79-81, Nov 3 1988, doi: 10.1038/336079a0.

[105] A. H. Courtney, W. L. Lo, and A. Weiss, "TCR Signaling: Mechanisms of Initiation and Propagation," (in eng), *Trends Biochem Sci,* vol. 43, no. 2, pp. 108-123, Feb 2018, doi: 10.1016/j.tibs.2017.11.008.

[106] M. K. Jenkins and R. H. Schwartz, "Antigen presentation by chemically modified splenocytes induces antigen-specific T cell unresponsiveness in vitro and in vivo," (in eng), *The Journal of experimental medicine,* vol. 165, no. 2, pp. 302-19, Feb 1 1987, doi: 10.1084/jem.165.2.302.

[107] F. A. Harding, J. G. McArthur, J. A. Gross, D. H. Raulet, and J. P. Allison, "CD28-mediated signalling co-stimulates murine T cells and prevents induction of anergy in T-cell clones," (in eng), *Nature,* vol. 356, no. 6370, pp. 607-9, Apr 16 1992, doi: 10.1038/356607a0.

[108] S. Bhatia, M. Edidin, S. C. Almo, and S. G. Nathenson, "Different cell surface oligomeric states of B7-1 and B7-2: implications for signaling," (in eng), *Proceedings of the National Academy of Sciences of the United States of America,* vol. 102, no. 43, pp. 15569-74, Oct 25 2005, doi: 10.1073/pnas.0507257102.

[109] L. I. Salazar-Fontana, V. Barr, L. E. Samelson, and B. E. Bierer, "CD28 Engagement Promotes Actin Polymerization Through the Activation of the Small Rho GTPase Cdc42 in Human T Cells," *The Journal of Immunology,* vol. 171, no. 5, pp. 2225-2232, 2003, doi: 10.4049/jimmunol.171.5.2225.

[110] Y. X. Tan, B. N. Manz, T. S. Freedman, C. Zhang, K. M. Shokat, and A. Weiss, "Inhibition of the kinase Csk in thymocytes reveals a requirement for actin remodeling in the initiation of full TCR signaling," (in eng), *Nature immunology,* vol. 15, no. 2, pp. 186-94, Feb 2014, doi: 10.1038/ni.2772.

[111] T. H. Watts, "Staying Alive: T Cell Costimulation, CD28, and Bcl-x_L," *The Journal of Immunology,* vol. 185, no. 7, pp. 3785-3787, 2010, doi: 10.4049/jimmunol.1090085.

[112] L. H. Boise *et al.*, "CD28 costimulation can promote T cell survival by enhancing the expression of Bcl-XL," (in eng), *Immunity,* vol. 3, no. 1, pp. 87-98, Jul 1995.

[113] K. A. Frauwirth *et al.*, "The CD28 signaling pathway regulates glucose metabolism," (in eng), *Immunity,* vol. 16, no. 6, pp. 769-77, Jun 2002.

[114] P. J. Martin, J. A. Ledbetter, Y. Morishita, C. H. June, P. G. Beatty, and J. A. Hansen, "A 44 kilodalton cell surface homodimer regulates interleukin 2 production by activated human T lymphocytes," (in eng), *J Immunol,* vol. 136, no. 9, pp. 3282-7, May 1 1986.

[115] J. D. Fraser, B. A. Irving, G. R. Crabtree, and A. Weiss, "Regulation of interleukin-2 gene enhancer activity by the T cell accessory molecule CD28," (in eng), *Science,* vol. 251, no. 4991, pp. 313-6, Jan 18 1991, doi: 10.1126/science.1846244.

[116] V. Kalia, S. Sarkar, S. Subramaniam, W. N. Haining, K. A. Smith, and R. Ahmed, "Prolonged interleukin-2Ralpha expression on virus-specific CD8+ T cells favors terminal-effector differentiation in vivo," (in eng), *Immunity,* vol. 32, no. 1, pp. 91-103, Jan 29 2010, doi: 10.1016/j.immuni.2009.11.010.

[117] R. R. Rao, Q. Li, K. Odunsi, and P. A. Shrikant, "The mTOR kinase determines effector versus memory CD8+ T cell fate by regulating the expression of transcription factors T-bet and Eomesodermin," (in eng), *Immunity,* vol. 32, no. 1, pp. 67-78, Jan 29 2010, doi: 10.1016/j.immuni.2009.10.010.

[118] J. Valenzuela, C. Schmidt, and M. Mescher, "The roles of IL-12 in providing a third signal for clonal expansion of naive CD8 T cells," (in eng), *J Immunol,* vol. 169, no. 12, pp. 6842-9, Dec 15 2002, doi: 10.4049/jimmunol.169.12.6842.

[119] H. D. Marshall, A. L. Prince, L. J. Berg, and R. M. Welsh, "IFN-alpha beta and self-MHC divert CD8 T cells into a distinct differentiation pathway characterized by rapid acquisition of effector functions," (in eng), *J Immunol,* vol. 185, no. 3, pp. 1419-28, Aug 1 2010, doi: 10.4049/jimmunol.1001140.

[120] P. Agarwal *et al.*, "Gene regulation and chromatin remodeling by IL-12 and type I IFN in programming for CD8 T cell effector function and memory," (in eng), *J Immunol,* vol. 183, no. 3, pp. 1695-704, Aug 1 2009, doi: 10.4049/jimmunol.0900592.

[121] E. L. Allard *et al.*, "Overexpression of IL-21 promotes massive CD8+ memory T cell accumulation," (in eng), *Eur J Immunol,* vol. 37, no. 11, pp. 3069-77, Nov 2007, doi: 10.1002/eji.200637017.

[122] M. F. Chevalier *et al.*, "HIV-1-Specific Interleukin-21⁺ CD4⁺ T Cell Responses Contribute to Durable Viral Control through the Modulation of HIV-Specific CD8⁺ T Cell Function," *Journal of virology,* vol. 85, no. 2, pp. 733-741, 2011, doi: 10.1128/jvi.02030-10.

[123] M. L. Janas, P. Groves, N. Kienzle, and A. Kelso, "IL-2 Regulates Perforin and Granzyme Gene Expression in CD8⁺ T Cells Independently of Its Effects on Survival and Proliferation," *The Journal of Immunology,* vol. 175, no. 12, pp. 8003-8010, 2005, doi: 10.4049/jimmunol.175.12.8003.

[124] M. E. Pipkin, J. A. Sacks, F. Cruz-Guilloty, M. G. Lichtenheld, M. J. Bevan, and A. Rao, "Interleukin-2 and inflammation induce distinct transcriptional programs that promote the differentiation of effector cytolytic T cells," (in eng), *Immunity,* vol. 32, no. 1, pp. 79-90, Jan 29 2010, doi: 10.1016/j.immuni.2009.11.012.

[125] J. A. Trapani and M. J. Smyth, "Functional significance of the perforin/granzyme cell death pathway," *Nature Reviews Immunology,* vol. 2, no. 10, pp. 735-747, 2002/10/01 2002, doi: 10.1038/nri911.

[126] R. V. Talanian *et al.*, "Granule-mediated Killing: Pathways for Granzyme B–initiated Apoptosis," *The Journal of experimental medicine,* vol. 186, no. 8, pp. 1323-1331, 1997, doi: 10.1084/jem.186.8.1323.

[127] R. A. Koup *et al.*, "Temporal association of cellular immune responses with the initial control of viremia in primary human immunodeficiency virus type 1 syndrome," vol. 68, no. 7, pp. 4650-4655, 1994. [Online]. Available: https://jvi.asm.org/content/jvi/68/7/4650.full.pdf.

[128] P. Borrow, H. Lewicki, B. H. Hahn, G. M. Shaw, and M. B. Oldstone, "Virus-specific CD8+ cytotoxic T-lymphocyte activity associated with control of viremia in primary human immunodeficiency virus type 1 infection," (in eng), *Journal of virology,* vol. 68, no. 9, pp. 6103-10, Sep 1994.

[129] N. Goonetilleke *et al.*, "The first T cell response to transmitted/founder virus contributes to the control of acute viremia in HIV-1 infection," (in eng), *The Journal of experimental medicine,* vol. 206, no. 6, pp. 1253-72, Jun 8 2009, doi: 10.1084/jem.20090365.

[130] A. Chowdhury *et al.*, "Differential Impact of In Vivo CD8+ T Lymphocyte Depletion in Controller versus Progressor Simian Immunodeficiency Virus-Infected Macaques," (in eng), *Journal of virology,* vol. 89, no. 17, pp. 8677-86, Sep 2015, doi: 10.1128/jvi.00869-15.

[131] J. E. Schmitz *et al.*, "Control of viremia in simian immunodeficiency virus infection by CD8+ lymphocytes," (in eng), *Science,* vol. 283, no. 5403, pp. 857-60, Feb 5 1999.

[132] Z. M. Ndhlovu *et al.*, "Magnitude and Kinetics of CD8+ T Cell Activation during Hyperacute HIV Infection Impact Viral Set Point," (in eng), *Immunity,* vol. 43, no. 3, pp. 591-604, Sep 15 2015, doi: 10.1016/j.immuni.2015.08.012.

[133] W. L. Dinges *et al.*, "Virus-specific CD8+ T-cell responses better define HIV disease progression than HLA genotype," (in eng), *Journal of virology,* vol. 84, no. 9, pp. 4461-8, May 2010, doi: 10.1128/jvi.02438-09.

[134] S. A. Migueles *et al.*, "CD8(+) T-cell Cytotoxic Capacity Associated with Human Immunodeficiency Virus-1 Control Can Be Mediated through Various Epitopes and Human Leukocyte Antigen Types," (in eng), *EBioMedicine,* vol. 2, no. 1, pp. 46-58, Jan 2015, doi: 10.1016/j.ebiom.2014.12.009.

[135] Z. M. Ndhlovu *et al.*, "High-dimensional immunomonitoring models of HIV-1-specific CD8 T-cell responses accurately identify subjects achieving spontaneous viral control," (in eng), *Blood,* vol. 121, no. 5, pp. 801-11, Jan 31 2013, doi: 10.1182/blood-2012-06-436295.

[136] M. R. Betts *et al.*, "HIV nonprogressors preferentially maintain highly functional HIV-specific CD8+ T cells," (in eng), *Blood,* vol. 107, no. 12, pp. 4781-9, Jun 15 2006, doi: 10.1182/blood-2005-12-4818.

[137] A. R. Hersperger *et al.*, "Increased HIV-specific CD8+ T-cell cytotoxic potential in HIV elite controllers is associated with T-bet expression," (in eng), *Blood,* vol. 117, no. 14, pp. 3799-808, Apr 7 2011, doi: 10.1182/blood-2010-12-322727.

[138] S. A. Migueles *et al.*, "Lytic granule loading of CD8+ T cells is required for HIV-infected cell elimination associated with immune control," (in eng), *Immunity,* vol. 29, no. 6, pp. 1009-21, Dec 19 2008, doi: 10.1016/j.immuni.2008.10.010.

[139] L. Trautmann *et al.*, "Upregulation of PD-1 expression on HIV-specific CD8+ T cells leads to reversible immune dysfunction," (in eng), *Nature medicine,* vol. 12, no. 10, pp. 1198-202, Oct 2006, doi: 10.1038/nm1482.

[140] C. L. Day *et al.*, "PD-1 expression on HIV-specific T cells is associated with T-cell exhaustion and disease progression," (in eng), *Nature,* vol. 443, no. 7109, pp. 350-4, Sep 21 2006, doi: 10.1038/nature05115.

[141] D. E. Kaufmann *et al.*, "Upregulation of CTLA-4 by HIV-specific CD4+ T cells correlates with disease progression and defines a reversible immune dysfunction," (in eng), *Nature immunology,* vol. 8, no. 11, pp. 1246-54, Nov 2007, doi: 10.1038/ni1515.

[142] C. Petrovas *et al.*, "PD-1 is a regulator of virus-specific CD8+ T cell survival in HIV infection," (in eng), *The Journal of experimental medicine,* vol. 203, no. 10, pp. 2281-92, Oct 2 2006, doi: 10.1084/jem.20061496.

[143] D. L. Barber *et al.*, "Restoring function in exhausted CD8 T cells during chronic viral infection," (in eng), *Nature,* vol. 439, no. 7077, pp. 682-7, Feb 9 2006, doi: 10.1038/nature04444.

[144] A. Saez-Cirion *et al.*, "HIV controllers exhibit potent CD8 T cell capacity to suppress HIV infection ex vivo and peculiar cytotoxic T lymphocyte activation phenotype," *Proceedings of the National Academy of Sciences of the United States of America,* vol. 104, no. 16, pp. 6776-81, Apr 17 2007, doi: 10.1073/pnas.0611244104.

[145] A. Saez-Cirion *et al.*, "Heterogeneity in HIV suppression by CD8 T cells from HIV controllers: association with Gag-specific CD8 T cell responses," (in eng), *J Immunol,* vol. 182, no. 12, pp. 7828-37, Jun 15 2009, doi: 10.4049/jimmunol.0803928.

[146] H. Streeck *et al.*, "Recognition of a Defined Region within p24 Gag by CD8⁺ T Cells during Primary Human Immunodeficiency Virus Type 1 Infection in Individuals Expressing Protective HLA Class I Alleles," *Journal of virology,* vol. 81, no. 14, pp. 7725-7731, 2007, doi: 10.1128/jvi.00708-07.

[147] S. A. Migueles *et al.*, "HLA B*5701 is highly associated with restriction of virus replication in a subgroup of HIV-infected long term nonprogressors," (in eng), *Proceedings of the National Academy of Sciences of the United States of America,* vol. 97, no. 6, pp. 2709-14, Mar 14 2000, doi: 10.1073/pnas.050567397.

[148] P. Kiepiela *et al.*, "Dominant influence of HLA-B in mediating the potential co-evolution of HIV and HLA," *Nature,* vol. 432, no. 7018, pp. 769-775, 2004/12/01 2004, doi: 10.1038/nature03113.

[149] R. S. Ntale *et al.*, "Temporal Association of HLA-B*81:01- and HLA-B*39:10-Mediated HIV-1 p24 Sequence Evolution with Disease Progression," *Journal of virology,* vol. 86, no. 22, p. 12013, 2012, doi: 10.1128/JVI.00539-12.

[150] Z. L. Brumme *et al.*, "Evidence of differential HLA class I-mediated viral evolution in functional and accessory/regulatory genes of HIV-1," (in eng), *PLoS pathogens,* vol. 3, no. 7, p. e94, Jul 2007, doi: 10.1371/journal.ppat.0030094.

[151] Z. L. Brumme *et al.*, "HLA-associated immune escape pathways in HIV-1 subtype B Gag, Pol and Nef proteins," (in eng), *PloS one,* vol. 4, no. 8, p. e6687, Aug 19 2009, doi: 10.1371/journal.pone.0006687.

[152] C. B. Moore, M. John, I. R. James, F. T. Christiansen, C. S. Witt, and S. A. Mallal, "Evidence of HIV-1 adaptation to HLA-restricted immune responses at a population level," (in eng), *Science,* vol. 296, no. 5572, pp. 1439-43, May 24 2002, doi: 10.1126/science.1069660.

[153] R. Draenert *et al.*, "Immune selection for altered antigen processing leads to cytotoxic T lymphocyte escape in chronic HIV-1 infection," (in eng), *The Journal of experimental medicine,* vol. 199, no. 7, pp. 905-15, Apr 5 2004, doi: 10.1084/jem.20031982.

[154] P. Ammaranond, J. Zaunders, C. Satchell, D. van Bockel, D. A. Cooper, and A. D. Kelleher, "A new variant cytotoxic T lymphocyte escape mutation in HLA-B27-positive individuals infected with HIV type 1," (in eng), *AIDS Res Hum Retroviruses,* vol. 21, no. 5, pp. 395-7, May 2005, doi: 10.1089/aid.2005.21.395.

[155] M. C. Iglesias *et al.*, "Escape from highly effective public CD8+ T-cell clonotypes by HIV," (in eng), *Blood,* vol. 118, no. 8, pp. 2138-49, Aug 25 2011, doi: 10.1182/blood-2011-01-328781.

[156] H. Crawford *et al.*, "Evolution of HLA-B*5703 HIV-1 escape mutations in HLA-B*5703-positive individuals and their transmission recipients," *The Journal of experimental medicine,* Research Support, N.I.H., Extramural

Research Support, Non-U.S. Gov't vol. 206, no. 4, pp. 909-21, Apr 13 2009, doi: 10.1084/jem.20081984.

[157] A. J. Leslie *et al.*, "HIV evolution: CTL escape mutation and reversion after transmission," *Nature medicine,* vol. 10, no. 3, pp. 282-9, Mar 2004. [Online]. Available: http://www.ncbi.nlm.nih.gov/entrez/query.fcgi?cmd=Retrieve&db=PubMed&dopt=Citation&list_uids=14770175.

[158] P. Ammaranond *et al.*, "HIV immune escape at an immunodominant epitope in HLA-B*27-positive individuals predicts viral load outcome," (in eng), *J Immunol,* vol. 186, no. 1, pp. 479-88, Jan 1 2011, doi: 10.4049/jimmunol.0903227.

[159] J. Martinez-Picado *et al.*, "Fitness cost of escape mutations in p24 Gag in association with control of human immunodeficiency virus type 1," (in eng), *Journal of virology,* vol. 80, no. 7, pp. 3617-23, Apr 2006, doi: 10.1128/jvi.80.7.3617-3623.2006.

[160] T. Miura *et al.*, "HLA-B57/B*5801 Human Immunodeficiency Virus Type 1 Elite Controllers Select for Rare Gag Variants Associated with Reduced Viral Replication Capacity and Strong Cytotoxic T-Lymphotye Recognition," *Journal of virology,* vol. 83, no. 6, p. 2743, 2009, doi: 10.1128/JVI.02265-08.

[161] J. K. Wright *et al.*, "Impact of HLA-B*81-Associated Mutations in HIV-1 Gag on Viral Replication Capacity," *Journal of virology,* vol. 86, no. 6, pp. 3193-3199, 2012, doi: 10.1128/jvi.06682-11.

[162] T. J. Markle, M. Philip, and M. A. Brockman, "HIV-1 Nef and T-cell activation: a history of contradictions," (in eng), *Future Virol,* vol. 8, no. 4, p. 10.2217/fvl.13.20, 2013, doi: 10.2217/fvl.13.20.

[163] L. Naidoo *et al.*, "Nef-mediated inhibition of NFAT following TCR stimulation differs between HIV-1 subtypes," (in eng), *Virology,* vol. 531, pp. 192-202, May 2019, doi: 10.1016/j.virol.2019.02.011.

[164] C. Aiken, J. Konner, N. R. Landau, M. E. Lenburg, and D. Trono, "Nef induces CD4 endocytosis: requirement for a critical dileucine motif in the membrane-proximal CD4 cytoplasmic domain," (in eng), *Cell,* vol. 76, no. 5, pp. 853-64, Mar 11 1994, doi: 10.1016/0092-8674(94)90360-3.

[165] Y. H. Kim, S. H. Chang, J. H. Kwon, and S. S. Rhee, "HIV-1 Nef plays an essential role in two independent processes in CD4 down-regulation: dissociation of the CD4-p56(lck) complex and targeting of CD4 to lysosomes," (in eng), *Virology,* vol. 257, no. 1, pp. 208-19, Apr 25 1999, doi: 10.1006/viro.1999.9642.

[166] S. Le Gall *et al.*, "Nef interacts with the mu subunit of clathrin adaptor complexes and reveals a cryptic sorting signal in MHC I molecules," (in eng), *Immunity,* vol. 8, no. 4, pp. 483-95, Apr 1998.

[167] A. Rosa *et al.*, "HIV-1 Nef promotes infection by excluding SERINC5 from virion incorporation," (in eng), *Nature,* vol. 526, no. 7572, pp. 212-7, Oct 8 2015, doi: 10.1038/nature15399.

[168] Y. Usami, Y. Wu, and H. G. Gottlinger, "SERINC3 and SERINC5 restrict HIV-1 infectivity and are counteracted by Nef," (in eng), *Nature,* vol. 526, no. 7572, pp. 218-23, Oct 8 2015, doi: 10.1038/nature15400.

[169] Y. Wu, B. Olety, E. R. Weiss, E. Popova, H. Yamanaka, and H. Gottlinger, "Potent Enhancement of HIV-1 Replication by Nef in the Absence of SERINC3 and SERINC5," (in eng), *MBio,* vol. 10, no. 3, Jun 11 2019, doi: 10.1128/mBio.01071-19.

[170] K. L. Collins, B. K. Chen, S. A. Kalams, B. D. Walker, and D. Baltimore, "HIV-1 Nef protein protects infected primary cells against killing by cytotoxic T lymphocytes," (in eng), *Nature,* vol. 391, no. 6665, pp. 397-401, Jan 22 1998, doi: 10.1038/34929.

[171] O. O. Yang *et al.*, "Nef-mediated resistance of human immunodeficiency virus type 1 to antiviral cytotoxic T lymphocytes," (in eng), *Journal of virology,* vol. 76, no. 4, pp. 1626-31, Feb 2002, doi: 10.1128/jvi.76.4.1626-1631.2002.

[172] H. Chen *et al.*, "TCR clonotypes modulate the protective effect of HLA class I molecules in HIV-1 infection," *Nature immunology,* vol. 13, no. 7, pp. 691-700, Jul 2012, doi: 10.1038/ni.2342.

[173] K. Ladell *et al.*, "A molecular basis for the control of preimmune escape variants by HIV-specific CD8+ T cells," (in eng), *Immunity,* vol. 38, no. 3, pp. 425-36, Mar 21 2013, doi: 10.1016/j.immuni.2012.11.021.

[174] A. Lissina, L. A. Chakrabarti, M. Takiguchi, and V. Appay, "TCR clonotypes: molecular determinants of T-cell efficacy against HIV," (in eng), *Current opinion in virology,* vol. 16, pp. 77-85, Feb 2016, doi: 10.1016/j.coviro.2016.01.017.

[175] J. R. Almeida *et al.*, "Antigen sensitivity is a major determinant of CD8+ T-cell polyfunctionality and HIV-suppressive activity," *Blood,* vol. 113, no. 25, pp. 6351-60, Jun 18 2009, doi: 10.1182/blood-2009-02-206557.

[176] C. T. Berger *et al.*, "High-Functional-Avidity Cytotoxic T Lymphocyte Responses to HLA-B-Restricted Gag-Derived Epitopes Associated with Relative HIV Control," *Journal of virology,* vol. 85, no. 18, pp. 9334-9345, 2011, doi: 10.1128/jvi.00460-11.

[177] B. Mothe *et al.*, "CTL Responses of High Functional Avidity and Broad Variant Cross-Reactivity Are Associated with HIV Control," *PloS one,* vol. 7, no. 1, p. e29717, 2012, doi: 10.1371/journal.pone.0029717.

[178] D. F. Nixon, A. R. M. Townsend, J. G. Elvin, C. R. Rizza, J. Gallwey, and A. J. McMichael, "HIV-1 gag-specific cytotoxic T lymphocytes defined with recombinant vaccinia virus and synthetic peptides," *Nature,* vol. 336, no. 6198, pp. 484-487, 1988/12/01 1988, doi: 10.1038/336484a0.

[179] A. Lissina *et al.*, "The link between CD8(+) T-cell antigen-sensitivity and HIV-suppressive capacity depends on HLA restriction, target epitope and viral isolate," (in eng), *Aids,* vol. 28, no. 4, pp. 477-86, Feb 20 2014, doi: 10.1097/qad.0000000000000175.

[180] X. Sun *et al.*, "Superimposed Epitopes Restricted by the Same HLA Molecule Drive Distinct HIV-Specific CD8⁺ T Cell Repertoires," *The Journal of Immunology,* vol. 193, no. 1, pp. 77-84, 2014, doi: 10.4049/jimmunol.1400375.

[181] E. L. Turnbull *et al.*, "HIV-1 epitope-specific CD8+ T cell responses strongly associated with delayed disease progression cross-recognize epitope variants efficiently," (in eng), *J Immunol,* vol. 176, no. 10, pp. 6130-46, May 15 2006, doi: 10.4049/jimmunol.176.10.6130.

Chapter 2. A robust and scalable TCR-based reporter cell assay to measure HIV-1 Nef-mediated T cell immune evasion

This chapter is adapted from the following published article of which I am a co-first author.

Anmole G*., Kuang X. T*., Toyoda M., Martin E., Shahid A., Le A. Q., Markle T., Baraki B., Jones R.B., Ostrowski M.A., Ueno T., Brumme Z.L., and Brockman, M. A. (2015). A robust and scalable TCR-based reporter cell assay to measure HIV-1 Nef-mediated T cell immune evasion. *J Immunol Methods, 426*, 104-113.

2.1. Contributions

Gursev Anmole and X Tallie Kuang contributed equally to this study. I use terms “we” and “our” to reflect that I did not complete all the work presented in **Chapter 2**. My primary roles in this study were: (1) to design and optimize the TCR signaling assay that was used to measure T cell reactivity to HIV antigens in the presence or absence of Nef; (2) to collect all data presented in Figure 2-1; (3) to participate in collection of data presented in other figures; (4) to train Tallie Kuang to use the TCR reporter assay so that she could run experiments independently; and (5) to prepare the initial draft of the manuscript and revisions for publication. Tallie Kuang generated the Nef mutant viruses, conducted assays involving viral infections, and sorted cells using FACS. Other co-authors contributed minor technical support (M.T, E.M., A.S., A.Q.L., T.M., B.B.), HIV or T cell specimens (R.B.J., M.O.) or supervision and mentorship (T.U., Z.L.B., M.A.B).

2.2. Abstract

HIV-1 evades cytotoxic T cell responses through Nef-mediated downregulation of HLA class I molecules from the infected cell surface. Methods to quantify the impact of Nef on T cell recognition typically employ patient-derived T cell clones; however, these assays are limited by the cost and effort required to isolate and maintain primary cell lines. The variable activity of different T cell clones and the limited number of cells generated by re-stimulation can also hinder assay reproducibility and scalability. Here, we describe a heterologous T cell receptor reporter assay and use it to study immune evasion by Nef. Induction of NFAT-driven luciferase following co-culture with peptide-pulsed or virus-infected target cells serves as a rapid, quantitative and antigen-specific measure of T cell recognition of its cognate peptide/HLA complex. We demonstrate that Nef-mediated downregulation of HLA on target cells correlates inversely with T cell receptor-dependent luminescent signal generated by effector cells. This method provides a robust, flexible and scalable platform that is suitable for studies to measure Nef function in the context of different viral peptide/HLA antigens, to assess the function of patient-derived Nef alleles, or to screen small molecule libraries to identify novel Nef inhibitors.

2.3. Introduction

HIV-1 infection elicits a rapid CD8+ cytotoxic T lymphocyte (CTL) response that targets viral peptide epitopes presented by Human Leukocyte Antigen class I (HLA-I) molecules. While CTL contribute to early control of HIV-1 replication [1]–[3], the virus quickly eludes this response to establish a persistent infection. Evasion from CTL is achieved by the selection of CTL escape mutations within or near targeted viral epitopes [4], as well as the actions of HIV-1 Nef, a 27-35 kD myrisoylated accessory protein that enhances plasma viremia and pathogenesis through various mechanisms [5], [6]. In particular, Nef's ability to downregulate HLA-I molecules, specifically HLA-A and –B alleles, reduces CTL recognition and killing of virus-infected cells [7]–[9]. Deletions or mutations in Nef have been identified in HIV-1 long-term non-progressors [10]–[13] and Nef alleles isolated from elite controllers have decreased *in vitro* ability to downregulate HLA-I compared to those from progressors [14], indicating that Nef contributes

significantly to disease outcome. As such, novel inhibitors of Nef are expected to be of clinical benefit.

The impact of Nef-mediated HLA-I downregulation on antiviral CTL activity has successfully been studied using traditional co-culture methods [7], [8], [15]–[17]. In a typical assay, a patient-derived CTL clone is incubated with HLA-expressing target cells that have been infected with HIV-1 harboring a wild type or mutant Nef sequence (e.g. ΔNef or the $M_{20}A$ variant that is defective for HLA-I downregulation [18]) and the extent of viral suppression is quantified by measuring HIV-1 p24 antigen levels in the culture supernatant over the course of 7 days. Alternatively, CTL cytolytic activity (or cytokine production) can be measured following co-culture with target cells expressing or not expressing functional Nef [19], [20]. While these approaches have contributed greatly to our mechanistic understanding of immunological effects of Nef-mediated HLA-I downregulation [21], [22], the use of primary T cells for such studies presents a number of challenges. First, isolation and maintenance of patient-derived epitope-specific CTL clones can be time consuming and costly. More importantly, *in vitro* expansion of CTL clones can introduce variability in cell purity and antiviral activity. Finally, the limited proliferative capacity of many CTL clones may preclude assay scale-up.

Here, we present a reporter T cell method to examine the immune evasion activity of Nef based in part on prior studies [23], [24]. This approach uses readily available molecular and cellular reagents to simulate natural T cell recognition. In this assay, a Jurkat T cell line serves as a modifiable “effector” cell population. These cells are transiently transfected with plasmids encoding TCR alpha and beta genes isolated from a primary CTL clone (conferring epitope/HLA specificity), CD8 alpha (to stabilize TCR-peptide/HLA interactions), and an NFAT-luciferase reporter vector (to quantify TCR-mediated signaling). CEM T cell lines stably or transiently expressing specific HLA-I alleles serve as “target” cell populations. These cells can be pulsed with epitopic peptide or infected with HIV-1. Co-culture of effector and target cells triggers antigen-specific TCR-dependent calcium flux in the effector cells, which results in quantifiable NFAT-driven luciferase expression that can be measured by luminescence. This highly flexible system provides a sensitive and scalable method to assess CTL recognition in the presence or absence of Nef.

2.4. Results

2.4.1. Antigen-specific reactivity of Jurkat effector cells expressing a TCR against HIV-1 Gag.

Previous studies have reported that heterologous expression of TCR in a Jurkat-derived CD8+ NFAT-luciferase reporter T cell line (Jurkat/MA) [33] conferred antigen-specific reactivity [24], [34]. However, in our hands, TCR-mediated luciferase expression in the Jurkat/MA cell line was consistently low, yielding signals less than 5-fold above negative controls. As an alternative strategy, we replicated this system using transient co-transfection of Jurkat "effector" cells with separate plasmid DNAs encoding TCR alpha, TCR beta, CD8 alpha, and an NFAT-luciferase reporter. TCR alpha and beta cDNAs were isolated from a human CTL clone (5B2) specific for the HLA-A*02-restricted FK10 epitope located within the HIV-1 Gag protein. Following electroporation, 40-50% of viable Jurkat cells expressed both GFP (a marker co-expressed by the TCR alpha and beta plasmids) and surface CD8 alpha, indicating relatively high transfection efficiency (**Figure 2.1A**).

To assess the utility of this method and to confirm that the response was peptide-specific, transfected Jurkat effector cells were incubated with CEM-A*02 target cells pulsed with either the TCR-matched (FK10) peptide or an HLA-matched but TCR mismatched (SL9) control peptide at an effector to target (E:T) ratio of 1:1. Robust luminescent signal was observed at 6 hours following co-culture when target cells were pulsed with FK10 peptide, but low background luminescence was seen when target cells were pulsed with SL9 peptide (**Figure 2-1B, left side**). Notably, the luminescent signal was responsive to FK10 peptide dose (~14-fold and ~10-fold induction with 30 ng/µL and 3 ng/µL peptide pulse, respectively, compared to SL9). For convenience, additional studies were conducted at the 6-hour time point.

To verify that TCR-mediated signaling was also HLA allele-specific, we co-cultured Jurkat effector cells with an HLA-mismatched target cell line (CEM-B*07) under similar conditions. Low background luminescence was observed in all cases (**Figure 2-1B, right side**). In addition, because Jurkat cells do not naturally express CD8 proteins, we assessed the CD8 dependence of 5B2 TCR by omitting this plasmid. We observed

~3-fold lower luminescent signal in the absence of CD8 **(Appendix Figure 2-1)** suggesting that this TCR can function in a CD8-independent manner.

To test the use of this Jurkat reporter cell assay to study other TCR-peptide-HLA combinations, we compared the *in vitro* response of 5B2 TCR with that of a second TCR (868), which recognizes the A*02-restricted Gag SL9 epitope [30]. Following co-culture with CEM-A*02 cells pulsed with the appropriate cognate peptide, we observed dose-dependent signaling by both TCR (**Figure 2-1C**) that was abolished when target cells were pulsed with the alternative (non-specific) peptide. The 868 TCR displayed higher background signaling and a shallower dose-response to cognate peptide, suggesting differences in antigen engagement between these TCR, but the biological relevance of this is not known. Next, we tested the ability of TCR clone 5B2 to respond to a panel of naturally occurring Gag FK10 sequence variants at peptide position 4 (K4R) or 9 (H9N, H9Y, H9S, H9Q). Our results indicated that the K4R polymorphism abrogated TCR recognition, resulting in signal that was ~9 fold less than FK10 and similar to that of negative control SL9 peptide **(Figure 2-1D)**. In contrast, all position 9 variants retained an ability to stimulate 5B2 TCR similar to wild type FK10.

Together, these results demonstrate that transient transfection of Jurkat T cells can be used to assess the antigen-specific function of a heterologous TCR in a peptide- and HLA-specific manner.

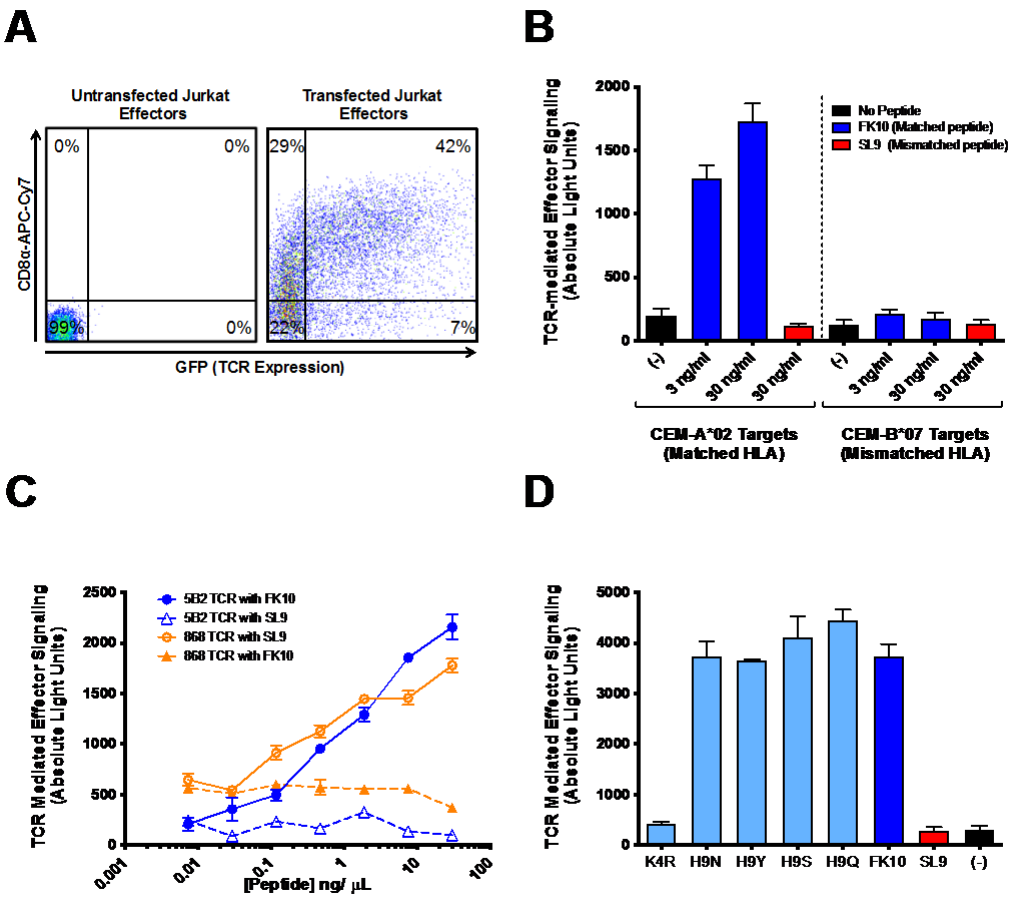

Figure 2-1. Jurkat cells transiently expressing a TCR specific for the HLA-A*02-restricted FK10 or SL9 epitope are responsive to antigen in a peptide- and HLA-specific manner.

(A) Representative dot plots illustrate efficient transfection of Jurkat cells. Expression of GFP (co-produced by the 5B2 TCR alpha/beta plasmids) and surface CD8alpha (allophycocyanin (APC)-Cy7) were detected in untransfected (left panel) and transfected cells (right panel) by flow cytometry at 20 hours following electroporation. (B) Transfected Jurkat cells displayed robust antigen-specific NFAT-luciferase signaling activity following co-culture with CEM-A*02 target cells pulsed with 3 ng/µl or 30 ng/µl FK10 peptide (blue bars) versus negative control (no peptide, black bars). Limited signaling following co-culture with CEM-A*02 target cells pulsed with irrelevant peptide (SL9, red bars) and HLA-mismatched CEM-B*07 target cells pulsed with either FK10 or SL9 peptide confirmed that this response was highly specific for the cognate antigen and HLA. (C) SL9-specific 868 TCR showed a dose dependent signal (solid orange line) when co-cultured with SL9-pulsed CEM-A*02 cells. Peptide concentrations were 30 ng/µl - 0.0073 ng/µl (4-fold serial dilutions). When TCRs were titrated with mismatched peptide, the signal remained at background levels and did not increase with increasing amounts of peptide. (D) 5B2 TCR displayed cross-reactivity, as it was able to recognize naturally occurring FK10 variants at position 9 (light blue bars) at 30 ng/µl; however, a lysine to arginine variant at position 4 abrogated TCR activity. Luminescence was measured at 6 hours using the Steady-glo luciferin kit (Promega) on a Tecan Infinite M200 plate reader. Luciferase results are presented as mean values from 3 co-culture replicates and error bars represent standard error mean (SEM).

2.4.2. Expression of HIV-1 Nef in target cells reduces TCR recognition

The ability of HIV-1 Nef to downregulate HLA-A and HLA-B alleles is well documented [35]. In order to test a range of HLA expression phenotypes on target cells, we examined the activity of wild type Nef_{SF2}, as well as $M_{20}A$ and $A_{72}xxA_{75}$ mutants that are expected to display reduced function [18], [36], HIV-1 subtype B and subtype C Nef alleles encoding 2004 consensus sequences, and empty vector (ΔNef, negative control). CEM-A*02 cells were transfected with each Nef allele (cloned into pSELECT-GFPzeo) and we assessed GFP (a marker of transfection) and surface HLA-A*02:01 expression 40 hours later using flow cytometry. Median fluorescence intensity (MFI) of HLA-A*02 staining was calculated for GFP positive cells in each case. As expected, Nef_{SF2} efficiently downregulated HLA-A*02 compared to ΔNef control, yielding a ~6-fold reduction in MFI (217 vs. 1332 units, respectively) (**Figure 2-2A**). Consensus subtype B and subtype C Nef alleles displayed activity that was similar to Nef_{SF2}, yielding HLA-A*02 MFIs of 183 and 267 units, respectively, that are also consistent with previous reports suggesting modestly lower HLA-I downregulation function for consensus subtype C Nef [37]. As expected, Nef $M_{20}A$ and $A_{72}xxA_{75}$ variants displayed MFIs between Nef_{SF2} and ΔNef (788 and 406, respectively), indicating impaired HLA-I downregulation function.

Next, we examined the ability of Jurkat effector cells expressing FK10-specific 5B2 TCR to recognize peptide-pulsed CEM-A*02 target cells expressing these Nef alleles. Co-culture assays were conducted as described in **2.6.4**, using unsorted Nef-transfected CEM-A*02 cells as targets. Consistent with reduced surface HLA-A*02 expression on target cells, TCR-dependent luminescent signal by effector cells following co-culture was lower when target cells expressed Nef_{SF2} compared to the ΔNef control (600 vs. 950 light units, respectively) (**Figure 2-2B, left panel**). These luminescence values were ~10 fold (Nef_{SF2}) and 15-fold (ΔNef) higher than those observed when target cells were pulsed with the mismatched SL9 peptide**.** Other Nef variants displayed intermediate effects on T cell recognition, as indicated by luminescent signals between 650 and 750 light units. A strong correlation was observed between luminescence generated by effector cells and HLA-A*02 expression on target cells (R_2=0.79, p=0.02) (**Figure 2-2C**), indicating that Nef-mediated reduction of HLA-I levels resulted in a impaired TCR stimulation.

The relatively high luminescent signal generated by FK10-pulsed target cells transfected with Nef_{SF2} (~10-fold greater than SL9-pulsed cells) was presumably due to the presence of untransfected target cells that expressed normal levels of HLA-A*02 and thus were able to capture FK10 peptide and present it to Jurkat effector cells. To test this issue directly, we sorted Nef-expressing target cells following transfection based either on their forward-scatter, side-scatter, and GFP expression (as a marker of transfection) parameters, or using these characteristics plus the absence of Annexin V to exclude early apoptotic cells. As expected, this strategy yielded a wider dynamic range of TCR-mediated luminescent signal in effector cells. We observed ~180 and ~800 light units upon co-culture with sorted Nef_{SF2} vs. ΔNef-transfected target cells, respectively (**Figure 2-2B, middle and right panels**), values that were ~3-fold and ~14-fold higher than SL9-pulsed control cells. Other Nef variants generated intermediate luciferase signals that were consistent with their level of HLA downregulation function. Similar results were observed with or without Annexin V staining, suggesting that removal of early apoptotic cells was not critical for assay reproducibility when cells were sorted based on GFP expression and size parameters based on healthy, unmanipulated cells. Overall, a very strong correlation was found between TCR-mediated signaling by effector cells and HLA-A*02 expression on sorted target cells, with or without Annexin V staining (R_2=0.96, p=0.0007) (**Figure 2-2C)**.

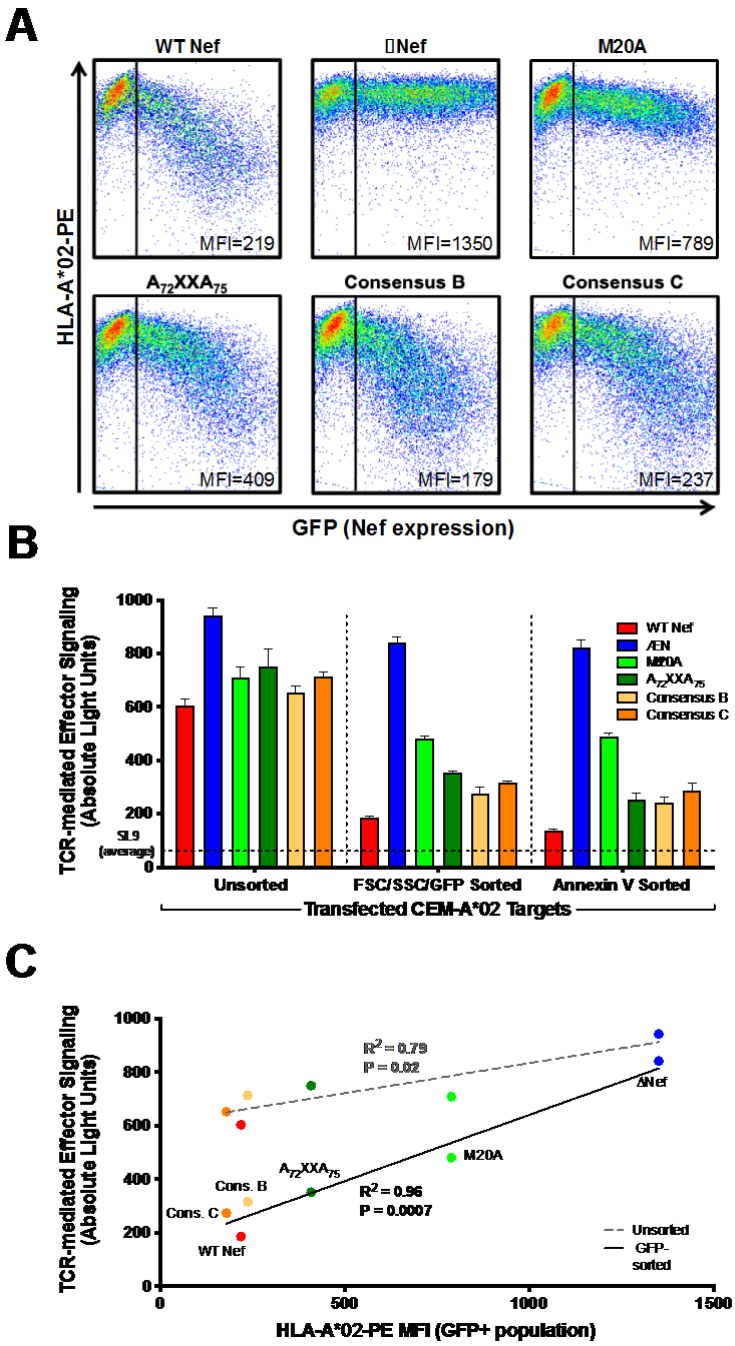

Figure 2-2. Response to HLA-A*02-FK10 is diminished by HIV-1 Nef.
(A) CEM-A*02 cells were transfected with a panel of HIV-1 Nef alleles, including wild type Nef_{SF2}; $M_{20}A$ or $A_{72}XXA_{75}$ mutants reported to display impaired HLA downregulation function; consensus HIV-1 subtype B or subtype C Nef sequences; or empty vector (ΔNef). Surface expression of HLA-A*02 (phycoerythrin; PE) was measured by flow cytometry at 20 hours following electroporation and median fluorescence intensity (MFI) was calculated for GFP positive cells (co-produced by pSELECT-Nef plasmids) in each case. **(B)** Transfected CEM-A*02 cells were left unsorted (left panel) or Nef-expressing cells were sorted by flow cytometry based on forward-scatter, side-scatter and GFP+

(FSC/SSC, middle panel), or these parameters plus Annexin V_{low} (FSC/SSC/Annexin V, right panel), prior to being pulsed with FK10 peptide and used as target cells in a co-culture with FK10-specific Jurkat effector cells. Luminescence was measured at 6 hours using the Steady-glo luciferin kit (Promega) on a Tecan Infinite M200 plate reader and are reported as light units (y-axis). Luciferase results are presented as mean values from 3 co-culture replicates and error bars represent standard error mean (SEM). Dashed line indicates the average background luminescent signal detected following co-culture of effector cells with control target cells pulsed with mismatched SL9 peptide. Control stimulations with PHA resulted in ~1700 absolute light units. **(C)** Linear regression analyses indicated a strong correlation between luminescent signal by effector cells with MFI of HLA-A*02 on unsorted target cells (R_2=0.79, p=0.02). This correlation was enhanced by sorting target cells for Nef expression as described above (R_2=0.96, p=0.0007).

2.4.3. Co-transfection of HLA and Nef alleviates need to sort target cells

To avoid the need to sort target cells, we evaluated the strategy of transfecting CEM cells with Nef and HLA-I expression plasmids. In this context, most cells that lack Nef should also be HLA-A*02-negative and thus unable to bind FK10 peptide or contribute to TCR-mediated luminescent signal following co-culture. Target cells were transfected with pHLA-A*02 and either pcDNA3.1-Nef_{SF2}-GFP or empty vector (ΔNef-GFP) prior to pulsing with FK10 or mismatched SL9 control peptide. Co-culture assays were conducted as described in **2.6.4**. Initial characterization of target cells by flow cytometry indicated typical transfection efficiency of >50% and ~60-fold reduction in HLA-A*02 surface expression for cells expressing Nef versus those transfected with ΔNef plasmid (**Figure 2-3A**). Following co-culture, we observed robust luminescent signal in response to FK10 peptide. This signal was maintained when target cells expressed HLA-A*02 alone or in combination with ΔNef plasmid (~10-14 fold higher vs. SL9-pulsed target cells) (**Figure 2-3B**). In contrast, FK10-pulsed target cells transfected with Nef_{SF2} plasmid generated very low signal (~2-fold higher than SL9 control). These results demonstrated that transient co-expression of HLA-I and Nef by target cells allowed detection of Nef-mediated T cell evasion without further isolation of Nef-expressing target cells.

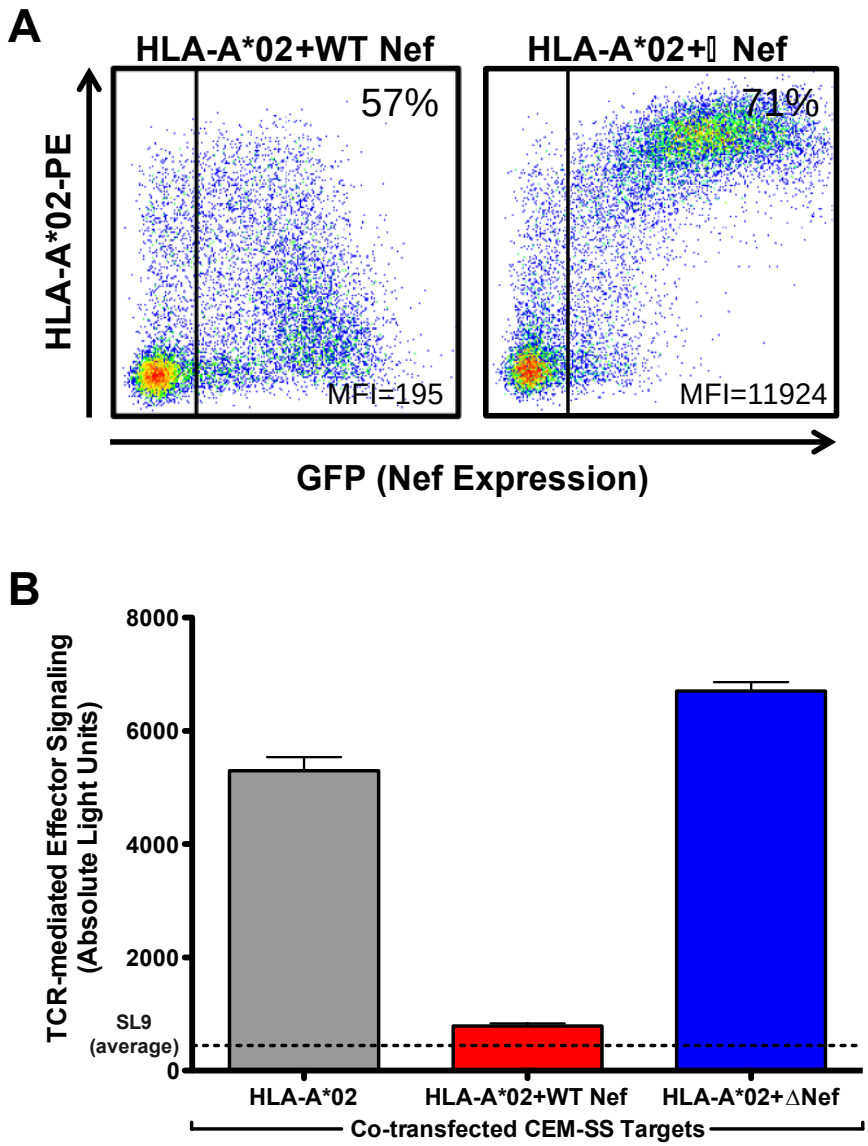

Figure 2-3. Co-transfection of Nef and HLA-A*02 in target cells eliminates the need to sort.
(A) Representative flow plots illustrate untransfected CEM-SS cells (left) and cells co-transfection with plasmids expressing HLA-A*02 and Nef_{SF2} (middle) or HLA-A*02 and ΔNef (right) The median fluorescence intensity (MFI) for HLA-A*02 (phycoerythrin, PE) was calculated using Nef-expressing (GFP+) cells. **(B)** Co-transfected CEM cells were pulsed with FK10 peptide and co-cultured with FK10-specific Jurkat effector cells. Luminescence was measured at 6 hours using the Steady-glo luciferin kit (Promega) on a $CentroXS_3$ plate reader (Berthhold Technologies) and are reported as light units (y-axis). Luciferase results are presented as mean values from 3 co-culture replicates and error bars represent standard error mean (SEM). Dashed line indicates the average background luminescent signal detected following co-culture of effector cells with control target cells pulsed with mismatched SL9 peptide.

2.4.4. Nef modulates recognition of HIV-infected target cells

Finally, we wanted to assess the ability of our method to recognize endogenous peptide antigen presented by HIV-infected cells in the presence or absence of Nef. In this context, uninfected target cells will not present viral peptide and thus should not contribute to TCR-mediated luminescent signal following co-culture with Jurkat effector cells. To do this, we infected GXR25-A*02 cells at an MOI=1 with VSV-g pseudotyped wild type HIV-1 or a ΔNef virus for use as targets in our assay. While not tested directly in these experiments, VSV-g pseudotyped envelope-defective strains or non-pseudotyped viruses could be used and may reduce safety concerns. The GXR25 reporter cell line produces GFP following productive HIV-1 infection through activation of a viral Tat-driven LTR promoter. We observed a high rate of productive infection by both wild type and ΔNef strains, as indicated by >60% of cells expressing GFP and intracellular Gag p24 at 40 hours post-infection **(Figure 2-4A)**. As expected, target cells infected with wild type virus downregulated surface HLA-A*02 to levels ~12-fold lower than that of cells infected with ΔNef (MFI 49 and 594, respectively). Co-culture assays using virus-infected GXR25 target cells were conducted as described in **3.1**. Uninfected GXR25-A*02 target cells and parental GXR25 cells lacking HLA-A*02 were used as additional controls. Co-culture of effector cells with GXR25-A*02 target cells infected with ΔNef generated ~11-fold higher TCR-dependent luminescent signal compared to those infected with wild type virus (673 light units and 59 light units, respectively) **(Figure 2-4B)**. Notably, luminescent signal following co-culture of effector cells with wild type HIV-1-infected GXR25-A*02 target cells was comparable to that of uninfected target cells and virus-infected GXR25 target cells lacking HLA-A*02. Together, these results demonstrate that this reporter T cell assay can be used to detect endogenous antigen presentation by virus-infected target cells, and also illustrate the ability of HIV-1 Nef to counteract T cell recognition.

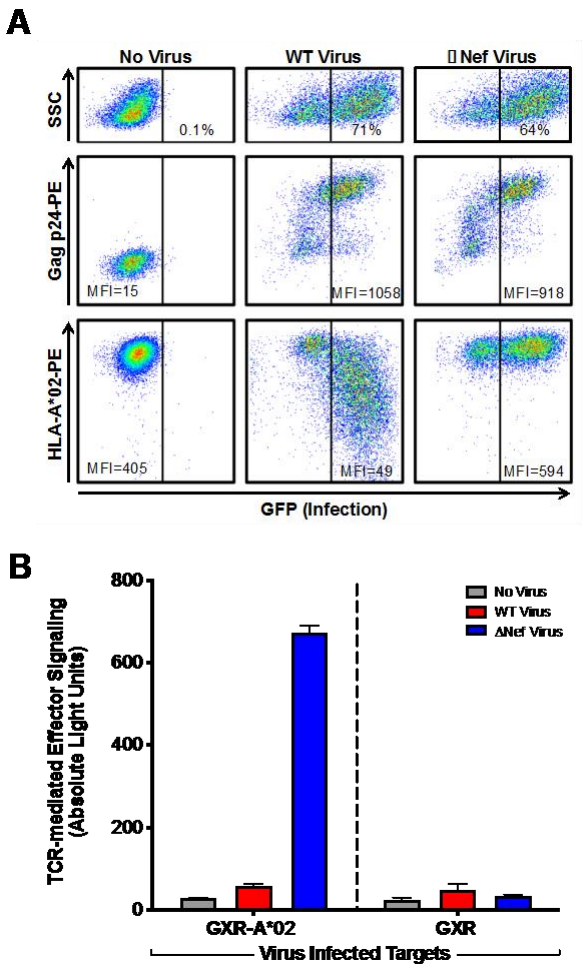

Figure 2-4. TCR+ Jurkat effector cells recognize endogenous FK10 presentation on HLA-A*02+ target cells.

(A) Representative flow plots illustrate the effects of wild type HIV-1 (strain NL4.3) or ΔNef strain on HLA-A*02 surface expression following infection of GXR-A*02 reporter T cells. Twenty hours later, high levels of HIV-1 infection were detected by cellular HIV-1-driven GFP (x-axis) and confirmed by staining for Gag p24 (phycoerythrin, PE) in GFP+ cells (middle panels). The effect of wild type Nef on HLA-A*02 was observed by HLA-A*02-PE cell surface staining. **(B)** GXR-A*02 cells (left panel) or parental GXR25 cells lacking A*02 (right panel) infected with wild type HIV-1 (strain NL4.3) or ΔNef strain, or uninfected control cells, were used as targets for co-culture with FK10-specific Jurkat effector cells. Luminescence was measured at 6 hours using the Steady-glo luciferin kit (Promega) on a Tecan Infinite M200 plate reader and are reported as light units (y-axis) Luciferase results are presented as mean values from 3 co-culture replicates and error bars represent standard error mean (SEM).

A

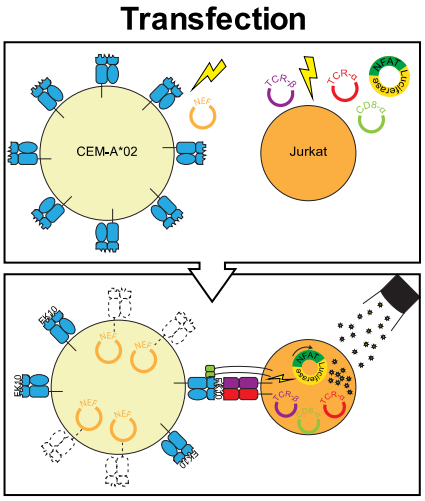
Transfection
CEM-A*02
Jurkat

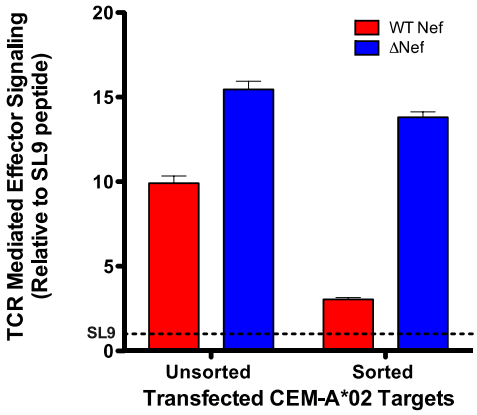
TCR Mediated Effector Signaling
(Relative to SL9 peptide)
WT Nef
ΔNef
20
15
10
5
SL9
0
Unsorted
Sorted
Transfected CEM-A*02 Targets

B

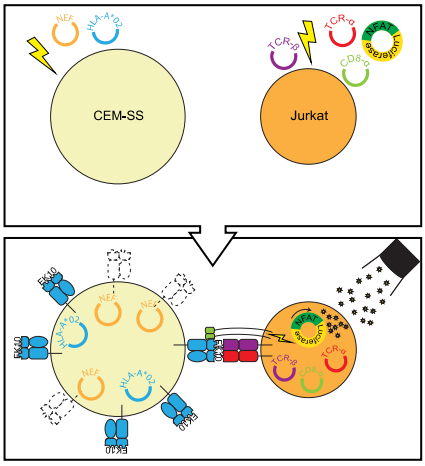
Co-Transfection
CEM-SS
Jurkat

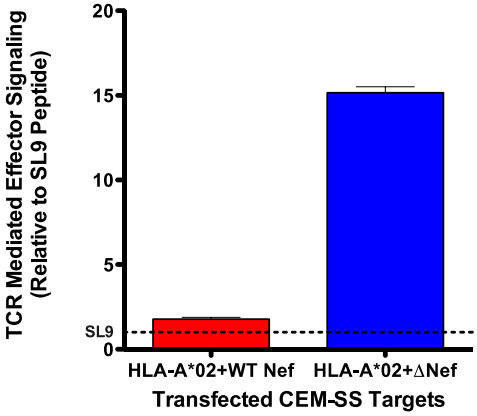
TCR Mediated Effector Signaling
(Relative to SL9 Peptide)
20
15
10
5
SL9
0
HLA-A*02+WT Nef
HLA-A*02+ΔNef
Transfected CEM-SS Targets

C

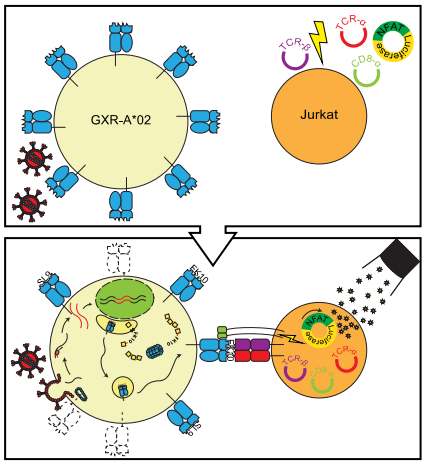
Infection
GXR-A*02
Jurkat

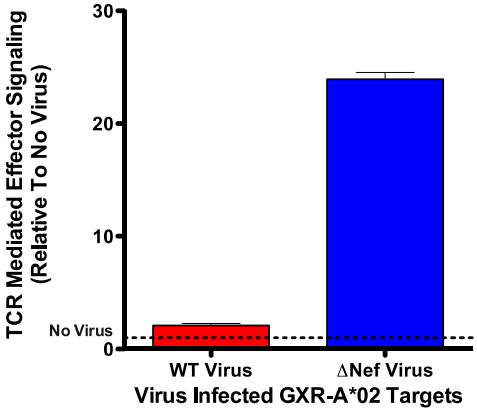
TCR Mediated Effector Signaling
(Relative To No Virus)
30
20
10
No Virus
0
WT Virus
ΔNef Virus
Virus Infected GXR-A*02 Targets

Figure 2-5. Overview of the Jurkat reporter cell assay and its variations. The three methods discussed in this report are illustrated. Target cells and TCR-expressing Jurkat effector cells are shown in beige and orange, respectively. Representative results for Nef-mediated effects on T cell recognition, expressed as fold-change from the negative control, are shown to the right of each panel. **(A)** In the "transfection" approach, HIV-1 Nef was transiently transfected into stable HLA-expressing CEM-A*02 cells, which were sorted based on GFP expression (or unsorted), pulsed with FK10 (or mismatched SL9) peptide and then used as targets for FK10-specific effector cells. Peptide- and HLA-dependent luminescent signal was observed, with a wider dynamic range if target cells were sorted prior to co-culture. However, in both cases the difference between ΔNef and WT Nef was statistically significant (both $p<0.0001$). FK10-specific signal is shown as the fold-change in absolute light units relative to mismatched SL9-pulsed target cells. **(B)** In the "co-transfection" approach, both Nef and HLA-A*02 were introduced into CEM cells, which were pulsed with FK10 or SL9 peptide and then used as targets for FK10-specific effector cells. Using this strategy, strong TCR-dependent signaling was observed without sorting of target cells. FK10-specific signal is shown as fold-change in absolute light units relative to mismatched SL9-pulsed target cells. A significant difference in TCR signaling was observed between target cells expressing HLA-A*02 plus ΔNef and those expressing HLA-A*02 plus WT Nef ($p<0.0001$). **(C)** In the "infection" approach, stable HLA-expressing GXR-A*02 reporter cells were infected with HIV-1 and then used as targets for FK10-specific effector cells. A benefit of this strategy is that it assesses endogenously derived viral peptides complexed with HLA-A*02. Virus-specific effector cell signaling was readily detected when target cells were infected with ΔNef virus, but not when they were infected with wild type HIV, demonstrating the profound ability of Nef to counteract T cell recognition. FK10-specific signal is shown as the fold-change in absolute light units relative to uninfected target cells. The difference between ΔNef virus and WT virus was significant ($p<0.0001$).

2.5. Discussion

In this report, we described a heterologous TCR reporter cell assay to measure the impact of HIV-1 Nef on T cell recognition of a viral antigen. We demonstrated that Jurkat effector cells transiently expressing a TCR isolated from a CTL clone specific for the HLA-A*02-restricted HIV-1 Gag FK10 epitope can specifically respond to target cells expressing this peptide. Importantly, effector cell recognition, measured as NFAT-driven luciferase activity, could be detected as early as 4 hours after co-culture, required HLA-A*02 expression on target cells and was sensitive to peptide dose. Moreover, the TCR-mediated response by effector cells was able to detect both peptide-pulsed as well as endogenous FK10 presented by HIV-infected target cells. Finally, we observed that HIV-1 Nef-mediated downregulation of HLA-I impaired TCR-dependent recognition of target cells in a variety of experimental contexts.

Figure 2-5 illustrates the key features of this assay, including the generation of effector and target cell populations and the role of Nef-mediated HLA-I downregulation on target cells. This method is highly versatile and modifications to the protocol will allow users to alter the TCR, peptide/HLA, and/or Nef sequence of interest. For example, we have adapted this system in our laboratory to study TCR-specific responses directed toward other HIV-1 epitopes, e.g. A*02-restricted Gag SL9 **(Figure 2-1C) and** B*27-restricted Gag KK10 **(Appendix Figure 5-2)** Using the transfection and co-transfection approaches **(Figure 2-5A and B),** target cells expressing different Nef alleles and viral epitopes can be easily explored, since these components are delivered using expression plasmids and exogenous peptides. Alternately, the viral infection approach can be used to examine endogenous peptide presentation (**Figure 2-5C**) by HIV-1 strains encoding diverse viral peptides and Nef variants.

Prior studies from our group have examined the ability of Nef to downregulate HLA-I using transient transfection approaches [29], [38]**.** Our assay extends and complements this method by looking more directly at the effect of HLA downregulation on TCR mediated effector response. While the effector activity of 5B2 TCR correlated linearly to Nef-mediated changes in HLA-A*02 levels **(Figure 2-2C),** the impact of Nef on other TCR, HLA alleles, and/or viral peptides may differ [22]. This method will provide a useful platform to investigate this question in future studies. It has also been observed that high TCR antigen sensitivity is associated with improved ability to control HIV-1 [39]–[41]. It will therefore be important to compare highly active TCR to less active clones in this assay system.

Many studies of Nef's immune evasion activity have used *in vitro* viral suppression assays to measure the replication of HIV-1 strains expressing wild type Nef or variants (such as $M_{20}A$) during co-culture with primary CTL clones (Ali et al., 2005; Collins et al., 1998; Mwimanzi et al., 2011). While these methods have demonstrated the importance of Nef to evade CTL, the assays require multiday co-culture to measure viral outgrowth and the use of primary T cells presents several challenges. *Ex vivo* expansion of CTL can be unreliable given the limited regenerative capacity of primary cells, which may lead to experimental variability. Indeed, CTL exhaustion is frequently observed in the context of chronic HIV-1 infection [43]–[45], resulting in loss of T cell lines during cloning and re-stimulation. The method described here employs more readily available immortalized cell lines, epitope-specific TCR expression plasmids and a

rapid luciferase reporting system, and therefore provides a flexible platform that can be modified according to researcher needs. Specifically, Jurkat effector cells can express any TCR of interest and CEM target cells may be transduced or transfected with any HLA allele of interest and any Nef isolate. The 6-hour detection time and assessment by luminescence allows for rapid measurement of TCR/peptide/HLA interactions following co-culture.

Despite these advantages, some potential limitations of this method merit mention. While we have shown that Jurkat effector cells expressing TCR and CD8 can be used to quantify the evasion activity of Nef in target cells, we have not directly compared them to primary CTL. It is possible that native CTL will display higher antigen sensitivity than transiently transfected Jurkat cells or that native CTL effector functions (e.g. cytolytic activity or cytokine expression) will provide a greater range of function (and thus a more precise measure of Nef evasion activity) than detection of luciferase by Jurkat cells. In addition, all of our experiments used CEM-derived target cell lines. Other cells (including primary cells) are expected to behave similarly, but each should be examined in light of experimental goals. Lastly, the mechanism of Nef-mediated HLA-I downregulation may differ slightly between cell types; indeed, Nef's proline-rich motif (which is mutated in the $A_{72}xxA_{75}$ variant used here) appears to be less important in CEM cells and other PTEN-deficient T cell lines compared to H9 cells or primary CD4+ T cells [46].

Altogether, our results indicate that a transient TCR reporter system can be used as a platform to specifically measure T cell recognition of viral antigen in the context of HIV-1 Nef. The relative simplicity and flexibility of this method may support larger-scale studies of Nef function, such as analysis of patient-derived Nef alleles and small molecule library screens to identify novel Nef inhibitors, and may be applied more broadly to the study of epitope-specific responses to HIV-1 and other pathogens.

2.6. Methods

2.6.1. Reagents

Plasmids and cell lines

The following reagents were obtained through the NIH AIDS Reagents Program, Division of AIDS, NIAID, NIH: pNL4.3 (Cat #114) from Dr. Malcolm Martin [25]; CEM-SS cell line (Cat #776) from Dr. Peter L. Nara [26]; and pHEF-VSVG (Cat #4693) from Dr. Lung-Ji Chang [27].

The CTL clone (5B2) specific for the HLA-A*02-restricted HIV-1 Gag FK10 epitope (FLGKIWPSYK; HIVHXB2 amino acid position 433-442) was isolated from an HIV-infected patient following written informed consent. Research ethics board approval was obtained from the University of Toronto, Canada (by M. Ostrowski). The pMSCV-A*02:01 retroviral vector was a gift from Dr. Christian Brander (IrsiCaixa, Spain). The CEM-derived GXR25 cell line containing an HIV-1 Tat-driven GFP reporter construct has been described previously [28]. Jurkat clone E6-1 cells (TIB-152) were purchased from the American Type Culture Collection; and RetroPack PT67 and HEK-293T cells were purchased from Clontech. Plasmids encoding wild type Nef (SF2 strain) and consensus HIV-1 subtype B or subtype C (2004 sequences, available at http://www.hiv.lanl.gov/content/sequence/NEWALIGN/align.html) were described previously [14], [29]. Other expression plasmids were purchased, as follows: pSELECT-GFPzeo and pORF9-hCD8A (InvivoGen); and pNFAT-Luciferase (Affymetrix).

Jurkat, CEM-SS and RetroPack PT67 cells were maintained in RPMI-1640 medium supplemented with 2mM L-glutamine, 100 U/ml Penicillin and 0.1 mg/ml Streptomycin (all from Sigma-Aldrich, Co.) plus 10% calf serum (Life Technologies, Inc) (R10+). Following HIV-1 infection, T cells were cultured in RPMI-1640 medium containing these supplements plus 20% calf serum (R20+). Cell lines transduced with HLA-A*02:01 or HLA-B*07:02 were maintained in R10+ supplemented with 0.5 µg/mL Puromycin to maintain HLA expression. RPMI-1640 medium lacking phenol red (Sigma-Aldrich, Co.) (R10+_NoPR) was used during co-culture to reduce quenching of luminescent signal. HEK-293T cells were maintained in DMEM (Lonza) containing 4.5 g/L glucose, 2mM L-glutamine, 100 U/ml Penicillin and 0.1 mg/ml Streptomycin, plus

10% calf serum (D10+). All cells were maintained, incubated, peptide pulsed, and co-cultured at 37°C with 5% CO2.

Viral stocks

Viruses were generated by transfection using Lipofectamine 3000 (Life Technologies, Inc.) according to the manufacturer's directions. To prepare retroviral vectors, lipid complexes (0.5 mL) containing 5 µg pMSCV-HLA-A*02:01 and 1 µg pHEF-VSVG in Opti-MEM (Life Technologies, Inc.) were added to RetroPack PT67 cells in a 25 cm2 flask containing 4.5 mL R10+. To prepare VSV-g pseudotyped HIV-1 stocks, lipid complexes (1.5 mL) containing 40 µg of pNL4.3 (containing the HIV-1 subtype B reference strain NL4.3) or pNL4.3□Nef (containing a Nef-deleted NL4.3 variant) plus 4 µg pHEF-VSVG in Opti-MEM were added to HEK-293T cells in a 75 cm2 flask containing 13.5 mL R10+. Cells were incubated for 6 hours, after which media was replaced with fresh R10+. Supernatant was collected at 48 hours post-transfection, cell debris was removed by centrifugation at 500 x g for 10 min, and aliquots were stored at -80°C until use. The infectivity of HIV-1 stocks was determined using GXR25 reporter cells as described previously [28].

2.6.2. Preparation of Jurkat effector T cells

Isolation and cloning of TCR alpha and TCR beta transcripts

Total RNA was extracted from 1 x106 5B2 T cells using the RNeasy Mini kit (Qiagen) and 125 ng RNA was used to prepare cDNA according to the 5' RACE protocol included with the SMARTer cDNA Synthesis Kit (Clontech). TCR cDNAs were amplified by nested PCR using Hi-Fidelity DNA polymerase (Roche) with the following gene-specific reverse primers: 1st round, TCRalpha_RevOutA: 5'-TGT CAG GCA GTG ACA AGC AG, TCRB1_1230: 5'-CCT GAC TGA ATG GGG AGA GTC ACA GGG, or TCRB2_1550: 5'-GAC ACT CCT GAA ATG CAA CCA GGC CC; 2nd round, TCRalpha_RevIn: 5'-CAG CAG TGT TTG GCA GCT CT, TCRB1_1090: 5'-AGA TTT CAG CCG TGA GTG TGC AGG, or TCRB2_1390: 5'-GGA ACA CAG ATT GGG AGC AGG TAC AGG AG. Thermocycler conditions for touchdown PCR were: 5 cycles at (95°C for 30 sec, 72°C for 3min); 5 cycles at (95°C for 30 sec, 70°C for 30 sec, 72°C for 3min); 30 cycles at (95°C for 30 sec, 68°C for 30 sec, 72°C for 3min); 72°C for 7 min. TCR alpha and beta products were confirmed by Sanger sequencing using the BigDye Terminator v3.1 kit on

an 3130xl Genetic Analyzer (Applied Biosystems, Inc.) and cloned into the SgrAI and NheI restriction sites of pSELECT-GFPzeo to generate pSELECT-5B2alpha (TRAV12-2*02; Genbank # KT207830) and pSELECT-5B2beta (TRBV7-2*01; Genbank # KT207831). The alpha and beta genes for TCR clone 868, which is specific for the A*02-restricted HIV-1 Gag SL9 epitope (SLYNTVATL; HIVHXB2 amino acid position 77-85) [30], were synthesized (Integrated DNA Technologies) according to their reported sequences and cloned similarly into pSELECT-GFPzeo.

Transfection of effector cells

Jurkat T cells were pelleted and resuspended at a concentration of 50 x106 cells/mL in Opti-MEM. A total of 10 x 106 cells (in 200 µl) were used for electroporation as follows. Cells were transferred to a 0.4 cm cuvette (Bio-Rad Laboratories, Inc.) containing 3 µg pSELECT-5B2alpha, 3 µg pSELECT-5B2beta, 5 µg pORF9-hCD8A and 10 µg pNFAT-luciferase and transfected using a Gene Pulser MXcellTM or a Gene Pulser XcellTM Electroporation System (Bio-Rad Laboratories, Inc.) with the following square-wave protocol: 250 or 500 V, 2000 µF, 3 msec, and 1 pulse. After a 10 min recovery at room temperature, cells were transferred into 10 mL R10+_NoPR and incubated 16-20 hours prior to use. Identical transfection conditions were used to produce effector cells expressing the 868 TCR (against HIV-1 Gag SL9). Transfection efficiency was assessed by flow cytometry to detect GFP (co-expressed with TCR) and surface expression of CD8 alpha (allophycocyanin (APC)-Cy7; clone SK1, BD Pharmingen).

2.6.3. Preparation of Nef expressing target cells

Construction of stable HLA-expressing CEM and GXR25 cell lines

CEM-SS cells and CEM-derived GXR25 reporter cells were stably transduced to express HLA-A*02:01 using a murine stem cell virus (MSCV; Clontech) retroviral vector. Briefly, 2 x 106 cells were pelleted and resuspended in 1 mL of undiluted retroviral supernatant (from 2.1.2) in a 6-well plate (Sarstedt, Inc.), centrifuged at 800 x g for 1 hour at 37°C, and then incubated for 24 hours. Next, 4 mL of R10+ supplemented with 5 µg/mL Puromycin was added and cells were incubated for an additional 48 hours. Cells were then pelleted and transferred to a 25 cm2 flask containing R10+ supplemented with 1 µg/mL Puromycin to select the vector-transduced population. HLA-A*02 surface expression was confirmed by flow cytometry (phycoerythrin (PE), clone BB7.2; BD

Pharmingen). CEM-SS cells were transduced similarly with HLA-B*07:02 for use as a negative (HLA-mismatched) control.

Transfection of target cells with HIV-1 Nef

CEM-SS derived CEM-A*02 cells were pelleted and re-suspended at a concentration of 50 x106 cells/mL in Opti-MEM, and 200 µL used for electroporation. Cells were transfected with 5 µg pSELECT-GFPzeo encoding either HIV-1 Nef from the reference strain SF2 [31] (NefSF2 ; wild type control), a Nef variant (M20A, A72xxA75, 2004 consensus subtype B or 2004 consensus subtype C), or empty pSELECT-GFPzeo (lacking Nef, negative control). Transfection was performed in a 96-well electroporation plate (Bio-Rad Laboratories, Inc.) using the following square-wave protocol: 250 V, 2000 µF, 25 msec and 1 pulse. After electroporation, cells were recovered for 10 min at room temperature, transferred to a 6 well plate at 2.5 x106/mL in R10+_NoPR and incubated for 20 hours. Cells were then collected, stained for HLA-A*02, and used as target cells in co-culture assays.

In an alternative protocol, HLA-A*02 was expressed transiently. For this, 2 x106 CEM-SS cells (250 µL) were co-transfected with 5 µg pcDNA3.1-HLA-A*02:01 and 5 µg pcDNA3.1-NefSF2-GFP fusion protein [32] or empty pcDNA3.1-GFP (negative control) by electroporation in 0.4 mm cuvettes, with the following Gene Pulser Xcell square-wave conditions: 250 V, 25 ms, and 1 pulse (Bio-Rad Laboratories, Inc). After electroporation, cells were recovered for 10 min at room temperature and then incubated at 2 x106 cells/mL (R10+_NoPR) for 20 hours in a 24 well plate. Cells were then collected, stained for HLA-A*02, and used as target cells in co-culture assays.

Isolation of Nef-transfected target cells

For the indicated experiments, GFPhigh target cells were sorted following electroporation using a BD FACSJazz cytometer to isolate live Nef-expressing cells based on forward and side scatter. In some cases, target cells were also stained using the APC-Annexin V apoptosis detection kit (BioLegend) and GFPhigh/Annexinlow cells were selected by sorting.

Infection of target cells with HIV-1

GXR25-A*02 or parental GXR25 (HLA-A*02-negative control) cells (1 x 106 each) were incubated with VSV-G pseudotyped HIV-1NL4.3 or HIV-1NL4.3-ΔNef in a

24-well plate overnight in a total volume of 500 µL D10+ at an MOI = 1 to achieve a high rate of infection. After 20 hours, 1 mL R20+ was added and cultures were incubated for an additional 24 hours to allow viral protein expression and processing of endogenous viral peptides. Productive HIV-1 infection was confirmed by detection of GFP (induced by the reporter cell) and intracellular Gag protein expression (clone KC57-PE; Beckman Coulter) by flow cytometry. Surface expression of HLA-A*02 was also assessed on HIV-1-uninfected (GFP-negative) and infected (GFP-positive) cells using flow cytometry.

2.6.4. Co-culture and luciferase assays

For peptide pulsed targets, Nef-expressing CEM-A*02 or CEM-SS cells (from 2.3.2) were resuspended in R10+_NoPR at 0.95 x106 cells/mL and 50,000 cells (52.5 µl) were added to each well of a white flat-bottom 96-well plate (Microlite 1+; Thermo). Either 2.1 µg FK10 peptide (an HLA-A*02-restricted HIV-1 Gag peptide recognized by the 5B2 TCR) or SL9 peptide (an HLA-A*02-restricted Gag recognized by the 868 TCR) in 17.5 µL was added to each well and cells were incubated for 1 hour. Virus-infected GXR25 or GXR25-A*02 target cells were re-suspended at 0.7 x106 cells/mL and 50,000 cells (70 µL) was added to each well. Jurkat effector cells were re-suspended at 1.65 x106/mL in R10+_NoPR and 50,000 cells (30 µl) were added to target cells, yielding an E:T ratio of 1:1. Preliminary analyses of E:T ratios ranging from 5:1 to 1:5 indicated that T cell activation could be observed under all conditions, but a 1:1 ratio consistently provided the best TCR-dependent signal versus non-specific background, so this was adopted for all additional studies. As a positive control the co-cultures were stimulated peptide free with phytohaemagglutinin (PHA) at 0.01 mg/mL.

Co-cultures were incubated for 6 hours prior to detection of luminescence using the Steady-glo luciferin kit (Promega). Briefly, 100 µl of luciferin substrate was added directly to each well and luminescence was observed using an Infinite M200 (Tecan) or CentroXS3 (Berthhold Technologies) plate reader with the following conditions: 3000 ms integration and 100 ms settle time.

2.7. Acknowledgements

We thank Vesna Mihajlovic for technical assistance in preparation of the 5B2 CTL clone. This work was supported by The Canadian HIV Cure Enterprise Team Grant (HIG-133050, to MAB) from the Canadian Institutes for Health Research (CIHR) in partnership with the Canadian Foundation for AIDS Research and the International AIDS Society; the Natural Sciences and Engineering Research Council of Canada (to MAB); and an AIDS International Collaborative Research Grant from the Ministry of Education, Science, Sports, and Culture of Japan (to TU). GA currently holds a masters scholarship from Canadian Association of HIV Research (CAHR) and Abbvie. XTK and AQL were supported by Frederick Banting and Charles Best Canada Graduate Scholarships from CIHR. EM was supported by a Master's Scholarship from the CAHR and Abbott Virology. ZLB was supported by a CIHR New Investigator Award and currently holds a Michael Smith Foundation for Health Research (MSFHR) scholar award. MAB holds a Canada Research Chair.

2.8 References

[1] P. Borrow, H. Lewicki, B. H. Hahn, G. M. Shaw, and M. B. Oldstone, “Virus-specific CD8+ cytotoxic T-lymphocyte activity associated with control of viremia in primary human immunodeficiency virus type 1 infection.,” *J. Virol.*, vol. 68, no. 9, pp. 6103–6110, 1994.

[2] J. T. Safrit, C. a Andrews, T. Zhu, D. D. Ho, and R. a Koup, “Characterization of human immunodeficiency virus type 1-specific cytotoxic T lymphocyte clones isolated during acute seroconversion: recognition of autologous virus sequences within a conserved immunodominant epitope.,” *J. Exp. Med.*, vol. 179, no. 2, pp. 463–472, 1994.

[3] R. A. Koup *et al.*, “Temporal association of cellular immune responses with the initial control of viremia in primary human immunodeficiency virus type 1 syndrome.,” *J. Virol.*, vol. 68, no. 7, pp. 4650–5, Jul. 1994.

[4] a J. McMichael and R. E. Phillips, “Escape of human immunodeficiency virus from immune control.,” *Annu. Rev. Immunol.*, vol. 15, pp. 271–296, 1997.

[5] H. W. Kestler *et al.*, “Importance of the nef gene for maintenance of high virus loads and for development of AIDS,” *Cell*, vol. 65, no. 4, pp. 651–662, 1991.

[6] K. K. Ariën and B. Verhasselt, “HIV Nef: role in pathogenesis and viral fitness.,” *Curr. HIV Res.*, vol. 6, no. 3, pp. 200–208, 2008.

[7] K. L. Collins, B. K. Chen, S. a Kalams, B. D. Walker, and D. Baltimore, “HIV-1 Nef protein protects infected primary cells against killing by cytotoxic T lymphocytes.,” *Nature*, vol. 391, no. 6665, pp. 397–401, 1998.

[8] O. O. Yang *et al.*, “Nef-mediated resistance of human immunodeficiency virus type 1 to antiviral cytotoxic T lymphocytes,” *J. Virol.*, vol. 76, no. 4, pp. 1626–1631, 2002.

[9] S. Adnan *et al.*, “Nef interference with HIV-1-specific CTL antiviral activity is epitope specific,” *Blood*, vol. 108, no. 10, pp. 3414–3419, 2006.

[10] G. Corró *et al.*, “Gene Derived from Long-Term Nonprogressor Children: Association of Attenuated Variants with Slow Progression to Pediatric AIDS,” *AIDS Res. Hum. Retroviruses*, vol. 28, no. 12, p. 120625113303009, 2012.

[11] N. J. Deacon *et al.*, “Genomic structure of an attenuated quasi species of HIV-1 from a blood transfusion donor and recipients.,” *Science*, vol. 270, no. 5238, pp. 988–91, Nov. 1995.

[12] J. C. Learmont *et al.*, “Immunologic and virologic status after 14 to 18 years of infection with an attenuated strain of HIV-1. A report from the Sydney Blood Bank Cohort.,” *N. Engl. J. Med.*, vol. 340, no. 22, pp. 1715–22, Jun. 1999.

[13] F. Kirchhoff, T. C. Greenough, D. B. Brettler, J. L. Sullivan, and R. C. Desrosiers, “Brief report: absence of intact nef sequences in a long-term survivor with nonprogressive HIV-1 infection.,” *N. Engl. J. Med.*, vol. 332, no. 4, pp. 228–32, Jan. 1995.

[14] P. Mwimanzi *et al.*, “Attenuation of multiple Nef functions in HIV-1 elite

controllers.," *Retrovirology*, vol. 10, no. 1, p. 1, Jan. 2013.

[15] P. Shankar, Z. Xu, and J. Lieberman, "Viral-specific cytotoxic T lymphocytes lyse human immunodeficiency virus-infected primary T lymphocytes by the granule exocytosis pathway.," *Blood*, vol. 94, no. 9, pp. 3084–3093, 1999.

[16] O. O. Yang *et al.*, "Efficient lysis of human immunodeficiency virus type 1-infected cells by cytotoxic T lymphocytes.," *J. Virol.*, vol. 70, no. 9, pp. 5799–5806, 1996.

[17] A. Ali, H. L. Ng, M. D. Dagarag, and O. O. Yang, "Evasion of cytotoxic T lymphocytes is a functional constraint maintaining HIV-1 Nef expression," *Eur. J. Immunol.*, vol. 35, no. 11, pp. 3221–3228, 2005.

[18] H. Akari, S. Arold, T. Fukumori, T. Okazaki, K. Strebel, and a Adachi, "Nef-induced major histocompatibility complex class I down-regulation is functionally dissociated from its virion incorporation, enhancement of viral infectivity, and CD4 down-regulation.," *J. Virol.*, vol. 74, no. 6, pp. 2907–2912, 2000.

[19] H. Tomiyama, H. Akari, A. Adachi, and M. Takiguchi, "Different effects of Nef-mediated HLA class I down-regulation on human immunodeficiency virus type 1-specific CD8(+) T-cell cytolytic activity and cytokine production.," *J. Virol.*, vol. 76, no. 15, pp. 7535–43, 2002.

[20] T. Ueno *et al.*, "CTL-mediated selective pressure influences dynamic evolution and pathogenic functions of HIV-1 Nef.," *J. Immunol.*, vol. 180, no. 2, pp. 1107–1116, 2008.

[21] U. S. Rajapaksa, D. Li, Y.-C. Peng, a. J. McMichael, T. Dong, and X.-N. Xu, "HLA-B may be more protective against HIV-1 than HLA-A because it resists negative regulatory factor (Nef) mediated down-regulation," *Proc. Natl. Acad. Sci.*, vol. 109, no. 33, pp. 13353–13358, 2012.

[22] D. Y. Chen, A. Balamurugan, H. L. Ng, W. G. Cumberland, and O. O. Yang, "Epitope targeting and viral inoculum are determinants of Nef-mediated immune evasion of HIV-1 from cytotoxic T lymphocytes.," *Blood*, vol. 120, no. 1, pp. 100–11, Jul. 2012.

[23] N. Schaft, B. Lankiewicz, J. W. Gratama, R. L. H. Bolhuis, and R. Debets, "Flexible and sensitive method to functionally validate tumor-specific receptors via activation of NFAT," *J. Immunol. Methods*, vol. 280, no. 1–2, pp. 13–24, 2003.

[24] K. Birkholz *et al.*, "A fast and robust method to clone and functionally validate T-cell receptors," *J. Immunol. Methods*, vol. 346, no. 1–2, pp. 45–54, 2009.

[25] a Adachi *et al.*, "Production of acquired immunodeficiency syndrome-associated retrovirus in human and nonhuman cells transfected with an infectious molecular clone.," *J. Virol.*, vol. 59, no. 2, pp. 284–291, 1986.

[26] P. L. Nara *et al.*, "Simple, rapid, quantitative, syncytium-forming microassay for the detection of human immunodeficiency virus neutralizing antibody.," *AIDS Res. Hum. Retroviruses*, vol. 3, no. 3, pp. 283–302, 1987.

[27] L. J. Chang, V. Urlacher, T. Iwakuma, Y. Cui, and J. Zucali, "Efficacy and safety analyses of a recombinant human immunodeficiency virus type 1 derived vector system.," *Gene Ther.*, vol. 6, no. 5, pp. 715–728, 1999.

[28] M. A. Brockman, G. O. Tanzi, B. D. Walker, and T. M. Allen, "Use of a novel GFP reporter cell line to examine replication capacity of CXCR4- and CCR5-tropic HIV-1 by flow cytometry.," *J. Virol. Methods*, vol. 131, no. 2, pp. 134–42, Feb. 2006.

[29] J. K. Mann *et al.*, “Ability of HIV-1 Nef to downregulate CD4 and HLA class I differs among viral subtypes.,” *Retrovirology*, vol. 10, no. April, p. 100, 2013.

[30] A. Varela-Rohena *et al.*, “Control of HIV-1 immune escape by CD8 T cells expressing enhanced T-cell receptor.,” *Nat. Med.*, vol. 14, no. 12, pp. 1390–5, Dec. 2008.

[31] J. A. Levy, A. D. Hoffman, S. M. Kramer, J. A. Landis, J. M. Shimabukuro, and L. S. Oshiro, “Isolation of lymphocytopathic retroviruses from San Francisco patients with AIDS.,” *Science*, vol. 225, no. 4664, pp. 840–2, Aug. 1984.

[32] T. Ueno, Y. Idegami, C. Motozono, S. Oka, and M. Takiguchi, “Altering effects of antigenic variations in HIV-1 on antiviral effectiveness of HIV-specific CTLs.,” *J. Immunol.*, vol. 178, no. 9, pp. 5513–5523, 2007.

[33] C. a. Aarnoudse, M. Krüse, R. Konopitzky, N. Brouwenstijn, and P. I. Schrier, “TCR reconstitution in Jurkat reporter cells facilitates the identification of novel tumor antigens by cDNA expression cloning,” *Int. J. Cancer*, vol. 99, no. October 2001, pp. 7–13, 2002.

[34] N. Schaft *et al.*, “A new way to generate cytolytic tumor-specific T cells: Electroporation of RNA coding for a T cell receptor into T lymphocytes,” *Cancer Immunol. Immunother.*, vol. 55, pp. 1132–1141, 2006.

[35] O. Schwartz, V. Maréchal, S. Le Gall, F. Lemonnier, and J. M. Heard, “Endocytosis of major histocompatibility complex class I molecules is induced by the HIV-1 Nef protein.,” *Nat. Med.*, vol. 2, no. 3, pp. 338–42, Mar. 1996.

[36] M. E. Greenberg, a. J. Lafrate, and J. Skowronski, “The SH3 domain-binding surface and an acidic motif in HIV-1 Nef regulate trafficking of class I MHC complexes,” *EMBO J.*, vol. 17, no. 10, pp. 2777–2789, 1998.

[37] J. K. Mann *et al.*, “Ability of HIV-1 Nef to downregulate CD4 and HLA class I differs among viral subtypes.,” *Retrovirology*, vol. 10, no. April, p. 100, 2013.

[38] X. T. Kuang *et al.*, “Impaired Nef function is associated with early control of HIV-1 viremia.,” *J. Virol.*, vol. 88, no. 17, pp. 10200–10213, 2014.

[39] M. C. Iglesias *et al.*, “Escape from highly effective public CD8 + T-cell clonotypes by HIV Escape from highly effective public CD8 ⊇ T-cell clonotypes by HIV,” vol. 118, no. 8, pp. 2138–2149, 2011.

[40] K. Ladell *et al.*, “A Molecular Basis for the Control of Preimmune Escape Variants by HIV-Specific CD8+ T Cells,” *Immunity*, vol. 38, no. 3, pp. 425–436, 2013.

[41] A. Lissina *et al.*, “The link between CD8+ T-cell antigen-sensitivity and HIV-suppressive capacity depends on HLA restriction, target epitope and viral isolate.,” *AIDS*, vol. 28, no. 4, pp. 477–86, 2014.

[42] P. Mwimanzi, Z. Hasan, R. Hassan, S. Suzu, M. Takiguchi, and T. Ueno, “Effects of naturally-arising HIV Nef mutations on cytotoxic T lymphocyte recognition and Nef’s functionality in primary macrophages.,” *Retrovirology*, vol. 8, no. 1, p. 50, 2011.

[43] O. O. Yang, H. Lin, M. Dagarag, H. L. Ng, R. B. Effros, and C. H. Uittenbogaart, “Decreased perforin and granzyme B expression in senescent HIV-1-specific cytotoxic T lymphocytes,” *Virology*, vol. 332, no. 1, pp. 16–19, 2005.

[44] B. Youngblood, E. J. Wherry, and R. Ahmed, “Acquired transcriptional programming in functional and exhausted virus-specific CD8 T cells,” *Curr. Opin.*

HIV AIDS, vol. 7, no. 1, pp. 50–57, 2012.

[45] M. Cella *et al.*, “NIH Public Access,” vol. 40, no. 4, pp. 949–954, 2011.

[46] J. D. Dikeakos *et al.*, “Small molecule inhibition of HIV-1-induced MHC-I down-regulation identifies a temporally regulated switch in Nef action.,” *Molecular biology of the cell*, vol. 21, no. 19. pp. 3279–3292, 2010.

Chapter 3. Dual HLA B*42 and B*81-reactive T cell receptors recognize more diverse HIV-1 Gag escape variants

This chapter is adapted from the following published article of which I am a co-first author.

Ogunshola F.*, Anmole G.*, Miller R. L., Goering E., Nkosi T., Muema D., Mann J., Ismail N., Chopera D., Ndung'u T., Brockman M.A.*, and Ndhlovu Z. M.* (2018). Dual HLA B*42 and B*81-reactive T cell receptors recognize more diverse HIV-1 Gag escape variants. *Nature communications, 9*(1), 5023-5023.

3.1. Contributions

Gursev Anmole and Funsho Ogunshola contributed equally to this study as co-first authors. Mark Brockman and Zaza Ndhlovu contributed equally to this study as co-senior authors and co-corresponding authors. I use terms "we" and "our" since I did not complete all the work presented in **Chapter 3.** My roles in this study were: (1) to design and conduct all TCR sequencing experiments **(Figure 3-3)**; (2) to isolate and synthesize paired TCR alpha/beta clones **(Figure 3-4);** (3) to assess the *in vitro* function of all TCR clones, including their reactivity to TL9 variants **(Figures 3-4 and 3-5)**; (4) to analyze all TCR function data and generate summary figures **(Figure 3-6)**; and (5) to generate all data described in **Appendix Figures 3-3, 3-4** and **Appendix Tables 3-2 and 3-3**. Rachel Miller provided technical assistance for TCR data collection, under my direction. Other co-authors contributed minor technical assistance (E.G., T.Nk., D.M., J.M., N.I., D.C.), access to HIV specimens (T.Nd.) or supervision and mentorship (M.A.B., Z.M.N.).

3.2. Abstract

Some closely related human leukocyte antigen (HLA) alleles are associated with variable clinical outcomes following HIV-1 infection despite presenting the same viral epitopes. Mechanisms underlying these differences remain unclear but may be due to intrinsic characteristics of the HLA alleles or responding T cell repertoires. Here we examine $CD8_+$ T cell responses against the immunodominant HIV-1 Gag epitope TL9 ($TPQDLNTML_{180-188}$) in the context of the protective allele B*81:01 and the less protective allele B*42:01. We observe a population of dual-reactive T cells that recognize TL9 presented by both B*81:01 and B*42:01 in individuals lacking one allele. The presence of dual-reactive T cells is associated with lower plasma viremia, suggesting a clinical benefit. In B*42:01 expressing individuals, the dual-reactive phenotype defines public T cell receptor (TCR) clones that recognize a wider range of TL9 escape variants, consistent with enhanced control of viral infection through containment of HIV-1 sequence adaptation.

3.3 Introduction

The rate of clinical progression following human immunodeficiency virus type 1 (HIV-1) infection is variable, with rare individuals maintaining plasma viral loads below 50 RNA copies mL^{-1} in the absence of therapy [1, 2]. Host and viral mechanisms associated with relative control of infection indicate that the ability of HIV-1 to adapt to a new host is a critical determinant of pathogenesis [3, 4]. Multiple lines of evidence support the central role of $CD8_+$ T cells in this process [5-7]. Expression of certain class I human leukocyte antigen (HLA) alleles, particularly at the HLA-B locus [8, 9], is associated with lower plasma viral loads, higher $CD4_+$ T cell counts and delayed onset of AIDS [10, 11]. Interaction between $CD8_+$ T cells and viral peptide epitopes presented on HLA determines breadth and other characteristics of the antiviral response [12, 13], while rapid development of viral mutations in targeted epitopes facilitates evasion from host immunity [3, 14, 15]. $CD8_+$ T cells that target epitopes derived from p24 Gag are associated with better control [16, 17], likely due to their relative immunodominance and greater fitness constraints on this major viral structural protein [15, 18-20].

Recognition of a peptide/HLA (pHLA) ligand by a $CD8_+$ T cell is determined by the sequence and functional characteristics of its T cell receptor (TCR) [21, 22]. The exceptional diversity of the TCR repertoire, generated by somatic recombination of variable (V), diversity (D), and joining (J) gene segments, junctional modifications, and differential pairing of α and β chains, has profound implications for immune coverage [23]. In addition to defining antigen specificity, TCR affinity for pHLA can dictate the strength of intracellular signaling events that modulate T cell effector functions, including cytotoxicity and proliferative capacity [24]. Characteristics of TCR clonotypes that contribute most effectively to $CD8_+$ T cell-mediated control of HIV-1 infection are largely unknown, since data linking individual TCR sequences with measures of antiviral function remains limited. In previous studies of p24 Gag epitopes TW10 ($TSTLQEQIGW_{240-249}$) and KK10 ($KRWIILGLNK_{263-272}$), presented on protective HLA alleles B*57:01 and B*27:05, respectively, $CD8_+$ T cell clones displaying higher functional avidity or greater ability to cross-recognize epitope variants were shown to have enhanced antiviral activity [25-28]. In the case of B*27-KK10, public TCR clonotypes, defined as having identical (or nearly identical) TCR β sequences in the antigen-specific repertoire of at least two unrelated individuals [22, 29], displaying high avidity against the consensus epitope were also associated with a more effective T cell response [28, 30].

Following infection with HIV-1 subtype C strains that are prevalent in sub-Saharan Africa, expression of HLA allele B*81:01 is associated with improved clinical outcomes [9, 31], while the genetically-related allele B*42:01 is less protective [16, 31-36]. Both alleles belong to the HLA B7 supertype [37, 38] and present similar viral peptides, including the immunodominant p24 Gag epitope TL9 ($TPQDLNTML_{180-188}$) [34, 39-42]. The magnitude of the TL9 response has been associated with lower plasma viremia and improved clinical outcome in the case of B*81:01 [43]. TL9 is located on helix 3 of the p24 protein, which is critical to form the mature viral capsid. Circulating subtype C strains display >99% sequence identity at all TL9 residues except positions 3 (88.5%) and 7 (93.5%) (HIV Databases; www.hiv.lanl.gov). Positions 3 and 7 are the principal sites for viral escape from $CD8_+$ T cell pressure [3, 40, 41, 44]; however, mutations at these residues also impair fitness [45], indicating that HIV-1 adaptation at TL9 must balance these counteracting pressures. Structural studies indicate that the TL9 residues exposed to T cells differ in its bound conformations with B*81:01 and B*42:01

[46], and some evidence suggests that enhanced antiviral T cell function is related to distinct TCR sequences elicited in the context of B*81:01 [40]. These observations are consistent with delayed viral escape in B*81:01 expressing individuals compared to B*42:01 expressing individuals [44] and selection of TL9 escape mutations by B*81:01 that tend to be more difficult to compensate for [45]. An improved understanding of clonotypic differences among CD8+ T cells responding to TL9 could highlight features that contribute to HIV-1 control in the context of B*81:01 and B*42:01.

Here we investigate the mechanisms associated with immune-mediated control of HIV-1 subtype C infection by examining the CD8+ T cell response to the immunodominant p24 Gag epitope TL9 in virus-infected individuals expressing HLA B*81:01 or B*42:01 alleles. We identify a subset of T cells that recognize TL9 epitope presented on both B*81:01 and B*42:01 alleles, despite individuals lacking one allele. The presence of a dual-reactive T cell population is associated with lower plasma viral loads after controlling for differences in HLA expression. Notably, the dual-reactive population in B*42:01 expressing individuals is dominated by several public TCR clonotypes that encoded *TRBV12-3*. In contrast, while mono- and dual-reactive populations in B*81:01 expressing individuals are enriched for *TRBV12-3* usage, no public clonotypes are observed. Comprehensive *in vitro* functional analyses of selected TCR clones demonstrated that B*81:01-derived clones and public dual-reactive B*42:01-derived clones display greater ability to cross-recognize HIV-1 Gag TL9 escape pathways compare to mono-reactive TCR clones isolated from B*42:01 expressing individuals. These results illustrate a use of HLA-tetramers and *in vitro* functional assays to identify and characterize TCR clonotypes that display enhanced ability to recognize a rapidly evolving HIV-1 infection.

3.4. Results

3.4.1. Characterizing CD8+ T cell responses in study participants

Population-level studies have demonstrated that HLA-B*81:01 is associated with better control of HIV-1 subtype C infection than the closely related allele B*42:01 [3, 9]; however, mechanisms to explain this remain unclear. To examine this, we recruited 21 treatment-naïve HIV-infected individuals expressing B*81:01 (n = 9), B*42:01 (n = 11), or both alleles (n = 1) from Durban, South Africa. Individuals co-expressing other protective

class I HLA alleles (namely B*57:03, B*58:01 and B*39:01) were excluded from this study. The clinical characteristics and class I HLA genotypes of participants are shown in **Table 3-1 and 3-2**, respectively. Consistent with prior reports [40, 47, 48], we observed that untreated B*81:01 expressing individuals displayed lower plasma viral loads (median 3.38 log_{10} RNA copies ml^{-1} [IQR 2.36-3.99]) compared to untreated B*42:01 expressing individuals (4.15 log_{10} RNA copies ml^{-1} [IQR 3.40-4.84]) (p=0.03, Mann-Whitney U-test) (**Figure 3-1A**). The difference in CD4 counts between groups was not statistically significant (median 625 cells μl^{-1} in B*81:01 vs. 555 cells μl^{-1} in B*42:01; p = 0.14, Mann-Whitney U-test). While the individual who co-expressed HLA-B*81:01 and B*42:01 alleles was not included in our analysis of clinical correlations, this participant displayed the lowest plasma viral load (2.11 log_{10} RNA copies ml^{-1}) and highest CD4 count (1,002 cells μl^{-1}).

HLA	B*81:01/B*42:01	B*81:01	B*42:01	(B*81:01 vs B*42:01) Pvalue
n	1	9	11	N/A
Female n (%)	1 (100%)	7 (77.8%)	10 (90.9%)	0.57[b]
Age (yr)	24	22.5 (22.25-28.5)[a]	22 (20.5-28.5) [a]	0.75[c]
CD4 counts, cells/mm^3	1002	625 (495-802) [a]	588 (479-673) [a]	0.14[c]
Viral load, log_{10} RNA copies/ml	2.11	3.38 (2.36-3.99) [a]	4.15 (3.40-4.84) [a]	0.03[c]

[a] Values expressed as median (interquartile range)
[b]Statistical test used: Fisher's exact test
[c]Statistical test used: Mann Whitney test
Excluded alleles: HLA-B*57:03; B*58:01; B*39:01
N/A means not applicable

Table 3-1. Demographic and clinical characteristics of the study participants.

All values in parenthesis were expressed as inter-quartile range. Participants with other protective alleles present in the cohort of study were excluded in the study.

Participants	HLA-A	HLA-B	HLA-C
PT1	33:03/34:02	53:01/81:01	04:01/04:01
PT2	02:00/34:00	14:01/81:01	08:00/08:00
PT3	01:01/30:01	81:01/81:01	04:01/18:00
PT4	23:01/29:02	53:01/42:01	03:04/17:00
PT5	30:01/34:02	35:01/42:01	02:10/17:01
PT6	43:01/74:01	57:01/81:01	04:01/07:01
PT7	01:01/29:11	13:02/81:01	06:02/18:01
PT8	01:01/29:02	45:01/81:01	06:02/18:01
PT9	23:01/68:02	14:02/81:01	08:02/18:00
PT10	02:05/33:01	42:01/58:02	07:01/17:01
PT11	29:02/29:02	42:01/45:01	06:02/17:01
PT12	26:01/30:02	15:18/42:01	17:01/18:00
PT13	30:01/32:01	42:01/58:02	06:02/17:01
PT14	02:01/30:01	42:01/45:07	16:01/17:01
PT15	01:01/74:01	35:01/81:01	04:01/18:01
PT16	02:05/29:02	42:01/45:07	16:01/17:01
PT17	29:01/30:01	15:22/42:01	04:01/17:01
PT18	30:01/68:02	14:02/42:01	08:02/17:01
PT19	23:01/30:01	42:01/57:02	07:01/17:00
PT20	02:00/34:00	14:01/81:01	08:00/08:00
PT21	30:01/68:01	42:01/81:01	04:01/17:01

Table 3-2. Detail class I HLA profiles of the study participants.

Immune targeting of dominant CD8+ T cell epitopes contributes to long-term suppression of HIV-1 viremia [49-51]. The p24 Gag-derived epitope TL9 is immunodominant in both B*81:01 and B*42:01 expressing individuals [39, 40], and the magnitude of the TL9 response has been associated with improved clinical outcome in the context of B*81:01 [43]. To characterize the TL9 response in our cohort, we quantified antigen-specific CD8+ T cells using B*81:01 and B*42:01 tetramers. We observed no difference in the frequency of tetramer+ CD8+ T cells between individuals expressing B*81:01 (median 2.08%) compared to B*42:01 (1.14%) (p=0.50; Student's T test) **(Figure 3-1B).** Notably, intra-patient comparison of responses in either B*81:01 or B*42:01 participants showed that TL9 was the most dominant response compared to other responses (p=<0.0001, Student's T test) by both tetramer staining and ELISPOT **(Appendix Figure 3-1A-C and Appendix Table 3-1)**. These data are consistent with previous studies [40, 46]. The proportion of TL9-specific CD8+ T cells expressing IFN-γ following peptide stimulation was also not significantly different between individuals expressing B*81:01 (median 47%) and B*42:01 (27%) (p=0.09, Student's T test) **(Figure 3-1C)**; however, the observed trend in favor of B*81:01 participants is consistent with prior work describing moderately higher TL9-specific IFN-γ secretion and higher functional avidity in the context of B*81:01 [40].

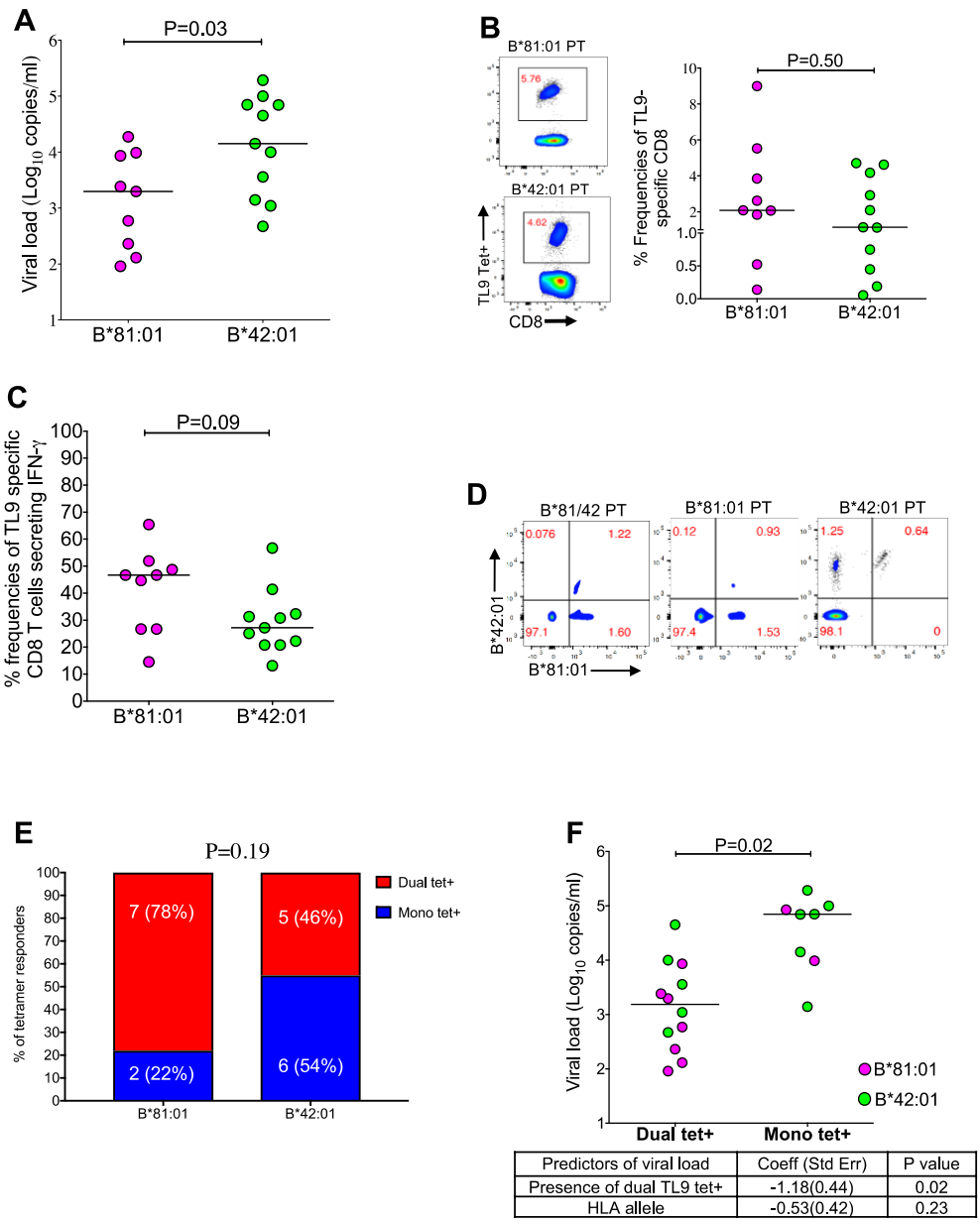

Predictors of viral load	Coeff (Std Err)	P value
Presence of dual TL9 tet+	-1.18(0.44)	0.02
HLA allele	-0.53(0.42)	0.23

Figure 3-1. A dual TL9 tetramer+ response is associated with lower plasma viral load.

A comparative analysis indicated lower plasma viral loads (log_{10}) among participants expressing B*81:01 compared to participants expressing B*42:01 (p=0.03, Mann-Whitney U-test test) (**A**). Representative flow plots display TL9 tetramer responses observed in one B*81:01 expressing individual (top) and one B*42:01 expressing individual (bottom). A comparative analysis of TL9 tetramer+ frequencies observed no difference between participants expressing B*81:01 compared to those expressing B*42:01 (p=0.5; Mann-Whitney U-test) (**B**). A comparative analysis of IFN-γ secretion following stimulation with TL9 peptide indicated a trend towards higher activity among individuals expressing B*81:01 versus B*42:01 (p=0.09, Mann-Whitney U-test) (**C**). Representative flow plots display the dual TL9 tetramer-reactive T cell population in

B*81/42:01 expressing participant, one B*81:01 expressing participant and one B*42:01 expressing participant (**D**). A higher proportion of B*81:01 expressing participants displayed dual tetramer reactivity (p=0.19, Chi-square test) (**E**). Multivariable linear regression analyses that included HLA allele and presence of dual tetramer-reactive T cells as independent variables indicated that dual-reactivity (p=0.02) but not HLA (p=0.23) was a significant determinant of plasma viral load (**F**). Data and figure provided by F. Ogunshola.

3.4.2 Dual HLA reactivity is associated with lower viral load

To investigate if there were any qualitative differences in TL9-specific CD8+ T cells restricted by these two HLA alleles, we first made a direct comparison between antigen-specific T cells in the individual who co-expressed B*81:01 and B*42:01. Intriguingly, when we double-stained cells from this individual with both HLA tetramers, we observed a dominant T cell subset that was labelled using the B*81:01-TL9 tetramer as well as a secondary subset that was labelled by both B*81:01-TL9 and B*42:01-TL9 tetramers, which we will refer to as the dual-reactive population **(Figure 3-1D)**.

To explore whether the dual-reactive T cell population was unique to this individual, we re-examined all study participants using both class I HLA tetramers. We observed dual-reactive TL9 responses in the majority of participants, indicating that a subset of CD8+ T cells elicited in the context of both B*81:01 and B*42:01 could cross-recognize TL9 bound to the other class I HLA allele, even when it was not expressed by the host. Representative results for two individuals are also shown in **Figure 3-1D**. The dual-reactive population was seen more frequently in individuals expressing B*81:01 (7 of 9; 78%) compared to B*42:01 (5 of 11; 46%) **(Figure 3-1E)**, but this difference was not statistically significant (p=0.19, Student's T test). While CD8+ T cell promiscuity is frequently observed towards peptide variants presented on the same HLA allele, we know of only one prior report that described CD8+ T cell cross-reactivity to the same peptide presented on two different class I HLA alleles [52]. In a multivariable linear regression model, we identified dual-reactivity, but not HLA, as a significant independent predictor of lower plasma viral load in our participants (p=0.02) **(Figure 3-1F)**, suggesting that this T cell phenotype is associated with a clinical benefit. We therefore hypothesized that features associated with dual-reactive CD8+ T cells could provide insight into mechanisms of HIV-1 control.

3.4.3 Constrained Vβ genes in B*42-derived dual-reactive TCR

The ability of dual-reactive CD8+ T cells to recognize TL9 bound to different, albeit related, class I HLA alleles suggested that they harbored distinct characteristics. Since individual TCR clonotypes have been associated with improved control of HIV-1 [26-28, 53-56], we analyzed the TCR repertoire found in mono- and dual-reactive TL9-specific T cells. First, we investigated TCR β expression using flow cytometry by co-staining PBMC with B*81:01- and B*42:01-TL9 tetramers plus a cocktail of Vβ-specific antibodies. Representative results for one B*42:01 expressing individual are shown in **Figure 3-2A**. Consistent with prior studies that described a high frequency of *TRBV12-3* gene usage among TL9-specific T cells [40, 41], we observed that both mono- and dual-reactive T cells from B*81:01 expressing individuals were highly enriched for Vβ 12-3/12-4 **(Figure 3-2B)**. In contrast, while mono-reactive T cells from B*42:01 individuals expressed multiple Vβ families, the dual-reactive T cells from these individuals were highly enriched for Vβ 12-3/12-4 **(Figure 3-2C)**. These results suggested that TCR clonotypes expressed by dual-reactive CD8+ T cells elicited in the context of HLA B*42:01 shared distinct features with T cells that dominated TL9 responses elicited by the more protective B*81:01 allele. To confirm these observations, we sorted mono- and dual-reactive T cells using FACS and generated separate TL9-specific cell lines. Similar Vβ staining profiles were observed following *ex vivo* expansion **(Appendix Figure 3-2)**, confirming that dual-reactive T cells were a *bona fide* population and not an artifact of tetramer staining.

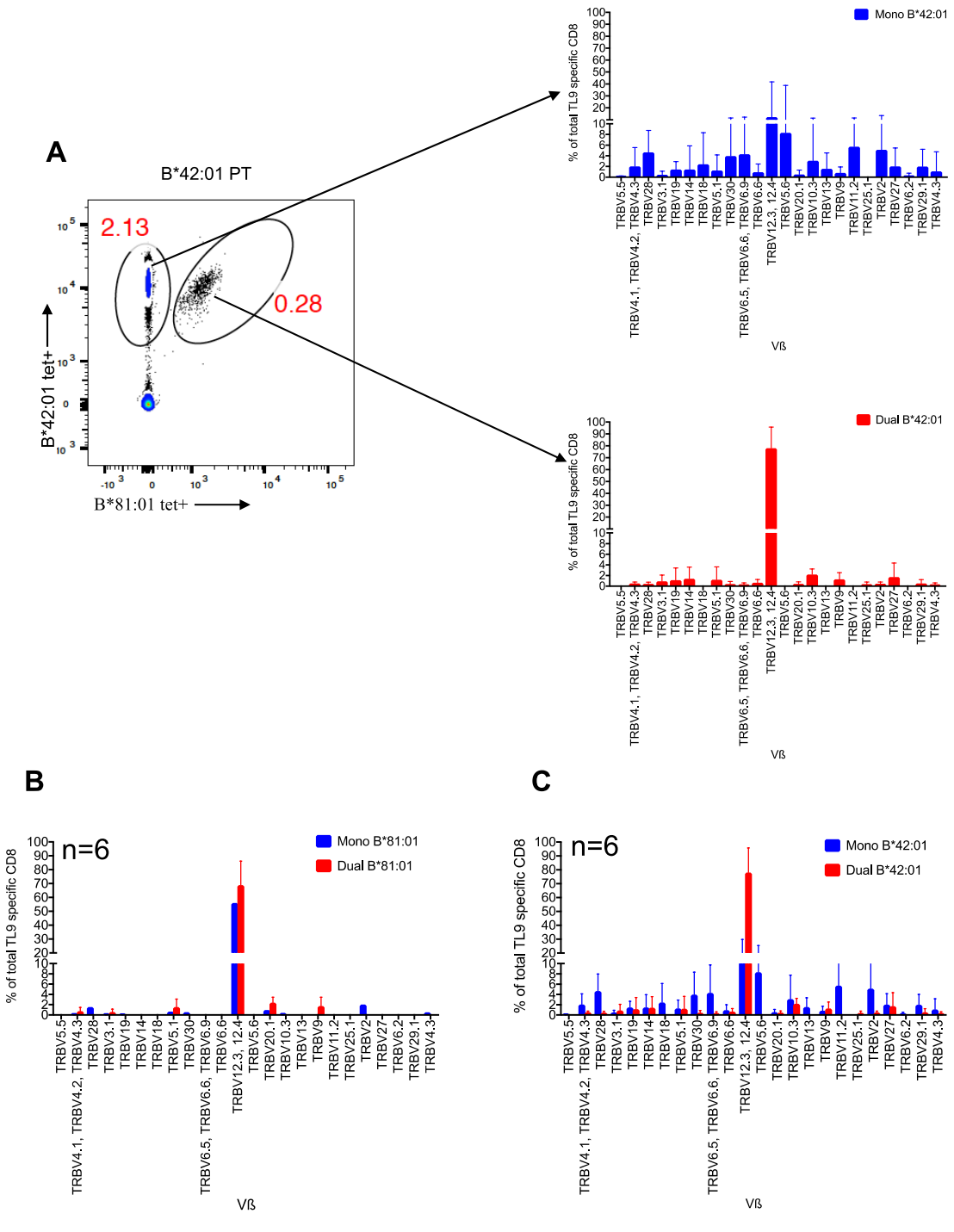

Figure 3-2. Enrichment of TCR Vβ 12-3/12-4 in dual-reactive T cells.

A representative flow plot for one B*42:01 expressing individual displays mono- and dual-TL9 tetramer reactive T cell populations and linked TCR Vβ expression profiles based on antibody staining (**A**). Aggregate results for TCR Vβ usage are shown for mono- (blue) and dual-reactive (red) T cells from six B*81:01 expressing individuals (**B**) or six B*42:01 expressing individuals (**C**). Data and figure provided by F. Ogunshola.

To gain additional molecular insight into the TCR clonotypes present within each TL9-specific T cell population, we sequenced the TCR β gene repertoire in single tetramer-labeled T cells isolated by FACS from three B*81:01 and three B*42:01 expressing individuals who displayed mono- and dual-reactive responses. Consistent with antibody staining results, Vβ gene usage for mono- and dual-reactive B*81:01-derived populations, as well as dual-reactive B*42:01-derived populations, was highly restricted to *TRBV12-3*/*12-4* **(Figure 3-3A, B)**. In contrast, while the mono-reactive population in one B*42:01 expressing individual (participant 11) was comprised largely of T cells encoding *TRBV12-3/12-4*, the primary Vβ gene present in the other two individuals (participants 13 and 17) was *TRBV7-9* **(Figure 3-3B)**. Notably, we observed that the dual-reactive population in all three B*42:01 expressing individuals was dominated by four public Vβ sequences (highlighted CDR3 regions in **Figure 3-3B**) that were never observed in B*81:01-derived TCR sequences. Enrichment of *TRBV12-3/12-4* usage by TL9-specific TCR in the context of B*81:01 as well as the public dual-reactive TCR in B*42:01 expressing individuals suggested that features of these TCR clonotypes contribute to control of HIV-1 infection.

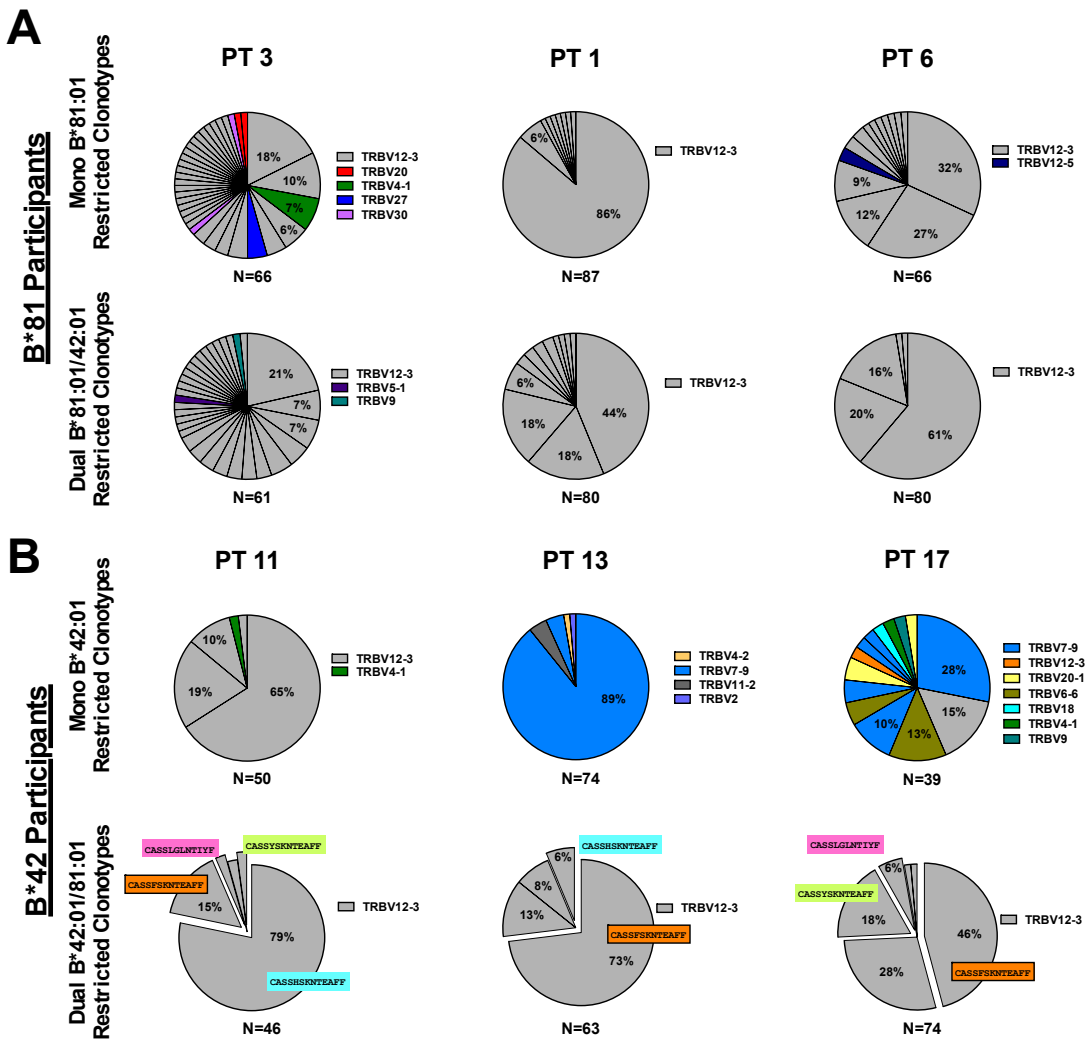

Figure 3-3. Molecular analysis of TCR β clonotypes in mono- and dual-reactive T cells.

TCR β sequencing was performed on single FACS-sorted mono- and dual-TL9 tetramer reactive T cells from three B*81:01 expressing participants (**A**) and three B*42:01 expressing participants (**B**). *TRBV* and CDR3 sequences were determined using the IMGT V-quest tool (www.imgt.org). The total number of sequences collected per population is indicated under each pie chart. Unique TCR β clones are displayed as wedges in the pie chart. The size of the wedge indicates the frequency of each sequence within the population and the color represents *TRBV* usage. TCR β sequences in mono- and dual-reactive populations from B*81:01 expressing individuals were highly enriched for *TRBV12-3/12-4* usage (indicated in grey); however, no public sequences were observed among these individuals. Mono-reactive populations from B*42:01 expressing individuals encoded diverse *TRBV* and also lacked public sequences. In contrast, dual-reactive populations from B*42:01 expressing individuals were enriched for *TRBV12-3/12-4* usage (grey), and these sequences were comprised predominately of four identical (public) TCR β clones (highlighted by colored boxes). Notably, these public clones were distinct from any TCR observed in B*81:01 individuals

3.4.4. Isolation and validation of TL9-specific TCR clones

To provide a more complete understanding of mono- and dual-reactive CD8+ T cell phenotypes, we identified the paired TCR α gene from eight dominant TCR clones representing the mono- and dual-reactive populations from B*81:01 and B*42:01 expressing individuals **(Figure 3-4A**) and directly assessed TCR function using a previously described *in vitro* reporter T cell assay [57]. Briefly, full-length TCR α/β genes were reconstructed and transiently expressed in Jurkat T cells. TCR-mediated NFAT signaling was quantified by luminescence following co-culture with HLA-expressing target cells presenting the TL9 epitope. Since methods used for TCR staining and sequencing could not distinguish between *TRBV12-3* and *TRBV12-4*, which differ by two amino acids in the CDR1, TCR β genes were synthesized encoding both alleles; however, only *TRBV12-3* constructs were functional **(Appendix Figure 3-3)**. TCR clones displayed dose-dependent responses to consensus TL9 over a range of peptide concentrations (5 nM to 20 µM) **(Appendix Figure 3-4)**, indicating that the reporter assay was sensitive and specific. Furthermore, reconstructed TCR maintained mono- or dual-reactivity against TL9 peptide-pulsed **(Figure 3-4B)** and HIV-infected **(Figure 3-4C)** target cells expressing B*81:01 or B*42:01, confirming that dual-reactive T cells were a distinct population in both B*81:01 and B*42:01 expressing individuals, and that phenotypic differences in pHLA specificity were due to TCR sequence.

A

TCR ID	Restriction	TRAV	TRAJ	CDR3 Alpha	TRBV	TRBJ	CDR3 Beta
7A10	B*42- Mono B*42 TL9	12-1*01	31*01	CVVNIRGNARLMF	12-3*01	2-1*01	CASSLGTLNEQFF
13A10	B*42- Mono B*42 TL9	16*01	18*01	CALRGRGSTLGRLYF	7-9*01	1-3*01	CASSSSLTGVTSYNEQFF
14A4	B*42- Dual B*42/81 TL9	13-1*01	38*01	CAATNAGNNRKLIW	12-3*01	1-1*01	CASSFSKNTEAFF
14D7	B*42- Dual B*42/81 TL9	13-1*01	38*01	CAATNAGNNRKLIW	12-3*01	1-1*01	CASSHSKNTEAFF
16A11	B*42- Dual B*42/81 TL9	13-1*01	38*01	CAACNAGNNRKLIW	12-3*01	1-1*01	CASSYSKNTEAFF
11A10	B*81- Mono B*81 TL9	26-1*01	23*01	CIVRGTYNQGGKLIF	12-3*01	2-1*01	CASSLGTLNEQFF
12A11	B*81- Dual B*81/42 TL9	26-2*01	30*01	CILRGLMNRDDKIIF	12-3*01	1-1*01	CASKQGVAEAFF
18A2	B*81- Dual B*81/42 TL9	26-1*01	39*01	CIVRGLNNAGNMLTF	12-3*01	1-3*01	CASSLGIDAIYF

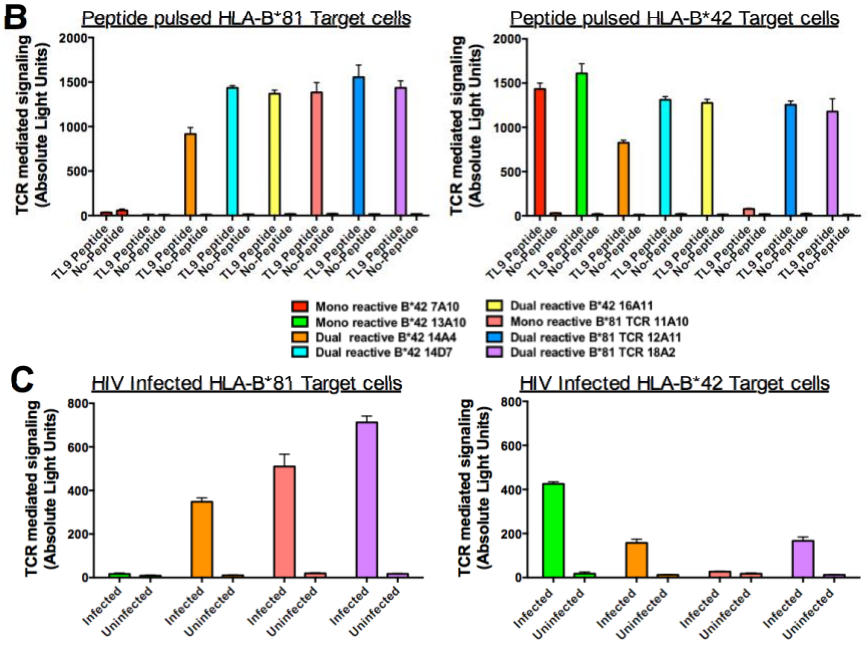

Figure 3-4. In vitro validation of TCR specificity and dual reactivity.

Details for the eight TL9-specific TCR clones investigated in this study are shown, including donor HLA, mono- or dual-reactivity phenotype, paired TCR α/β V gene usage and CDR3 sequences (**A**). Jurkat T cells were co-transfected with TCR α/β, CD8 α and an NFAT-driven luciferase reporter vector, and then co-cultured with TL9 peptide-pulsed (**B**) or HIV-infected (**C**) target cells stably expressing B*81:01 or B*42:01. TCR-dependent NFAT signaling was quantified by luminescence. The expected mono- or dual-reactive phenotype was observed for all reconstructed TCR clones, as indicated by greater luminescence (absolute light units, y-axis) in the presence of TL9-pulsed or virus-infected target cells compared to no-peptide or uninfected controls. Assays were conducted at least three times. Results from a representative experiment are shown as the mean of three co-culture reactions, plus standard deviation.

3.4.5. Analyses of TL9 variant recognition by TCR clones

The ability of TCR to cross-recognize epitope variants is associated with enhanced antiviral activity of $CD8_+$ T cells [26, 27, 58]. If indeed the dual-reactive

population contributes to control of HIV-1, we hypothesized that it should be able to respond to a variety of TL9 variants. To explore this, we assessed the ability of each reconstructed TCR to respond to a panel of 180 peptides representing TL9 and all possible single amino-acid TL9 variants. These results are displayed as heat maps in **Figure 3-5** and also provided in the Appendix Data file. Collectively, the eight TCR clones recognized 114 (of 171, 67%) TL9 variants at a normalized luminescence value of 0.1 or greater (which was ~10-fold above negative control wells). In addition to consensus TL9, individual B*81:01-derived clones responded to 67 (11A10, mono-reactive), 53 (12A11, dual), and 94 (18A2, dual) variant peptides, while B*42:01-derived clones responded to 48 (7A10, mono), 46 (13A10, mono), 54 (14A4, public dual), 34 (16A11, public dual), and 34 (14D7, public dual) variant peptides. No correlation was observed between the total breadth of TL9 variant recognition and dual-reactivity, suggesting that qualitative features of TCR function contributed to this phenotype. The three TCR clones isolated from B*81:01 expressing individuals (one mono- and two dual-reactive) displayed similar overall TL9 variant cross-recognition profiles, as demonstrated by Spearman R-values >0.80 for all pair-wise associations; however, greater breadth against variants at position 4 (aspartic acid) was seen for clone 18A2. In contrast, the five TCR clones isolated from B*42:01 expressing individuals displayed more disparate cross-recognition profiles, which was reflected by pair-wise Spearman R-values between 0.12 and 0.67. Notable differences were observed among B*42:01-derived TCR clones for recognition of TL9 peptide variants at positions 3 and 7, which are discussed below. To further evaluate the degree of functional similarity among these TCR clones, we performed a hierarchical clustering analysis based on their TL9 variant recognition profiles. Results are shown as a dendrogram in **Figure 3-5**. We observed that all three of the public dual-reactive B*42:01-derived clones grouped together with bootstrap values of 100. Furthermore, this group of public clones clustered more closely with the three B*81:01-derived clones (bootstrap value of 97), compared to the two mono-reactive B*42:01-derived clones. Together, these results indicate that the epitope binding properties of the public dual-reactive B*42:01-derived TCR clones are more similar to those of clones elicited in the context of the more protective B*81:01 allele, despite TL9 peptide being presented on a different HLA allele.

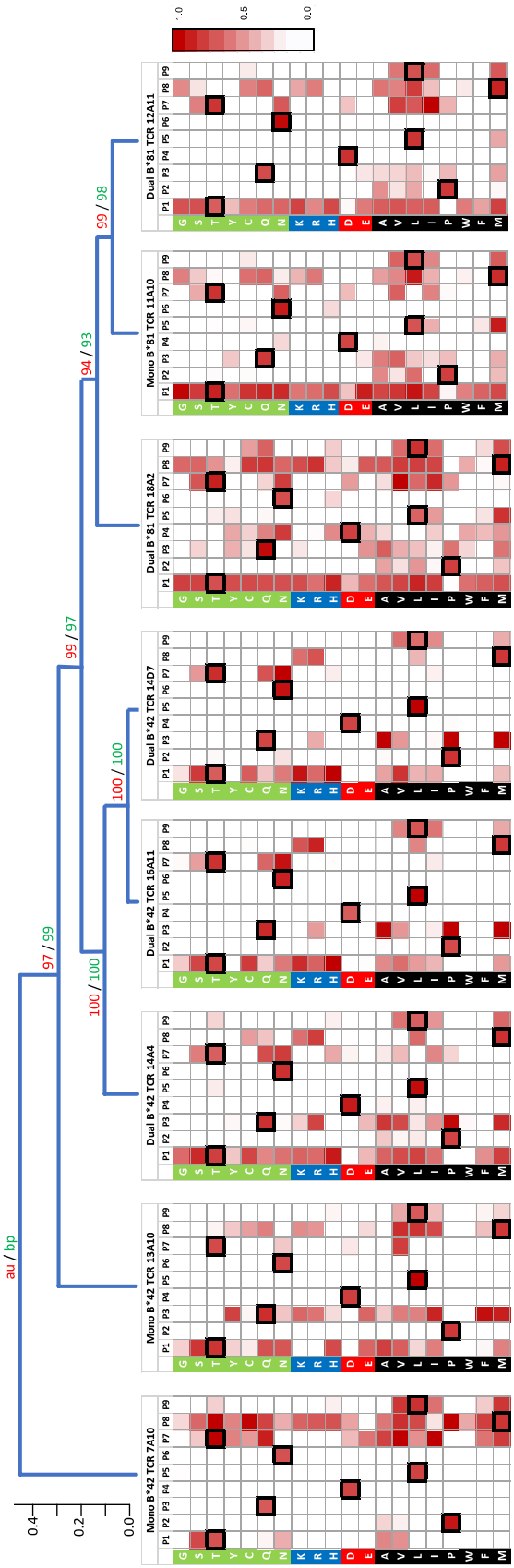
au / bp
0.4
0.2
0.0
97 / 99
100 / 100
99 / 97
100 / 100
94 / 93
99 / 98
1.0
0.5
0.0
Mono B*42 TCR 7A10
Mono B*42 TCR 13A10
Dual B*42 TCR 14A4
Dual B*42 TCR 16A11
Dual B*42 TCR 14D7
Dual B*81 TCR 18A2
Mono B*81 TCR 11A10
Dual B*81 TCR 12A11
P1 P2 P3 P4 P5 P6 P7 P8 P9
G S T Y C Q N K R H D E A V L I P W F M

Figure 3-5. Functional clustering of TCR clones based on TL9 variant recognition profiles.

TCR recognition of TL9 variants was assessed by pulsing target cells expressing the donor HLA (B*81:01 or B*42:01) with a panel of 180 peptides encompassing all single amino acid substitutions at epitope positions 1 through 9 prior to co-culture with Jurkat T cells expressing the TCR of interest. TCR-dependent NFAT signaling was quantified by luminescence. Values were normalized to the mean signal obtained for consensus TL9 (set to 1.0), which was tested nine times in each experiment. Results are displayed as heatmaps, where the warmer color reflects higher relative luminescence values indicative of better TCR recognition. Peptide positions are shown at the top of each heatmap; amino acid substitutions on the consensus TL9 backbone are shown on the left-hand side. Amino acids are grouped according to chemical properties: polar residues (G, S, T, Y, C, Q, N) are highlighted in green; basic residues (K, R, H) are blue; acidic residues (D, E) are red; and hydrophobic residues (A, V, L, I, P, W, F, M) are black. For reference, the consensus TL9 residue at each position is indicated using a box. TCR were grouped according to their functional profiles by hierarchical clustering using correlation distances and single linkage methods (5,000 iterations) implemented in pvclust (http://stat.sys.i.kyoto-u.ac.jp/ prog/pvclust/). The dendrogram (top) displays approximately unbiased (au) p-values in red text and bootstrap probability (bp) values in green text. The three B*81:01-derived TCR clustered with bp values of 93 or higher. The three public dual-reactive B*42:01-derived TCR clustered with bp values of 100; and, notably, they grouped more closely with B*81:01 clones (bp value of 97), rather than mono-reactive B*42:01-derived TCR.

3.4.6. Dual-reactive TCR recognize more TL9 escape mutations

We observed substantial differences in TL9 variant recognition among TCR clones, particularly at epitope positions 3 and 7. To examine the impact of these differences on viral adaptation, we restricted our analysis to 19 TL9 polymorphisms present in circulating HIV-1 subtype C sequences at a prevalence of ~0.1% or greater, which were considered as viable escape mutations. The ability of each TCR to recognize this panel of mutants is illustrated as a SequenceLogo in **Figure 3-6** (panels A-H). Collectively, the eight TCR clones recognized 16 (of 19, 84%) TL9 escape mutants; none responded to a threonine, glycine or aspartic acid substitution at position 3, which together accounted for 26.1% of circulating variant sequences. These results were highly consistent with prior studies of T cell cross-reactivity based on IFN-γ ELISPOT assays using PBMC [40, 41, 43], with 7 (of 8; 88%) TCR clones recognizing serine at position 7 or alanine at position 3, whereas responsiveness to other natural polymorphisms at position 3 (histidine, 13%; serine, 13%; threonine, 0%) and position 7 (valine, 75%; methionine, 25%) were less common. While the total number of TL9 escape mutants recognized by B*81:01-derived TCR clones (range, 8-14), public dual-

reactive B*42:01-derived clones (6-9) and mono-reactive B*42:01-derived clones (6-7) was not significantly different between groups, we observed that the two mono-reactive B*42:01-derived TCR clones responded primarily to variants located at either position 7 (for 7A10) **(Figure 3-6A)** or position 3 (for 13A10) **(Figure 3-6B)**, indicating a limited ability to control escape mutations that occur at the other residue. In contrast, B*81:01-derived TCR clones and public dual-reactive B*42:01-derived clones each displayed broader recognition of variants at both position 3 and 7 **(Figure 3-6C-H)**, suggesting a distinct mechanism(s) of binding that accommodated changes at these residues. B*81:01-derived TCR clones also displayed broader recognition of TL9 variants at position 5. These results demonstrate functional differences among TCR clonotypes that may contribute to control of naturally occurring TL9 variants, particularly at epitope positions 3 and 7.

HIV-1 adaptation to $CD8_+$ T cells is highly dynamic [59, 60], but escape in TL9 is limited by functional constraints [45]. Since common TL9 variants, such as serine at position 7 (S7; 23.4% of non-consensus sequences in LANL), are presumed to encounter a relatively lower barrier to escape compared to rare variants, such as isoleucine at this position (I7: 0.7%), we reasoned that TCR recognition of more common TL9 variants would be beneficial for viral control. To explore this, we plotted these 19 TL9 polymorphisms using pie charts with wedges sized according to their prevalence in subtype C sequences **(Figure 3-6I-P)** and then determined the percent coverage of TL9 escape mutations for each TCR by calculating the proportion of total sequence variation that was recognized (see wedges highlighted in Red). Based on this frequency-adjusted analysis, individual clones displayed 22% **(Figure 3-6J)** to 67% **(Figure 3-6P)** coverage of TL9 variants. While differences between groups were not statistically significant, B*81:01-derived TCR clones and public dual-reactive B*42:01 clones tended to display greater coverage (40-67% and 36-41%, respectively) compared to the mono-reactive B*42:01 clones (22% and 32%). These results indicate that individual TCR clonotypes display variable capacity to recognize more common TL9 variants that are likely to constitute preferential escape mutants.

Since codon usage places additional constraints on viral sequence evolution, we reasoned that TCR recognition of transitional variants would hinder the development of TL9 escape. For example, substitution of glutamine at position 3 (Q3) with serine (S3) requires a minimum of two nucleotide changes with transition through proline (P3) or a

stop codon. Thus, TCR recognition of the P3 variant would be expected to prevent formation of S3, even in cases where the TCR did not respond to the S3 variant itself. For each TCR clone, we determined which TL9 escape mutations were inhibited due to recognition of critical transitional variants (see Yellow wedges in **Figures 3-6I-P**). We then calculated the total coverage of TL9 escape pathways by summing the proportion of variant sequences that were recognized or prevented by each TCR (i.e. Red plus Yellow wedges). Based on this pathway-adjusted analysis, individual TCR clones displayed 32% to 83% coverage of TL9 escape mechanisms. Notably, B*81:01-derived clones (range, 57-83%, **Figure 3-6N-P**) and public dual-reactive B*42:01-derived clones (range, 52-83%, **Figure 3-6K-M)** displayed broader coverage compared to mono-reactive B*42:01-derived clones (both 32%, **Figure 3-6I-J**) ($p = 0.05$ and $p = 0.11$, respectively; Student's T test); highlighted by one public dual-reactive B*42:01-derived clone (14A4) and one B*81:01-derived clone (18A2). Notably, extended coverage of TL9 escape pathways was due mainly to the ability of TCR clones 14A4 (**K**), 14D7 (**L**), 16A11 (**M**), 11A10 (**N**), and 12A11 (**O**) to respond to the P3 variant, which is anticipated to impair development of the S3 escape mutation that accounts for 16.5% of TL9 variant sequences. Together, these results illustrate the functional diversity that exists among antigen-specific T cells and demonstrate the impact of TCR sequence on recognition of HIV-1 Gag TL9 escape mutations. This work highlights the role of TCR clonotype differences as a correlate of HIV-1 control in the context of HLA B*81:01 and B*42:01.

A

TCR 7A10
Mono-B*42:01
TRBV12-3

I

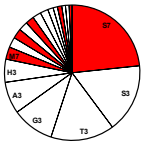

Variant Epitope Recognition (R): 32%
Escape Pathway Recognition (Y+R): 32%

B

TCR 13A10
Mono-B*42:01
TRBV7-9

J

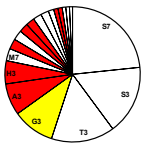

Variant Epitope Recognition (R): 22%
Escape Pathway Recognition (Y+R): 32%

C

TCR 14A4
Dual-B*42:01
TRBV12-3

K

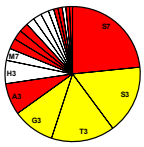

Variant Epitope Recognition (R): 41%
Escape Pathway Recognition (Y+R): 83%

D

TCR 14D7
Dual-B*42:01
TRBV12-3

L

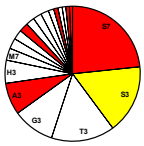

Variant Epitope Recognition (R): 36%
Escape Pathway Recognition (Y+R): 52%

E

TCR 16A11
Dual-B*42:01
TRBV12-3

M

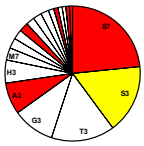

Variant Epitope Recognition (R): 36%
Escape Pathway Recognition (Y+R): 52%

F

TCR 11A10
Mono-B*81:01
TRBV12-3

N

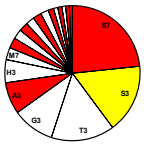

Variant Epitope Recognition (R): 42%
Escape Pathway Recognition (Y+R): 58%

G

TCR 12A11
Dual-B*81:01
TRBV12-3

O

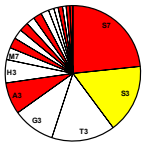

Variant Epitope Recognition (R): 40%
Escape Pathway Recognition (Y+R): 57%

H

TCR 18A2
Dual-B*81:01
TRBV12-3

P

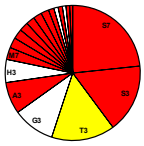

Variant Epitope Recognition (R): 67%
Escape Pathway Recognition (Y+R): 83%

Figure 3-6. Enhanced recognition of TL9 escape by B*81:01-derived and B*42:01-derived dual-reactive TCR clones.

The ability of each TCR clone to respond to HIV-1 escape mutants was determined by comparing its recognition profile to a panel of 19 naturally occurring subtype C TL9 variants, found at a prevalence of ~0.1% or greater in the LANL HIV Sequence Database (HIV Databases; http://www.hiv.lanl.gov). Recognition breadth for each TCR is illustrated as a SequenceLogo, demonstrating variable responsiveness towards relevant TL9 mutations located primarily at epitope positions 3 and 7. Mono-reactive TCR from B*42:01 expressing individuals displayed narrower profiles that recognized TL9 variants at either position 7 (7A10, **A**) or position 3 (13A10, **B**), whereas public dual-reactive B*42:01-derived clones (**C-E**) and B*81:01-derived clones (**F-H)** demonstrated broader ability to recognize TL9 variants at both positions 3 and 7. To account for constraints on TL9 escape, epitope variants were displayed using pie charts where the size of each wedge is proportional to variant frequency in circulating subtype C isolates (**I-P**). Serine at position 7 (S7), serine at position 3 (S3), and threonine at position 3 (T3) accounted for the majority (55%) of population-level variation. For each chart, the wedge is shaded in Red (R) if the TCR responded to the escape mutant or in Yellow (Y) if the TCR recognized all transitional mutations required to generate that escape mutant from consensus TL9. The sum of all Red wedges is displayed under each chart as the total percentage of Variant Epitope Recognition and the sum of all shaded wedges, Red plus Yellow, is displayed as the total percentage of Escape Pathway Recognition, where recognition of all circulating TL9 variants would be 100%. Overall, B*81:01-derived TCR (**N-P**) and public dual-reactive B*42:01-derived TCR (**K-M**) displayed better ability to cross-recognize circulating TL9 escape variants and pathways compared to mono-reactive B*42:01-derived clones (**I-J**).

3.5. Discussion

The characteristics that determine effectiveness of adaptive host immune responses to rapidly evolving pathogens such as HIV-1 are not fully defined. In this study, we examined the $CD8_+$ T cell response against the immunodominant HIV-1 p24 Gag TL9 epitope in the context of two closely related class I HLA alleles, B*81:01 and B*42:01, that display differential abilities to control viral subtype C infection [9]. We identified a population of dual HLA tetramer-reactive T cells that recognized TL9 presented in the context of either B*42:01 or B*81:01 alleles and observed that the presence of this dual-reactive population was an independent predictor of lower plasma viral load. In B*42:01 expressing individuals, dual-reactive populations were dominated by public TCR clonotypes that encoded *TRBV12-3*. A comprehensive *in vitro* functional analysis of selected TCR clones indicated that B*81:01-derived clones (regardless of mono- or dual-reactive phenotype) and public dual-reactive B*42:01-derived TCR clones displayed greater ability to recognize TL9 escape pathways, compared to mono-reactive

clones from B*42:01 expressing individuals. While the dual-reactive T cell phenotype reported here is a phenomenon of tetramer binding to pHLA that is not expressed by the host, our results indicate that it identifies T cell subsets within diverse antigen-specific repertoires that share important features, including Vβ gene sequences and the ability to recognize HIV-1 epitope variants. A similar dual HLA-reactive phenotype has been described for one CTL clone [52], but here we demonstrate the extent to which dual-reactive T cells exist *in vivo* and link this phenotype to functional characteristics of individual TCR clonotypes. It will be critical to examine this phenomenon further to see if it is a common feature of T cell responses elicited in the context of other HLA supertypes, such as members of the B57 family that also show differential abilities to control HIV-1 infection [9].

It is important to note that antigen sensitivity appeared to be independent of cross-reactivity for TCR examined in this study. While more detailed biochemical analyses will be necessary to fully assess the affinity of TL9-specific TCR clones, our reporter assay provides a surrogate measure of antigen sensitivity based on strength of NFAT signalling. The activities of dual-reactive B*42:01-derived TCR clones were lower compared to those of mono-reactive B*42:01-derived clones. We observed similar differences in the sensitivity of representative TCR clones tested over a range of TL9 concentrations **(Appendix Figure 3-3)**, indicating that this result was not an artefact of peptide dose. In addition, TCR sensitivity towards consensus TL9 did not correlate with cross-recognition of TL9 variants in our more comprehensive analysis, although it will be important to confirm this observation using a larger panel of TL9-specific TCR clones.

Although B*81:01 and B*42:01 are both members of the B7 supertype and known to present many of the same HIV-1 peptides, the dual-reactive T cell phenotype is unexpected since structural data indicated that TL9 adopts a distinct conformation upon binding to each allele [46]. Our analysis demonstrated that B*81:01-derived TCR clones and public dual-reactive B*42:01-derived clones recognized TL9 variants at both principal sites of viral escape, position 3 and 7. This is interesting since both residues are buried in the B*81:01 structure, while position 7 is solvent-exposed in the context of B*42:01 [46]. It remains to be determined whether TCR recognition reflects direct binding to these TL9 variants, or rather is due to conformational changes in the pHLA or indirect effects on other TL9 residues. In contrast, mono-reactive B*42:01-derived TCR displayed breadth against TL9 variants at either position 3 or position 7, but not both.

While both types of mono-reactive TCR may be present within the repertoire of B*42:01 expressing individuals, skewing of the immune response towards either mono-reactive TCR subset could facilitate viral escape at the alternative TL9 position.

Our detailed functional data provides insight into characteristics of TL9-specific TCR clones that might be overlooked using more conventional methods based on HIV-1 sequences alone. For example, all TCR clones were sensitive to changes at TL9 position 6, demonstrating that this highly conserved polar asparagine residue is critical in the context of both HLA alleles, despite it being solvent-exposed in the B*81:01 structure and buried in the B*42:01 structure [46]. In addition, most TCR were sensitive to changes at position 4, indicating that this negatively charged, polar aspartic acid residue (which is solvent-exposed in both structures [46]) is critical for recognition; however, the B*81:01-derived clone 18A2 tolerated mutations at this residue, suggesting a distinct mechanism of interaction in this case. Structural flexibility is a crucial feature of the interaction between TCR and pHLA [61-63]; thus, changes in conformation induced upon TCR binding may be relevant to recognize TL9 variants in the context of both B*81:01 and B*42:01. Because such conformational rearrangements are difficult to predict [64], more detailed structural analyses will be necessary to explore this issue. In the absence of such data, we are unable to define structural determinants of cross-reactivity for the TCR clones examined in our study. Nevertheless, our results highlight peptide-recognition properties that may contribute to future studies of these and other TL9-specific TCR.

This work extends prior efforts to examine TL9-specific $CD8_+$ T cell responses. In particular, Leslie et al. [40] and Geldmacher et al. [41] observed enrichment of *TRBV12-3* usage in B*81:01 and some B*42:01 expressing individuals, while Leslie et al. [40] and Kloverpris et al [34] described public TCR ß sequences in B*42:01 expressing individuals that correspond to the dual-reactive TCR clones 14A4 (CASSFSKNTEAFF) and 14D7 (CASSHSKNTEAFF) examined here and demonstrated that the presence of these public clones was associated with TL9 immunodominance [34]. These earlier reports suggested that $CD8_+$ T cell responses in B*81:01 expressing individuals displayed broader recognition of TL9 variants, but individual T cell clones (or TCR clonotypes) were not explored. Here, we re-discovered public TCR ß clonotypes in B*42:01 expressing individuals by their dual HLA-reactive phenotypes. Extensive functional analyses of selected TCR clones demonstrated substantial diversity in their

abilities to recognize TL9 variants. Our results emphasize the role of cross-reactive public TCR clones encoding *TRBV12-3* for effective TL9 responses in B*42:01 expressing individuals; however, differences in TL9 variant recognition among these public clones also suggests a functional hierarchy that may be clinically relevant. Furthermore, it should be noted that B*42:01-derived clone 7A10 encoded *TRBV12-3* but did not demonstrate dual-reactivity or broad recognition of TL9 escape variants, indicating that phenotypic differences among TCR were not driven entirely by V gene usage.

Several observations from this study are relevant for the design of vaccines or therapeutics. Vaccine antigens that can elicit effective cross-reactive TCR clonotypes might provide better protection against HIV-1 infection or enhance the ability of the immune system to recognize latent viral reservoirs encoding escape variants. We observed that public dual-reactive TCR clones from B*42:01 expressing individuals were unique in their ability to recognize a proline variant at TL9 position 3 (Q3P). It would be interesting to examine *ex vivo* responses to this rare TL9 variant as a surrogate marker for public dual-reactive T cells HIV-infected individuals or vaccine recipients; or to consider vaccination with this variant TL9 sequence to elicit a more broadly reactive T cell response in B*42:01 expressing individuals. We have also identified and validated the recognition profiles of eight TL9-specific TCR clones, including several with dual HLA-reactive phenotypes. These TCR clones may be attractive products for future T cell therapy strategies that aim to reduce or eliminate viral reservoirs encoding escape mutations in the context of HIV-1 subtype C infection.

In summary, we have identified characteristics of TCR clonotype sequence and function that are associated with variable control of HIV-1 infection in the context of B*81:01 and B*42:01. We observed a unique dual HLA-reactive $CD8_+$ T cell population that was highly enriched for a small number of public TCR clonotypes in B*42:01 expressing individuals. Mono- and dual-reactive TCR clones from individuals expressing the protective B*81:01 allele displayed broad recognition of TL9 variants, suggesting that they provide comparable abilities to contain HIV-1 Gag escape mutants. In contrast, only public dual-reactive TCR clones from B*42:01 expressing individuals displayed similar broad TL9 variant recognition, suggesting that these public clonotypes provide enhanced ability to control HIV-1 escape mutants in the context of this less protective HLA allele. While additional studies will be necessary to fully assess the structural mechanisms and

clinical relevance of these observations, this work provides a strong foundation and rationale to further explore the impact of TCR clonotype differences on HIV-1 outcomes. Together, our results highlight the feasibility and use of detailed molecular analyses that link TCR sequences with functional characteristics to improve understanding of T cell responses against diverse and rapidly evolving pathogens. Similar investigations might be beneficial to enhance the development of vaccines and T cell-based immunotherapies against HIV or other human diseases.

3.6. Methods

3.6.1. Study subjects

Twenty-one antiretroviral naïve individuals were enrolled in Durban, South Africa through the HIV Pathogenesis Programme (HPP) acute infection cohorts. The clinical characteristics are shown in **Table 1**. All individuals were infected with HIV-1 subtype C. The Biomedical Research Ethics Committee of the University of KwaZulu-Natal and the Massachusetts General Hospital Ethics committee approved this study. All subjects provided written informed consent.

3.6.2. HLA typing

HLA typing was conducted by the laboratory of Dr. Mary Carrington (National Cancer Institute, Fredrick, USA), as previously described [9]. DNA samples obtained from peripheral blood mononuclear cells (PBMC) were first oligo-typed using Dynal RELITM reverse Sequence Specific Oligonucleotide (SSO) kits for the HLA-A, HLA-B and HLA-C loci (Dynal Biotech). Genotypes were refined to the allelic level using the Dynal Biotech Sequence Specific priming (SSP) kits in conjunction with the previous SSO type. In cases where alleles were still not well-defined at the allelic level, sequence-specific primers were used [65]. All class I HLA alleles in the IMGT allele release 24.0 were considered in the typing.

3.6.3. Tetramer staining, cell sorting and cell line generation

To identify and characterize TL9-specific $CD8^+$ T cell populations, PBMC were first stained with a cell-viability dye (Fixable Blue Dead Cell Stain Kit, Invitrogen) for 10

minutes at room temperature. Cells were washed with 2% fetal calf serum (FCS) in phosphate buffered saline (PBS) and then stained with B*42:01-APC and/or B*81:01-PE TL9 HLA class I tetramers (obtained from the laboratory of Dr. Soren Buus), for 30 mins at room temperature. Subsequently, cells were washed, and surface stained with anti-CD8-BV786, CD3-BV711 and CD4-BV650 for 20 minutes at room temperature. Stained cells were analyzed by flow cytometry and/or tetramer-specific $CD8_+$ T-cells were sorted for TCR sequencing. To generate TL9-specific $CD8_+$ T-cell lines, cells were pulsed with 5 µl (200 µg ml_{-1}) of TL9 peptide at 37 ºC for 3 hours and subsequently cultured in RPMI medium containing 10% heat-inactivated fetal calf serum (R10 medium) supplemented with 50 units ml_{-1} of recombinant human interleukin 2 (IL-2) (R10/50 medium) for 2 weeks. Expanded TL9-specific $CD8_+$ T cells were validated for specificity by tetramer staining and isolated using a cell sorter (BD FACSAria, Germany).

3.6.4. Tetramer intracellular cytokine staining and ELISPOT assay

To assess the functional quality of TL9-specific $CD8_+$ T cells, PBMC from B*81:01 and B*42:01 subjects were stimulated with 1.2 µl (200 µg ml_{-1}) of TL9 peptide for 6 hours. After stimulation, cells were stained with an equal mixture of B*81:01 and B*42:01 TL9 tetramers for 30 minutes at room temperature, washed in PBS containing 2% FCS and then stained with viability dye, anti-CD8-BV786, CD3-BV711, and CD4-BV650 for 20 minutes at room temperature. Cells were fixed, permeabilized, stained intracellularly with anti-IFN-γ-PE-Cy7 and analyzed on the BD LSRFortessa. HIV-1 immune responses were enumerated by IFN-γ enzyme-linked immunosorbent spot (ELISPOT) assay as previously described [9, 66]. Briefly, PBMCs were stimulated with optimal HIV-1 subtype C peptide corresponding to each patient's HLA-A, B and C alleles at a final concentration of 2 µg ml_{-1} peptide.

3.6.5. TCR Vβ antibody staining

TCR Variable β (Vβ) expression on mono- and dual-$tetramer_+$ cells was assessed by flow cytometry as described previously [67]. PBMC were stained with B*81:01 and/or B*42:01 TL9 tetramers conjugated to different fluorochromes, followed by TCR Vβ family labeling using IOTest Beta Mark TCR Vβ repertoire Kit (Beckman

Coulter, Pasadena, United States) for 30 minutes at room temperature. Subsequently, cells were stained with viability dye, anti-CD8-BV786, CD3-BV711, and CD4-BV650. The percentage of each Vβ family was determined for a minimum of 100,000 $CD8_+$ T cells using FlowJo software (Treestar, Ashland, United States). TCR Vβ staining was also performed on expanded mono- and dual- TL9 $tetramer_+$ cell lines.

3.6.6. TCR sequencing

Amplification of TCR β CDR3 coding regions from single T cells was performed as described previously by Han et al [68] with modifications to obtain ~230 bp amplicons for Sanger sequencing (ABI 3130xl). Primers are included in **Appendix Tables 3-2 and 3-3**. The one-step SuperScript III kit (ThermoFisher) was used for RT-PCR and Expand High Fidelity PCR system (Roche) was used for subsequent rounds. TCR α amplicons were TOPO cloned and screened to ensure productive CDR3 rearrangement. Sequences were examined using the ImMunoGeneTics (IMGT)/V-quest tool (www.imgt.org) to characterize Variable gene usage and CDR3 diversity. Full-length TCR alleles were reconstructed using Variable and Constant gene sequences obtained from the IMGT database, codon-optimized using the CodonOpt tool (Integrated DNA Technologies; www.idtdna.com) and synthesized as double-stranded DNA gBlocks by IDT. Full-length genes were cloned into pSELECT_GFPzeo (Invivogen) for functional studies.

3.6.7. TCR reporter assay

TCR antigen recognition was examined using a previously described *in vitro* reporter T cell assay [57]. Briefly, Jurkat T cells were co-transfected with TCR α, TCR β, CD8 α and NFAT-driven luciferase reporter plasmids by electroporation (BioRad MxCell). Target cells consisted of a CEM-derived GXR cell line [69] stably expressing either HLA-B*42:01 or B*81:01. TCR-transfected Jurkat effector cells (50,000 cells) were co-cultured with 50,000 target cells either pulsed with 20 μM TL9 peptide (purchased from GenScript at >90% purity) or infected with HIV-1 in a total volume of 100 μL, and TCR recognition activity was quantified by luminescence after 6 hours (Tecan M200). Viral stocks were generated by co-transfection of HEK293T cells with pBR4.3ΔNefΔEnv and pVSV-g using Lipofectamine 2000 (ThermoFisher Scientific). Infected GXR target cells were isolated by FACS based on GFP expression prior to co-culture with Jurkat T

cells. To screen antigen cross-recognition, a peptide panel consisting of all single amino acid TL9 variants (180 total peptides) was purchased from GenScript. This panel was prepared using microscale synthesis methods and individual peptides were aliquoted to 96-well plates at 0.5 to 2.0 mg total weight and >75% purity. Target cells were pulsed with ~20 μM peptide; however, due to variations in peptide sequence, total weight, Molar weights and purity, actual concentrations were anticipated to range between 8.4 and 20 μM.

3.6.8. HIV sequence analysis

To determine the frequency of naturally occurring Gag TL9 variants in HIV-1 subtype C infection, all subtype C TL9 amino acid sequences (N=5,481) were downloaded from the Los Alamos National Laboratory (LANL) HIV sequence database (www.hiv.lanl.gov) and analyzed. Sequences encoding consensus TL9 (N=4,526), multiple substitutions or mixed residues (combined N=217) and those appearing fewer than five times (N=53) were removed to generate a list of the most probable single amino acid TL9 variants (N=685). The proportion of each variant within this population was calculated to determine the likelihood of viral escape. Critical transition mutations (i.e. those that must to occur for consensus TL9 to evolve into escape variants) were identified using the standard amino acid codon table for eukaryotes. Sequence conservation frequencies for TL9 residues were estimated using the QuickAlign tool on the LANL web site (based on N=1,865 protein sequences).

3.6.9. Statistical analysis

Statistical analyses were conducted using Prism software, version 6.0 (GraphPad, Inc.). Two-tailed tests were employed, and p-values less than 0.05 were considered to be significant. Comparisons between groups of continuous variables were assessed using parametric (unpaired Student's T) or non-parametric (Mann-Whitney U) tests. Differences in categorical variables between groups were assessed using Fisher's exact test. A multivariable linear regression analyses was conducted using Stata, version 14 (Stata Corp), to assess the independent predictive ability of HLA and dual reactivity on plasma viral loads. Hierarchical clustering analysis was performed using pvclust software [70] (http://stat.sys.i.kyoto-u.ac.jp/prog/pvclust), implemented in R. Data was grouped according to correlation distances using single linkage methods.

Approximately unbiased (au) p-values and bootstrap probability (bp) values were based on 5,000 iterations.

3.6.10. Data availability

Participants specimens, primary cell data, reagents for TCR sequencing and reporter cell assays used for peptide screening are available from the corresponding authors on reasonable request. Contact Zaza M. Ndhlovu (zndhlovu@mgh.harvard.edu) with requests regarding reagents and resource sharing for participant specimens, sequences and primary cell data. Similar requests regarding TCR sequencing and reporter cell assays used for peptide screening should be directed towards Mark A. Brockman (mark_brockman@sfu.ca). Paired TCR sequences are available through Genbank, accession codes: [MH918759-MH918774].

3.7. Acknowledgements

This work was supported in part through the Sub-Saharan African Network for TB/HIV Research Excellence (SANTHE), a DELTAS-Africa Initiative (Grant # DEL-15-006). The DELTAS-Africa Initiative is an independent funding scheme of the African Academy of Sciences's Alliance for Accelerating Excellence in Science in Africa and supported by the New Partnership for Africa's Development Planning and Coordinating Agency with funding from the Wellcome Trust [Grant # 107752/Z/15/Z] and the Government of the United Kingdom. Additional funding was received from the National Institutes of Health, U.S.A (R37-AI080289, R01-AI102660 and UM1-AI126617), the International AIDS Vaccine Initiative (UKZNRSA1001), and the Canadian Institutes for Health Research (HIG-133050). Z.M.N. is supported by an HHMI International research scholar award (Grant #55008743); M.A.B. is supported by the Canada Research Chairs Program and T.N. is supported by the South Africa Research Chairs Initiative. We thank Dr. Bruce Walker for providing clinical samples, part of the funding and for his insightful discussion during preparation of this manuscript. We also thank Natalie Kinloch, Xiaomei Kuang, and Zabrina Brumme for technical assistance and helpful discussions during preparation of this manuscript. The views expressed in this publication are those of the authors and not necessarily those of the funding agencies or partner organizations.

3.8. References

[1] S. G. Deeks and B. D. Walker, "Human immunodeficiency virus controllers: mechanisms of durable virus control in the absence of antiretroviral therapy," (in eng), *Immunity,* vol. 27, no. 3, pp. 406-16, Sep 2007, doi: 10.1016/j.immuni.2007.08.010.

[2] S. A. Migueles and M. Connors, "Long-term nonprogressive disease among untreated HIV-infected individuals: clinical implications of understanding immune control of HIV," (in eng), *Jama,* vol. 304, no. 2, pp. 194-201, Jul 14 2010, doi: 10.1001/jama.2010.925.

[3] A. J. Frater *et al.*, "Effective T-cell responses select human immunodeficiency virus mutants and slow disease progression," *Journal of virology,* Research Support, Non-U.S. Gov't vol. 81, no. 12, pp. 6742-51, Jun 2007, doi: 10.1128/JVI.00022-07.

[4] Y. Kawashima *et al.*, "Adaptation of HIV-1 to human leukocyte antigen class I," *Nature,* vol. 458, no. 7238, pp. 641-5, Apr 2 2009, doi: 10.1038/nature07746.

[5] B. Walker and A. McMichael, "The T-cell response to HIV," (in eng), *Cold Spring Harbor perspectives in medicine,* vol. 2, no. 11, Nov 01 2012, doi: 10.1101/cshperspect.a007054.

[6] R. A. Koup *et al.*, "Temporal association of cellular immune responses with the initial control of viremia in primary human immunodeficiency virus type 1 syndrome," *J Virol,* Research Support, Non-U.S. Gov't

Research Support, U.S. Gov't, P.H.S. vol. 68, no. 7, pp. 4650-5, Jul 1994. [Online]. Available: http://www.ncbi.nlm.nih.gov/pubmed/8207839.

[7] P. Borrow, H. Lewicki, B. H. Hahn, G. M. Shaw, and M. B. Oldstone, "Virus-specific CD8+ cytotoxic T-lymphocyte activity associated with control of viremia in primary human immunodeficiency virus type 1 infection," (in eng), *Journal of virology,* vol. 68, no. 9, pp. 6103-10, Sep 1994.

[8] S. A. Migueles *et al.*, "HLA B*5701 is highly associated with restriction of virus replication in a subgroup of HIV-infected long term nonprogressors," (in eng), *Proceedings of the National Academy of Sciences of the United States of America,* vol. 97, no. 6, pp. 2709-14, Mar 14 2000, doi: 10.1073/pnas.050567397.

[9] P. Kiepiela *et al.*, "Dominant influence of HLA-B in mediating the potential co-evolution of HIV and HLA," (in eng), *Nature,* vol. 432, no. 7018, pp. 769-75, Dec 09 2004, doi: 10.1038/nature03113.

[10] R. A. Kaslow *et al.*, "Influence of combinations of human major histocompatibility complex genes on the course of HIV-1 infection," (in eng), *Nature medicine,* vol. 2, no. 4, pp. 405-11, Apr 1996.

[11] X. Gao *et al.*, "Effect of a single amino acid change in MHC class I molecules on the rate of progression to AIDS," (in eng), *The New England journal of medicine,* vol. 344, no. 22, pp. 1668-75, May 31 2001, doi: 10.1056/nejm200105313442203.

[12] R. Draenert *et al.*, "Constraints on HIV-1 evolution and immunodominance revealed in monozygotic adult twins infected with the same virus," *J Exp Med,* vol. 203, no. 3, pp. 529-39, Mar 20 2006. [Online]. Available: http://www.ncbi.nlm.nih.gov/entrez/query.fcgi?cmd=Retrieve&db=PubMed&dopt=Citation&list_uids=16533886

[13] A. Kosmrlj *et al.*, "Effects of thymic selection of the T-cell repertoire on HLA class I-associated control of HIV infection," (in eng), *Nature,* vol. 465, no. 7296, pp. 350-4, May 20 2010, doi: 10.1038/nature08997.

[14] A. J. Leslie *et al.*, "HIV evolution: CTL escape mutation and reversion after transmission," *Nature medicine,* vol. 10, no. 3, pp. 282-9, Mar 2004. [Online]. Available: http://www.ncbi.nlm.nih.gov/entrez/query.fcgi?cmd=Retrieve&db=PubMed&dopt=Citation&list_uids=14770175.

[15] H. Crawford *et al.*, "Evolution of HLA-B*5703 HIV-1 escape mutations in HLA-B*5703-positive individuals and their transmission recipients," *J Exp Med,* Research Support, N.I.H., Extramural

Research Support, Non-U.S. Gov't vol. 206, no. 4, pp. 909-21, Apr 13 2009, doi: 10.1084/jem.20081984.

[16] P. Kiepiela *et al.*, "CD8+ T-cell responses to different HIV proteins have discordant associations with viral load," (in eng), *Nature medicine,* vol. 13, no. 1, pp. 46-53, Jan 2007, doi: 10.1038/nm1520.

[17] N. Goonetilleke *et al.*, "The first T cell response to transmitted/founder virus contributes to the control of acute viremia in HIV-1 infection," (in eng), *J Exp Med,* vol. 206, no. 6, pp. 1253-72, Jun 8 2009, doi: 10.1084/jem.20090365.

[18] O. O. Yang *et al.*, "Determinant of HIV-1 mutational escape from cytotoxic T lymphocytes," *J Exp Med,* vol. 197, no. 10, pp. 1365-75, May 19 2003, doi: 10.1084/jem.20022138.

[19] J. K. Wright *et al.*, "Gag-protease-mediated replication capacity in HIV-1 subtype C chronic infection: associations with HLA type and clinical parameters," (in eng), *Journal of virology,* vol. 84, no. 20, pp. 10820-31, Oct 2010, doi: 10.1128/jvi.01084-10.

[20] M. A. Brockman *et al.*, "Early selection in Gag by protective HLA alleles contributes to reduced HIV-1 replication capacity that may be largely compensated for in chronic infection," *Journal of virology,* vol. 84, no. 22, pp. 11937-49, Nov 2010, doi: 10.1128/JVI.01086-10.

[21] S. J. Davis and P. A. van der Merwe, "The structure and ligand interactions of CD2: implications for T-cell function," *Immunol Today,* Research Support, Non-U S Gov't

Review vol. 17, no. 4, pp. 177-87, 1996.

[22] S. J. Turner, P. C. Doherty, J. McCluskey, and J. Rossjohn, "Structural determinants of T-cell receptor bias in immunity," (in eng), *Nature reviews. Immunology,* vol. 6, no. 12, pp. 883-94, Dec 2006, doi: 10.1038/nri1977.

[23] J. Nikolich-Zugich, M. K. Slifka, and I. Messaoudi, "The many important facets of T-cell repertoire diversity," (in eng), *Nature reviews. Immunology,* vol. 4, no. 2, pp. 123-32, Feb 2004, doi: 10.1038/nri1292.

[24] A. Lissina, L. A. Chakrabarti, M. Takiguchi, and V. Appay, "TCR clonotypes: molecular determinants of T-cell efficacy against HIV," (in eng), *Current opinion in virology,* vol. 16, pp. 77-85, Feb 2016, doi: 10.1016/j.coviro.2016.01.017.

[25] K. H. Lee *et al.*, "The immunological synapse balances T cell receptor signaling and degradation," (in eng), *Science (New York, N.Y.),* vol. 302, no. 5648, pp. 1218-22, Nov 14 2003, doi: 10.1126/science.1086507.

[26] H. Chen *et al.*, "TCR clonotypes modulate the protective effect of HLA class I molecules in HIV-1 infection," *Nat Immunol,* vol. 13, no. 7, pp. 691-700, Jul 2012, doi: 10.1038/ni.2342.

[27] K. Ladell *et al.*, "A molecular basis for the control of preimmune escape variants by HIV-specific CD8+ T cells," (in eng), *Immunity,* vol. 38, no. 3, pp. 425-36, Mar 21 2013, doi: 10.1016/j.immuni.2012.11.021.

[28] M. C. Iglesias *et al.*, "Escape from highly effective public CD8+ T-cell clonotypes by HIV," *Blood,* vol. 118, no. 8, pp. 2138-49, Aug 25 2011, doi: 10.1182/blood-2011-01-328781.

[29] J. J. Miles, D. C. Douek, and D. A. Price, "Bias in the alphabeta T-cell repertoire: implications for disease pathogenesis and vaccination," (in eng), *Immunology and cell biology,* vol. 89, no. 3, pp. 375-87, Mar 2011, doi: 10.1038/icb.2010.139.

[30] S. J. Turner, N. L. La Gruta, K. Kedzierska, P. G. Thomas, and P. C. Doherty, "Functional implications of T cell receptor diversity," (in eng), *Current opinion in immunology,* vol. 21, no. 3, pp. 286-90, Jun 2009, doi: 10.1016/j.coi.2009.05.004.

[31] R. S. Ntale *et al.*, "Temporal association of HLA-B*81:01- and HLA-B*39:10-mediated HIV-1 p24 sequence evolution with disease progression," (in eng), *Journal of virology,* vol. 86, no. 22, pp. 12013-24, Nov 2012, doi: 10.1128/jvi.00539-12.

[32] F. Bihl *et al.*, "Impact of HLA-B alleles, epitope binding affinity, functional avidity, and viral coinfection on the immunodominance of virus-specific CTL responses," *J Immunol,* vol. 176, no. 7, pp. 4094-101, Apr 1 2006. [Online]. Available: http://www.ncbi.nlm.nih.gov/pubmed/16547245.

[33] J. M. Carlson *et al.*, "Correlates of protective cellular immunity revealed by analysis of population-level immune escape pathways in HIV-1," *Journal of virology,* vol. 86, no. 24, pp. 13202-16, Dec 2012, doi: 10.1128/JVI.01998-12.

[34] H. N. Kloverpris *et al.*, "CD8+ TCR Bias and Immunodominance in HIV-1 Infection," (in eng), *J Immunol,* vol. 194, no. 11, pp. 5329-45, Jun 01 2015, doi: 10.4049/jimmunol.1400854.

[35] Y. Moosa *et al.*, "Case report: mechanisms of HIV elite control in two African women," *BMC Infect Dis,* vol. 18, no. 1, p. 54, Jan 25 2018, doi: 10.1186/s12879-018-2961-8.

[36] C. K. Koofhethile *et al.*, "CD8+ T cell breadth and ex vivo virus inhibition capacity distinguish between viremic controllers with and without protective HLA class I alleles," *Journal of virology,* May 18 2016, doi: 10.1128/JVI.00276-16.

[37] A. Sette and J. Sidney, "Nine major HLA class I supertypes account for the vast preponderance of HLA-A and -B polymorphism," (in eng), *Immunogenetics,* vol. 50, no. 3-4, pp. 201-12, Nov 1999.

[38] J. Sidney, B. Peters, N. Frahm, C. Brander, and A. Sette, "HLA class I supertypes: a revised and updated classification," *BMC Immunol,* vol. 9, p. 1, Jan 22 2008, doi: 10.1186/1471-2172-9-1.

[39] P. J. Goulder *et al.*, "Differential narrow focusing of immunodominant human immunodeficiency virus gag-specific cytotoxic T-lymphocyte responses in infected African and caucasoid adults and children," *Journal of virology,* vol. 74, no. 12, pp. 5679-90., 2000. [Online]. Available: http://www.ncbi.nlm.nih.gov/cgi-bin/Entrez/referer?http://jvi.asm.org/cgi/content/abstract/74/12/5679.

[40] A. Leslie *et al.*, "Differential selection pressure exerted on HIV by CTL targeting identical epitopes but restricted by distinct HLA alleles from the same HLA supertype," (in eng), *J Immunol,* vol. 177, no. 7, pp. 4699-708, Oct 01 2006.

[41] C. Geldmacher *et al.*, "Minor viral and host genetic polymorphisms can dramatically impact the biologic outcome of an epitope-specific CD8 T-cell response," *Blood,* vol. 114, no. 8, pp. 1553-62, Aug 20 2009, doi: 10.1182/blood-2009-02-206193.

[42] H. N. Kloverpris *et al.*, "HIV control through a single nucleotide on the HLA-B locus," *Journal of virology,* vol. 86, no. 21, pp. 11493-500, Nov 2012, doi: 10.1128/JVI.01020-12.

[43] C. Geldmacher *et al.*, "CD8 T-cell recognition of multiple epitopes within specific Gag regions is associated with maintenance of a low steady-state viremia in human immunodeficiency virus type 1-seropositive patients," *Journal of virology,* vol. 81, no. 5, pp. 2440-8, Mar 2007, doi: 10.1128/JVI.01847-06.

[44] R. S. Ntale *et al.*, "Temporal association of HLA-B*81:01- and HLA-B*39:10-mediated HIV-1 p24 sequence evolution with disease progression," *J Virol,* vol. 86, no. 22, pp. 12013-24, Nov 2012, doi: 10.1128/JVI.00539-12.

[45] J. K. Wright *et al.*, "Impact of HLA-B*81-associated mutations in HIV-1 Gag on viral replication capacity," *J Virol,* vol. 86, no. 6, pp. 3193-9, Mar 2012, doi: 10.1128/JVI.06682-11.

[46] H. N. Kloverpris *et al.*, "A molecular switch in immunodominant HIV-1-specific CD8 T-cell epitopes shapes differential HLA-restricted escape," (in eng), *Retrovirology,* vol. 12, p. 20, Feb 20 2015, doi: 10.1186/s12977-015-0149-5.

[47] A. Leslie *et al.*, "Additive contribution of HLA class I alleles in the immune control of HIV-1 infection," (in eng), *Journal of virology,* vol. 84, no. 19, pp. 9879-88, Oct 2010, doi: 10.1128/jvi.00320-10.

[48] H. A. Prentice *et al.*, "HLA-B*57 versus HLA-B*81 in HIV-1 infection: slow and steady wins the race?," (in eng), *Journal of virology,* vol. 87, no. 7, pp. 4043-51, Apr 2013, doi: 10.1128/jvi.03302-12.

[49] P. J. Goulder *et al.*, "Evolution and transmission of stable CTL escape mutations in HIV infection," (in eng), *Nature,* vol. 412, no. 6844, pp. 334-8, Jul 19 2001, doi: 10.1038/35085576.

[50] P. J. Goulder *et al.*, "Late escape from an immunodominant cytotoxic T-lymphocyte response associated with progression to AIDS," *Nature medicine,* Research Support, Non-U.S. Gov't vol. 3, no. 2, pp. 212-7, Feb 1997. [Online]. Available: http://www.ncbi.nlm.nih.gov/pubmed/9018241.

[51] F. Pereyra *et al.*, "HIV control is mediated in part by CD8+ T-cell targeting of specific epitopes," (in eng), *Journal of virology,* vol. 88, no. 22, pp. 12937-48, Nov 2014, doi: 10.1128/jvi.01004-14.

[52] S. C. Threlkeld *et al.*, "Degenerate and promiscuous recognition by CTL of peptides presented by the MHC class I A3-like superfamily: implications for vaccine development," *J Immunol,* vol. 159, no. 4, pp. 1648-57, Aug 15 1997. [Online]. Available: http://www.ncbi.nlm.nih.gov/pubmed/9257824.

[53] T. M. Allen *et al.*, "De novo generation of escape variant-specific CD8+ T-cell responses following cytotoxic T-lymphocyte escape in chronic human immunodeficiency virus type 1 infection," (in eng), *Journal of virology,* vol. 79, no. 20, pp. 12952-60, Oct 2005, doi: 10.1128/jvi.79.20.12952-12960.2005.

[54] T. Ueno, Y. Idegami, C. Motozono, S. Oka, and M. Takiguchi, "Altering effects of antigenic variations in HIV-1 on antiviral effectiveness of HIV-specific CTLs," (in eng), *J Immunol,* vol. 178, no. 9, pp. 5513-23, May 01 2007.

[55] J. R. Almeida *et al.*, "Antigen sensitivity is a major determinant of CD8+ T-cell polyfunctionality and HIV-suppressive activity," *Blood,* vol. 113, no. 25, pp. 6351-60, Jun 18 2009, doi: 10.1182/blood-2009-02-206557.

[56] T. Akahoshi, T. Chikata, Y. Tamura, H. Gatanaga, S. Oka, and M. Takiguchi, "Selection and accumulation of an HIV-1 escape mutant by three types of HIV-1-specific cytotoxic T lymphocytes recognizing wild-type and/or escape mutant

epitopes," (in eng), *Journal of virology,* vol. 86, no. 4, pp. 1971-81, Feb 2012, doi: 10.1128/jvi.06470-11.

[57] G. Anmole *et al.*, "A robust and scalable TCR-based reporter cell assay to measure HIV-1 Nef-mediated T cell immune evasion," (in eng), *Journal of immunological methods,* vol. 426, pp. 104-13, Nov 2015, doi: 10.1016/j.jim.2015.08.010.

[58] G. M. Gillespie *et al.*, "Cross-reactive cytotoxic T lymphocytes against a HIV-1 p24 epitope in slow progressors with B*57," *AIDS,* vol. 16, no. 7, pp. 961-72, May 3 2002. [Online]. Available: https://www.ncbi.nlm.nih.gov/pubmed/11953462.

[59] J. E. Sunshine *et al.*, "Fitness-Balanced Escape Determines Resolution of Dynamic Founder Virus Escape Processes in HIV-1 Infection," *Journal of virology,* vol. 89, no. 20, pp. 10303-18, Oct 2015, doi: 10.1128/JVI.01876-15.

[60] M. R. Henn *et al.*, "Whole genome deep sequencing of HIV-1 reveals the impact of early minor variants upon immune recognition during acute infection," *PLoS Pathog,* vol. 8, no. 3, p. e1002529, 2012, doi: 10.1371/journal.ppat.1002529.

[61] O. Y. Borbulevych *et al.*, "T cell receptor cross-reactivity directed by antigen-dependent tuning of peptide-MHC molecular flexibility," *Immunity,* vol. 31, no. 6, pp. 885-96, Dec 18 2009, doi: 10.1016/j.immuni.2009.11.003.

[62] B. E. Willcox *et al.*, "TCR binding to peptide-MHC stabilizes a flexible recognition interface," (in eng), *Immunity,* vol. 10, no. 3, pp. 357-65, Mar 1999.

[63] K. M. Armstrong, K. H. Piepenbrink, and B. M. Baker, "Conformational changes and flexibility in T-cell receptor recognition of peptide-MHC complexes," *Biochemistry Journal,* vol. 415, no. 2, pp. 183-96, Oct 15 2008, doi: 10.1042/BJ20080850.

[64] J. J. Miles, J. McCluskey, J. Rossjohn, and S. Gras, "Understanding the complexity and malleability of T-cell recognition," *Immunology and cell biology,* vol. 93, no. 5, pp. 433-41, May-Jun 2015, doi: 10.1038/icb.2014.112.

[65] M. Bunce, "PCR-sequence-specific primer typing of HLA class I and class II alleles," (in eng), *Methods in molecular biology (Clifton, N.J.),* vol. 210, pp. 143-71, 2003.

[66] C. F. Thobakgale *et al.*, "Human immunodeficiency virus-specific CD8+ T-cell activity is detectable from birth in the majority of in utero-infected infants," (in eng), *Journal of virology,* vol. 81, no. 23, pp. 12775-84, Dec 2007, doi: 10.1128/jvi.00624-07.

[67] D. Bernal-Estevez, R. Sanchez, R. E. Tejada, and C. Parra-Lopez, "Chemotherapy and radiation therapy elicits tumor specific T cell responses in a breast cancer patient," (in eng), *BMC cancer,* vol. 16, p. 591, Aug 03 2016, doi: 10.1186/s12885-016-2625-2.

[68] A. Han, J. Glanville, L. Hansmann, and M. M. Davis, "Linking T-cell receptor sequence to functional phenotype at the single-cell level," (in eng), *Nature biotechnology,* vol. 32, no. 7, pp. 684-92, Jul 2014, doi: 10.1038/nbt.2938.

[69] M. A. Brockman, G. O. Tanzi, B. D. Walker, and T. M. Allen, "Use of a novel GFP reporter cell line to examine replication capacity of CXCR4- and CCR5-tropic HIV-1 by flow cytometry," *J Virol Methods,* vol. 131, no. 2, pp. 134-42, Feb 2006, doi: 10.1016/j.jviromet.2005.08.003.

[70] R. Suzuki and H. Shimodaira, "Pvclust: an R package for assessing the uncertainty in hierarchical clustering," *Bioinformatics,* vol. 22, no. 12, pp. 1540-2, Jun 15 2006, doi: 10.1093/bioinformatics/btl117.

Chapter 4. Structural and functional characterization of an expanded panel of HLA-B*42 TL9 specific TCR

4.1. Contributions

In this chapter, I use the terms “we” and “our” in cases where I did not conduct all of the presented work. My direct roles in this project were: 1) to gather all of the TCR sequences and *in vitro* functional data; 2) to develop and implement an Illumina-based protocol to collect paired TCR alpha/beta sequences; and 3) to manage multiple external collaborations, including expert technical, bioinformatics and structural biology support to strengthen data collection and analysis. Technical assistance for Illumina sequencing (described in **Figure 4-2**) was provided by Winnie Dong at the BC Center for Excellence in HIV/AIDS. Bioinformatics assistance to develop a TCR sequence analysis pipeline (summarized in **Figure 4-3**) was provided by Jeff Knaggs at the BC Center for Excellence in HIV/AIDS. I also trained and supervised an undergraduate student, Nathan Chatron, who assisted in the collection of functional data using large peptide screens (shown in **Figure 4-4**, **4-5**, **4-6** and **4-7)**. Finally, the laboratory of Dr. George Gao (Chinese Academy for Sciences), led by Dr. Shuguang Li, completed all of the structural biology work (shown in **Figures 4-6** and **4-8)**.

4.2. Introduction

HLA-B*81 is associated with control of HIV-1 subtype C infection [1, 2]. HIV-infected individuals who express B*81 display significantly lower plasma viral loads and slower disease progression compared to population averages. Interestingly, the closely related HLA-B*42 allele is not typically associated with viral control [1, 3-8], despite the fact that B*81 and B*42 both belong to the HLA B7 supertype [9, 10] and both alleles present a very similar array of HIV-derived peptide epitopes, including the immunodominant Gag p24 epitope TL9 (TPQDLNTML) [11-13]. Detailed studies of the CD8+ T cell response to TL9 in the setting of B*81 and B*42 may provide new insight into mechanisms that contribute to HIV control.

In our previous study [14] (also **Chapter** 3 of this thesis), we identified a unexpected population of CD8+ T cells that displayed dual-reactivity for TL9 bound to both B*81 and B*42, which was also associated with lower plasma viral loads in our South Africa cohort. We validated the dual-reactive phenotype of individual TCR clones using a Jurkat reporter cell assay. Notably, we observed that dual-reactive TCR clones were enriched for use of the *TRBV12-3* gene and that the dual-reactive population in B*42 individuals was dominated by several public TCR alpha/beta clonotypes, including one that was found in all three B*42 individuals tested. Furthermore, dual-reactive TCR clones from B*42 individuals (as well as TCR clones encoding *TRBV12-3* derived from B*81 individuals) demonstrated a greater capacity to recognize TL9 variants, suggesting that cross-reactivity towards viral escape mutants is a critical mechanism of HIV control in this setting. However, our conclusions were based largely on data from eight TCR clones, including only five clones derived from B*42 individuals. This chapter aims to address several questions that remained after completion of our prior study, specifically:

1) Can we strengthen our observations (and conclusions) by examining a larger panel of TL9-specific TCR clones? In particular, will other dual-reactive TCR clones display a similar profile of cross-reactivity and recognition of TL9 escape variants?
2) Is TCR antigen sensitivity associated with cross-reactivity towardsTL9 peptide variants?
3) What are the structural determinants of TL9 specificity and dual-reactivity?
4) How can we selectively elicit or expand dual-reactive TCR responses?

Here, I present a more comprehensive sequence, functional and structural analysis of TL9-specific TCR clonotypes from B*42 and B*81 individuals, focusing on features of dual-reactive TCR clones derived from B*42 individuals that may contribute to HIV control. I describe my efforts to develop an Illumina-based sequencing strategy to identify paired TCR alpha/beta genes from single-cell T cells, provide additional *in vitro* functional analysis of selected B*42-derived TCR clones, and highlight the exciting results of a collaboration to define the ternary structure of dual-reactive TCR bound to peptide/HLA antigens.

4.3. Results

4.3.1. High-throughput paired TCR sequencing identifies new clones

To expand our panel of B*42 TL9-specific TCR clones for functional studies, I initially used nested PCR and Sanger-based methods (as described in **Chapter 3**) to amplify and sequence additional TCR alpha gene products from clones with known TCR beta sequences in order to generate additional paired information. This targeted sequencing approach generated data for eight additional B*42-derived TCR clones, resulting in a total of 13 TCR clones that could be pursued for functional studies (shown in **Figure 4-1**).

To further enhance our capacity to collect paired TCR alpha/beta sequence data from single T cells, I collaborated with scientists at the BC Centre for Excellence in HIV/AIDS (Vancouver, BC) to establish an Illumina-based sequencing strategy. To do this, we adapted the primer set and methods described by Han et al. [15] and optimized them for the BC Centre's standard workflow using an Illumina miSeq instrument. The barcoding strategy was adopted from Lapointe et al. [16]. Briefly, I used existing first-round RT-PCR products (described in Chapter 3) as templates for a nested 2$_{nd}$ round PCR reaction to attach universal Illumina linkers and a 3$_{rd}$ round PCR reaction to attach unique forward and reverse barcodes to each product, thus allowing multiplexed products to be analyzed on the Illumina Miseq instrument. The final amplification strategy (shown in **Figure 4-2**) will allow PCR amplicons from up to 20 96-well plates (up to 1920 individual cells) to be combined on a single sequencing run. I also worked with an expert in bioinformatics to develop a dedicated TCR sequence analysis pipeline (illustrated in **Figure 4-3).** This automated pipeline de-multiplexes the Illumina samples, cleans the data (i.e. removes primer-dimer and other products of unexpected size), and determines the most likely TCR gene usage and CDR3 motifs. The final data is then exported as a csv file, allowing the composition of the TCR repertoires, such as clonal frequencies, to be examined. Using this new approach, I re-sequenced all of the mono and dual-reactive T cell populations described in Chapter 3 (N=12 96-well plates) and successfully isolated additional paired TCR sequences. Notably, with the Sanger-based methods, we were able to generate paired alpha/beta sequences for 27 TCR clonotypes across all 12 PCR plates. Using the Illumina-based strategy, we isolated a total of 49

paired TCR clonotypes, including all 27 that were known from Sanger sequencing, plus 22 new clones. In addition to the improved throughput and robustness of the data, the Illumina-based method requires substantially less time and effort.

A

TCR ID	TRAV	TRAJ	CDR3 Alpha	TRBV	TRBJ	CDR3 Beta
7A10	12-1*01	31*01	CVVNIRGNARLMF	12-3*01	1-3*01	CASRFGTGSGNTIYF
7C12	19*01	53*01	CALSGPMPLNSGGSNYKLTF	12-3*01	2-1*01	CASLHYSGTGNDNEQFF
7A4	26-2*01	39*01	CILRGLFNAGNMLTF	12-3*01	2-6*01	CASSLGSSGANVLTF
13A10	16*01	18*01	CALRGRGSTLGRLYF	7-9*01	2-1*01	CASSSSLTGVTSYNEQFF
13D8	19*01	56*01	CALSDFPGANSKLTF	11-2*01	1-3*01	CASSLFGLEPTSGNTIYF
13B11	12-1*01	26*01	CVVTLYGQNFVF	7-9*01	1-3*01	CASSSTQTGVSVSGNTIYF

B

TCR ID	TRAV	TRAJ	CDR3 Alpha	TRBV	TRBJ	CDR3 Beta
14A4	13-1*01	38*01	CAATNAGNNRKLIW	12-3*01	1-1*01	CASSFSKNTEAFF
14A9	26-1*01	39*01	CIVRTFLNNAGNMLTF	12-3*01	1-1*01	CASSLAGEAFF
14A10	26-1*01	49*01	CIVRSFLTNTGNQFYF	12-3*01	1-3*01	CASSLGASEAFF
14D7	13-1*01	38*01	CAATNAGNNRKLIW	12-3*01	1-1*01	CASSHSKNTEAFF
16A12	26-1*01	39*01	CIVRGLYNAGNMLTF	12-3*01	1-3*01	CASSLGANTIYF
16A11	13-1*01	38*01	CAACNAGNNRKLIW	12-3*01	1-1*01	CASSYSKNTEAFF
16A7	26-1*01	39*01	CIVRAPSNAGNMLTF	12-3*01	1-3*01	CASSLGLNTIYF

Figure 4-1. Expanded panel of B*42-TL9 specific TCR clones.
Sanger-based sequencing was used to identify additional TCR alpha genes that paired with existing TCR beta data from Chapter 3. In total, 13 TCR derived from B*42 individuals were selected for functional analysis. **Panel A** shows the characteristics of six mono B*42-TL9 specific TCR clones. **Panel B** shows characteristics of seven dual B*42/B*81-TL9 specific TCR clones. Highlighted clone IDs (first column) indicate the five

clones that were assessed in **Chapter 3** (and [14]). Dual-reactive TCR highlighted in red text represent public clonotypes, based on our analysis of only three B*42 individuals.

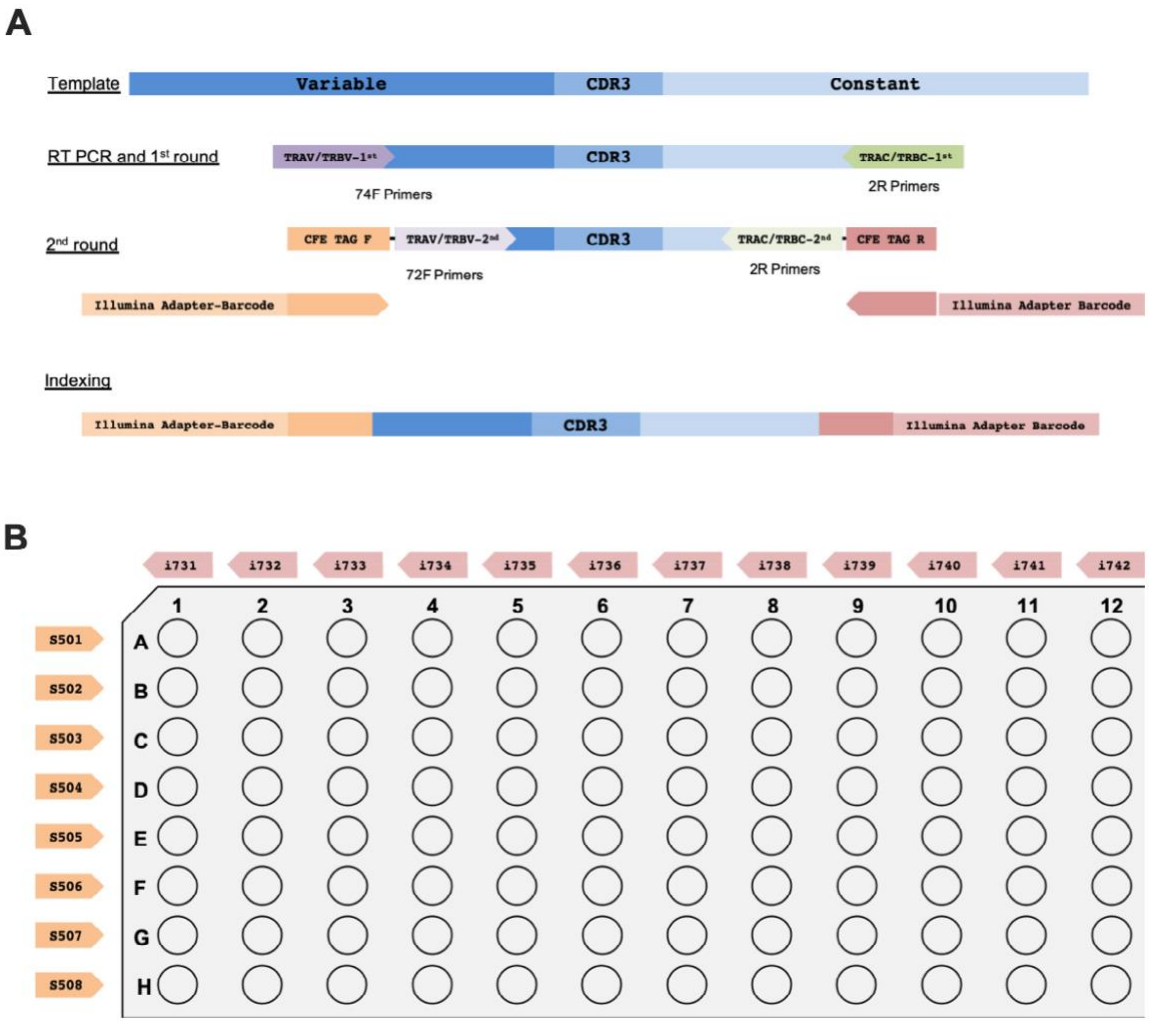

Figure 4-2. TCR amplification strategy for Illumina based sequencing.

TCR amplification is conducted from a single cell to generate paired TCR alpha and beta sequences. The primer and amplification strategy is highlighted in panel (A). First round RT-PCR is performed with a cocktail of forward and reverse primers encompassing both TCR alpha and beta genes. First round primer sequences are shown in the Appendix Table 3-2. This is followed by a second round nested PCR that attaches universal forward and reverse nucleotide tags, labelled “CFE TAG F” and “CFE TAG R”. The 2nd round primer sequences and the TAG sequences are included in Appendix Table 4-1. This is followed by an 3rd round indexing reaction that attaches a unique, 8-nt long, sequence and the Illumina adapter sequence to the contents of each well PCR reaction,

which ideally contains TCR from one T-cell (B). We have access to a barcoding strategy where 1920 unique TCR amplification reactions can be individually barcoded and have 4 sets of “S” series and 5 sets of “i” series barcodes for use and this panel is representation of 96 samples.

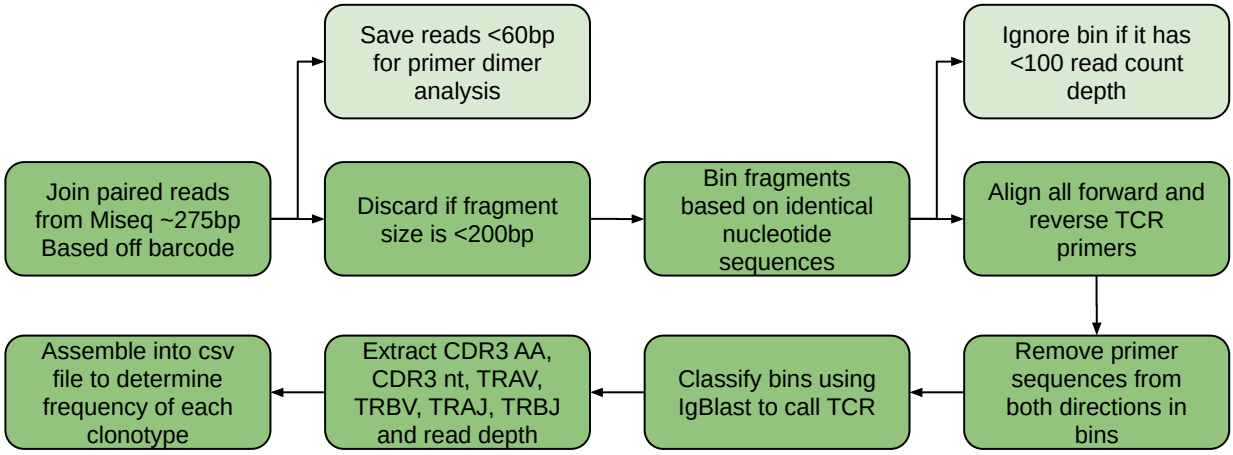

Figure 4-3. Data analysis pipeline for TCR MiSeq.
This figure summarizes the current analysis pipeline for TCR sequencing using the Miseq. This automated pipeline de-multiplexes, cleans and bins TCR sequences for analysis. TCR clones are classified using IgBlast and results are exported as a csv file – allowing the frequency of individual clones and the composition of the repertoire to be determined.

4.3.2. Dual-reactive B*42-derived TCR clones display increased ability to recognize TL9 peptide variants

To extend my analysis of TL9-specific TCR clones presented in **Chapter 3** (and [14]), I selected seven additional TCR clones isolated from B*42 individuals for functional studies (for a total of 13 B*42-derived TCR; see **Figure 4-1**). I chose to focus on B*42-derived TCR clones in order to confirm the striking functional differences that we observed between mono and dual-reactive TCR clones from this population. To generate peptide recognition profiles for the eight new TCR clones, each TCR was synthesized and tested for reactivity towards a panel of TL9 variants using our Jurkat reporter assay, as described in Chapter 3. Briefly, GXR-B*42 cells were pulsed with 2.1 µg of peptide (either TL9 or one of 171 single amino acid variants) and then co-cultured with Jurkat cells expressing TCR, CD8 and an NFAT-driven luciferase reporter vector. TCR recognition of each peptide variant was measured as the amount of NFAT-driven luminescence (absolute light units), normalized to the average of the nine co-cultures containing wildtype TL9. A representative heat map, summarizing the recognition data for TCR clone 14A4 is shown in **Figure 4-4 A**. Here, the intensity of red indicates the strength of signaling for each peptide variant; black boxes highlight wildtype TL9

residues. Representative heat maps for all TCR clones are included in **Appendix Figure 4-1**. To assess similarity in the patterns of TL9 variant recognition among clones, we conducted a hierarchical clustering analysis for data from all 13 B*42-derived TCR clones using correlation distances and single linkage methods (5,000 iterations), implemented in PVCLUST (http://stat.sys.i.kyoto-u.ac.jp/ prog/pvclust/). As shown by the dendrogram in **Figure 4-4 B**, the dual-reactive TCR clones formed a distinct cluster compared to mono-reactive clones, suggesting that they share distinct peptide-recognition properties. This is consistent with data presented in **Chapter 3,** which further indicated that dual-reactive B*42-derived TCR were functionally more similar to B*81-derived TCR, compared to mono-reactive B*42-derived TCR.

In Chapter 3, I observed that dual-reactive TCR clones displayed an enhanced ability to recognize naturally occurring HIV escape and "escape pathway" variants **(Figure 3-6).** I therefore wanted to assess this phenotype in the new B*42-derived TCR clones. However, a limitation of the prior study is that TL9 escape variant peptides were examined only at a single, high concentration of peptide (20 μM). To overcome this concern, I repeated this analysis of all 13 B*42-derived TCR clones using a range of lower doses for wildtype TL9 and variant peptides (20 μM, 1.3 μM, 0.09 μM and 0 μM). In addition to testing the pathway variants described in Chapter 3 (namely, Q3P, Q3K, Q3E, Q3R), I also looked more carefully at the four most common single amino-acid mutations observed in TL9 (T7S, Q3S, Q3T, and Q3G; highlighted in the grey box in **Figure 4-5 A**), which are each present at a frequency of 10% or greater in HIV-1 subtype C sequences from the Los Alamos National Laboratory's HIV Sequence Database (http://www.hiv.lanl.gov). Representative results of TL9 and Q3P peptide titrations for four TCR clones are shown in **Figure 4-5 B.** Summary results for all TCR clones and all peptides are shown as a in **Figure 4-5 C**. For this analysis, I set a conservative threshold for TCR recognition, such that signal strengths below 0.25 relative light units compared to wildtype TL9 at the 1.3μM peptide dose were considered to be negative. In the figure, green boxes indicate recognition, red boxes indicate no recognition and orange boxes indicate scenarios where the escape mutation itself is not recognized, but all pathway mutations leading to the variant are recognized by the TCR clone. A specific example of this is TCR 14A4, which does not recognize Q3S, but does recognize the pathway mutation Q3P. In order for HIV to mutate from Q to S, it must adopt a pathway P to eventually escape. These results confirm the observations of my

earlier studies (Chapter 3) and suggest that the ability of TCR clones to recognize certain intermediate mutations may prevent HIV from adapting most efficiently to the CD8+ T cell response. Indeed, when I assessed the expected ability of each TCR clone to recognize common HIV escape variants and pathways leading to these variants (i.e. by calculating a total recognition score that was the sum of the frequency of each mutation recognized plus those blocked by pathway recognition; maximum value of 65), I found that the dual-reactive TCR clones displayed a significantly higher ability to recognize HIV escape variants compared to mono-reactive clones (**Figure 4-5 D**).

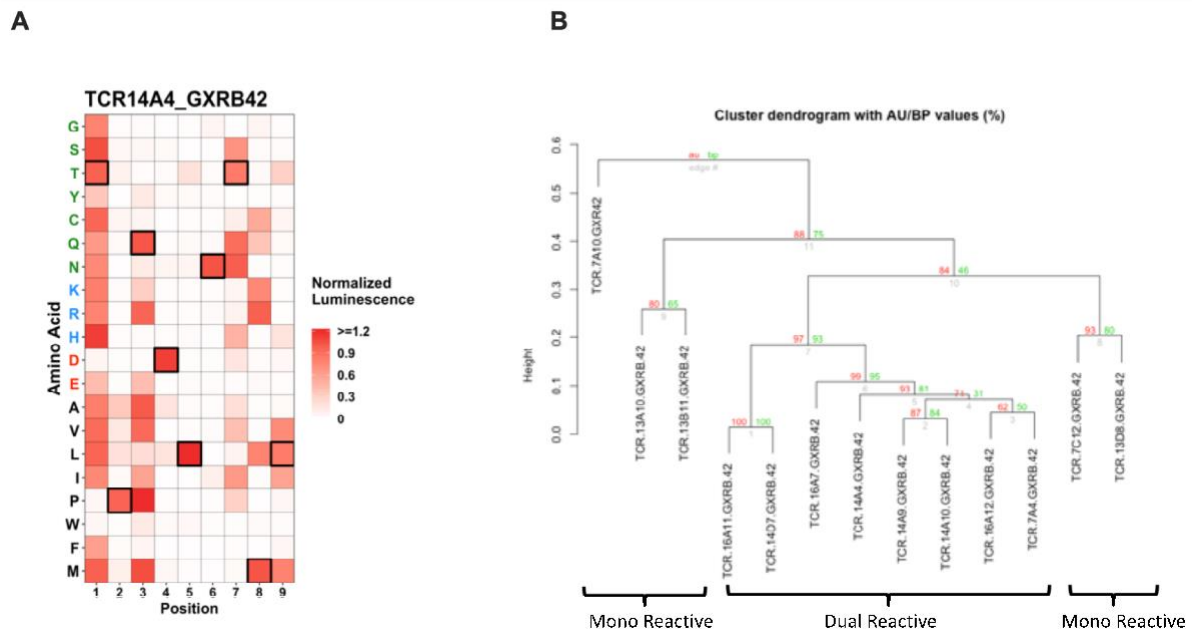

Figure 4-4. Peptide variant screen and hierarchical clustering of cross-reactivity profiles indicated dual reactive TCR form a functional cluster.
A) Representative heat map summarizing cross reactivity profile of TCR 14A4 towards TL9 variants spanning all 20 amino acids substituted from TL9 positions 1-9. Intensity of heat map indicates strength of signaling relative to WT TL9 (boxes). The On the y-axis are amino acids and the x- axis are the positions 1-9. This was conducted for the 8 additional clones that are a part of this follow-up study (listed in figure 1) and the cross-reactivity profiles were subjected to hierarchical clustering using correlation distances and single linkage methods (5,000 iterations) implemented in pvclust (http://stat.sys.i.kyoto-u.ac.jp/ prog/pvclust/) **(B)**. The dual reactive TCR cluster more closely with one another compared to the mono TCR. The dendrogram (top) displays approximately unbiased (au) p-values in red text and bootstrap probability (bp) values in green text.

4.3.3. Antigen sensitivity and TCR cross reactivity

In addition to cross-reactivity towards HIV escape variants, the level of antigen sensitivity that a TCR displays towards wildtype or variant peptides is also expected to contribute to CD8+ T-cell mediated control [17]. Thus, linked data on TCR cross-reactivity and antigen sensitivity may provide a more complete functional understanding of how an individual's TCR repertoire contributes to HIV control. The Jurkat reporter cell assay that I have used offers a somewhat unique measure of antigen sensitivity that might be useful to compare TCR clones. Specifically, because the assay detects NFAT-mediated signaling following co-culturing with peptide-pulsed cells, it provides a quantifiable value of signaling strength (presumably related to Calcium flux) that might differ among clones exposed to the same dose of an antigen.

To assess antigen sensitivity, I tested the reactivity of all 13 B*42-derived TCR clones to a limiting dose of wildtype TL9 peptide (**Figure 4-6 A;** y-axis refers to fold induction of each TCR relative to no peptide). Both, the mono- and the dual-reactive TCR clones displayed a broad range of signaling capacities using this assay. As such, no association was found between the sensitivity of a TCR clone for wildtype TL9 and its ability to cross-recognize TL9 variants. For example, the mono-reactive TCR clone 13A10 and the dual-reactive clone 14A9 displayed similar high antigen sensitivities, though their cross-reactivity profiles are markedly different. Nevertheless, the TCR clone with the highest antigen sensitivity for wildtype TL9 (namely, 14A10) is also dual-reactive, suggesting that this clonotype might be particularly beneficial for HIV control. A similar rank-order of TCR signaling function was observed in repeated tests using smaller panel of TCR clones (**Figure 4-6 B**), showing the reproducibility of these results and demonstrating that TCR 14A10 displayed significantly higher signaling capacity compared to other TCR clonotypes.

A

Name	Sequence	Alignment	Freq	Pathway
T7S	TPQDLNSML	------S--	23.4	-
Q3S	TPSDLNTML	--S------	16.5	P
Q3T	TPTDLNTML	--T------	15.2	P/K
Q3G	TPGDLNTML	--G------	10.1	E/R
Q3A	TPADLNTML	--A------	7.6	P/E
Q3G	TPHDLNTML	--H------	5.5	-
T7M	TPQDLNMML	------M--	2.9	-
Q3E	TPEDLNTML	--E------	2.5	-
T7A	TPQDLNAML	------A--	2.3	-
Q3V	TPVDLNTML	--V------	2.2	L/E
M9F	TPQDLNTMF	--------F	2.0	-
L5M	TPQDMNTML	----M----	2.0	-
P2S	TSQDLNTML	-S-------	1.9	-
L5I	TPQDINTML	----I----	1.3	-
Q3R	TPRDLNTML	--R------	1.0	-
T7V	TPQDLNVML	------V--	1.0	I/M/A
Q3D	TPDDLNTML	--D------	0.9	-
Q3P	TPPDLNTML	--P------	0.9	-
T7I	TPQDLNIML	------I--	0.7	-

B

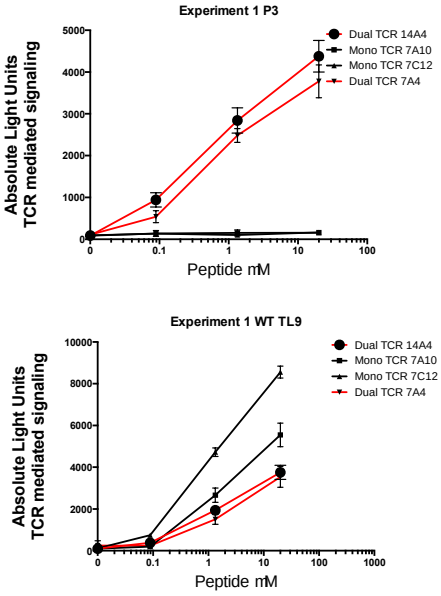

C

TCR Name	TL9	T7S	Q3S	Q3T	Q3G	Q3P	Q3K	Q3E	Q3R
Mono 7A10	+	+	-	-	-	-	-	-	-
Mono 7C12	+	-	-	-	-	-	-	-	-
Mono 13A10	+	-	-	-	-	-	+	+	+
Mono 13D8	+	+	-	-	-	-	-	+	+
Mono 13B11	+	+	-	+	-	-	+	-	+
Dual 14A4	+	+	-	-	-	+	-	-	+
Dual 7A4	+	+	-	-	-	+	+	-	+
Dual 14A9	+	+	-	-	-	+	-	-	+
Dual 14A10	+	+	-	-	-	+	-	-	+
Dual 14D7	+	+	-	-	-	+	-	-	+
Dual 16A7	+	+	-	-	-	+	-	+	-
Dual 16A11	+	+	-	-	-	+	-	-	-
Dual 16A12	+	+	-	-	-	+	+	-	+

~1.33uM of Peptide and >0.25 WT TL9 signal

D

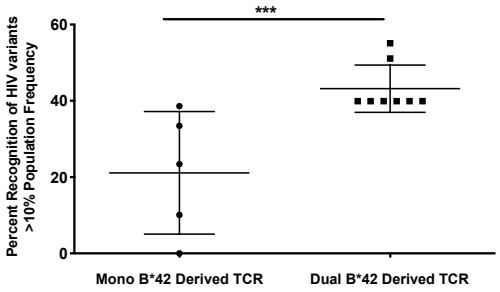

Figure 4-5. Dual reactive TCR have increased capacity to recognize HIV escape. The frequency of naturally occurring single amino acid TL9 variants is shown in panel **A**. "Pathway" amino acids substitutions required to achieve eventual escape are listed in the table under the "Pathway" column. For the cross reactivity analysis, we focused on testing TCR cross reactivity to variants present at a frequency of >10% in the total single amino acid variant sequence space (HIV LANL). Wild-type, escape and pathway to escape peptides (TL9, T7S, Q3S, Q3T, Q3G, Q3P) were titrated on HLA B*42 expressing GXR target cells and these were co cultured with reporter Jurkat cells to measure signaling. Representative graphs (**B**) showing wild-type and Q3P where the x-axis indicates absolute light units, from the Jurkat reporter cell and the x-axis is showing peptide dose and error bars indicate a mean and SEM of 3 co-culture replicates **(C)**. A

recognition score was given If TCR recognized the HIV escape variant or all pathway variants at 1.33μM peptide with signaling capacity >0.25 compared to wild-type TL9. The "recognition score" of a variant is simply the frequency at which it is present at a population level. (**D**) Sum of scores is shown on the y-axis and as illustrated, dual reactive TCR have significantly higher levels HIV escape recognition compared to the mono TCR. The statistical test preformed was a Mann-Whitney test, p=0.0008. These data are representative of N=2.

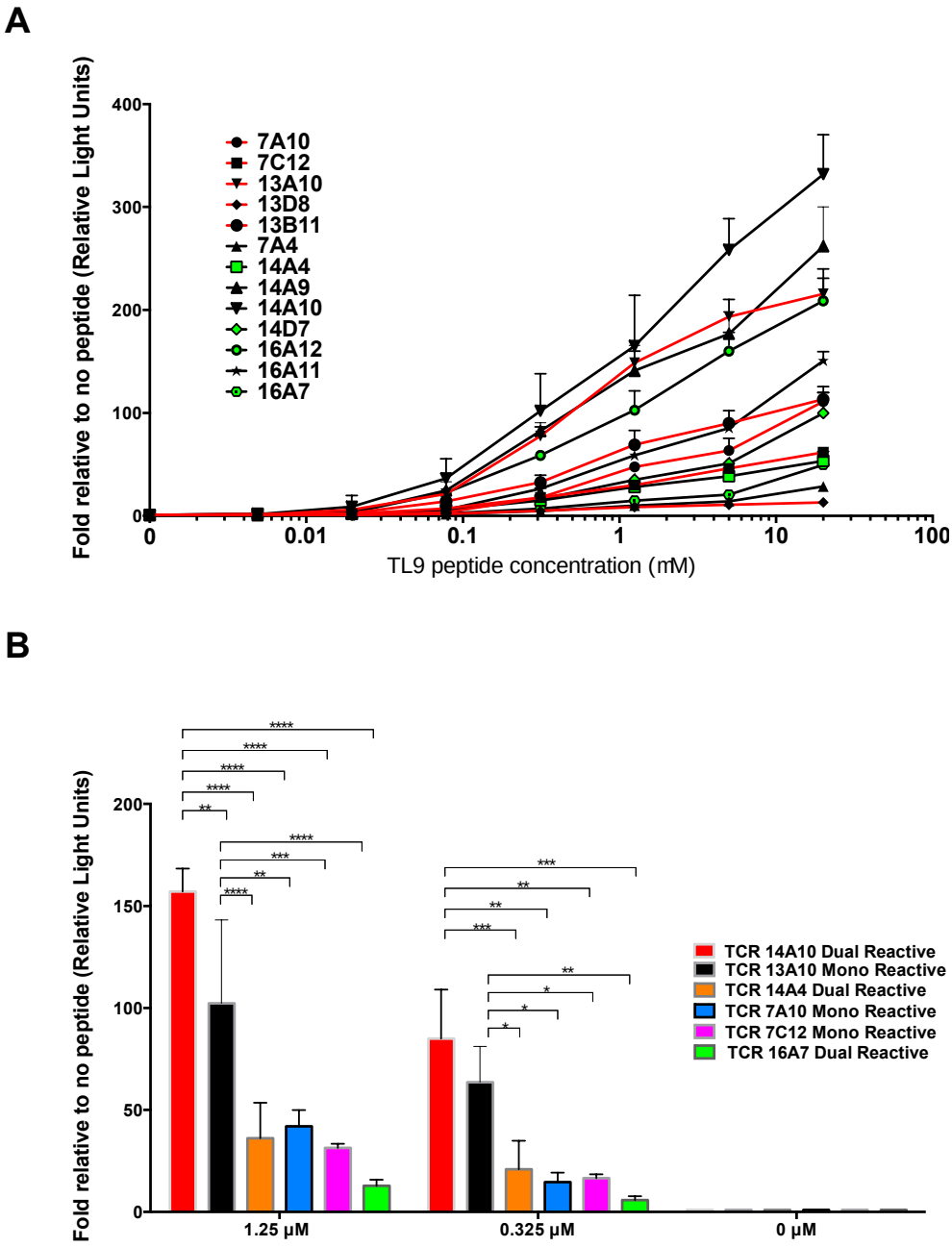

Figure 4-6. TCR have a range of antigen sensitivity across Mono and Dual TCR. (**A**) To assess antigen sensitivity, TCR reactivity was tested over a range of TL9 concentrations. The y-axis indicates fold-change relative to no peptide controls (relative light units) while the x-axis displays the peptide concentration in µM. Red lines indicate mono-B*42-reactive TCR and black lines indicate dual-reactive TCR. "Pubic" TCR clones are highlighted using green symbols. A wide range of TCR signaling capacities was observed among mono- and dual-reactive TCR clones, indicating that cross-reactivity did not necessary correlate with antigen sensitivity. Data represents one experiment with 3 technical replicates. (**B**) The dual-reactive TCR clone 14A10 displayed the highest antigen sensitivity in repeated tests compared to other representative mono- and dual-reactive clones. Results represent the mean ± S.D. of combined data from at least 2 independent experiments (4 for TCR 14A4 and 3 for TCR 13A10). Significance was assessed using a two-way ANOVA adjusted for multiple comparisons (* ≤0.05; ** ≤0.01;*** ≤0.001; ****<0.0001). The y-axis indicates TCR signaling capacity fold relative to no peptide (relative light units) and x-axis indicated peptide dose.

4.3.4. Structural determinants of TCR binding and cross-reactivity

A prior report by Kloverpris et al. [6] demonstrated that the TL9 peptide adopts distinct conformations upon binding to HLA-B*81 and B*42 (see **Figure 4-7 A and B)**. In particular, the structures show that the asparagine residue located at TL9 position 6 (N6) is exposed to solvent (and presumably exposed to TCR) when the peptide is bound to B*81, whereas this residue is buried in the HLA binding groove when the peptide is bound to B*42. At the time, these structural results were consistent with several other reports from the Goulder and Koup laboratories [11, 13, 18] that observed different TCR repertoires associated with TL9-specific CD8+ T cells from B*81 versus B*42 individuals, including selective *TRBV12-3* gene usage in responses from B*81 individuals.

Given this background, our observation that some TCR clones were dual-reactive for TL9 bound to both B*42 and B*82 was unexpected. Based on my functional data, dual-reactive B*42-derived TCR clones displayed very similar peptide recognition profiles as B*81-derived clones, which suggested to us that these TCR were likely to use similar mechanisms to engage peptide/HLA. However, it is hard to reconcile this model with the reported peptide/HLA structures, since they seem to be inconsistent with a shared mechanism of TCR binding. I considered several possible solutions to this problem. One plausible scenario is that TCR engagement influences the conformation of the TL9 peptide bound to HLA. If true, the structures from Kloverpris et al. may be the lowest energy state in the absence of TCR, but we would expect to find a different structure in the presence of TCR. Alternatively, the dual-reactive TCR might engage both TL9/HLA molecules using an unusual orientation that was unaffected by changes at

residue N6. We decided that the only way to conclusively address this question was to attempt to gather structural information for our dual-reactive TCR clones.

To do this, we established a collaboration with Dr. George Gao's laboratory at the Chinese Academy of Sciences, who has expertise in x-ray crystallography of immune receptors. In consultation with the Gao lab, we defined a list of priority TCR clones that displayed high antigen sensitivity and dual-reactivity. Using my paired TCR alpha/beta sequences, their lab expressed the proteins and generated crystal structures of two dual-reactive TCR bound to TL9/HLA antigens. TCR clone 14A9 was successfully crystalized with TL9 bound to B*81 and B*42 (at 2.7 Å and 2.1 Å resolution, respectively) (**Figure 4-7**); while TCR clone 14A4 was crystalized with TL9 bound to B*42 (at 2.5 Å resolution) (**Appendix 4-2)**. Three key observations can be made from these tri-partite TCR/peptide/HLA structures. First, the two structures for TCR 14A9 displayed only minimal differences, demonstrating that this TCR clone engaged TL9/B*42 and TL9/B*81 using an identical binding mechanism. Second, the TL9 peptide adopted a "B*81-like" conformation in the TCR 14A9 structure with TL9/B*42, with peptide residue N6 pointed outwards to form a major site of contact with the TCR. The same B*81-like TL9 conformation was also observed in the structure of TCR 14A4 with TL9 bound to B*42 **(Appendix Figure 4-2)**. This suggests that the TL9 peptide can undergo a conformational change on B*42 concomitant with TCR binding, explaining the ability of dual-reactive TCR clones to engage both peptide/HLA ligands. Finally, and perhaps most remarkably, both dual-reactive TCR clones displayed an unconventional interaction with TL9 peptide that relied on their CDR2 beta domain (rather than CDR3 [19]), which is defined by the *TRBV12-3* gene. Similar "germ-line" biased recognition of viral peptides has been described previously [20] but to our knowledge this is the first example of a TCR interaction where the CDR3 beta domain contributes nothing to peptide binding. This unusual interaction by the CDR2 beta domain is focused on peptide residue N6, providing a simple mechanism to explain the enrichment of the *TRBV12-3* gene in TCR clones from B*81 individuals and in dual-reactive TCR clones from B*42 individuals. Additional studies will be necessary to validate these results, including structures of mono-reactive clones to demonstrate that TCR can also engage TL9/B*42 in the conformation that is expected based on prior studies by Kloverpris et al [6].

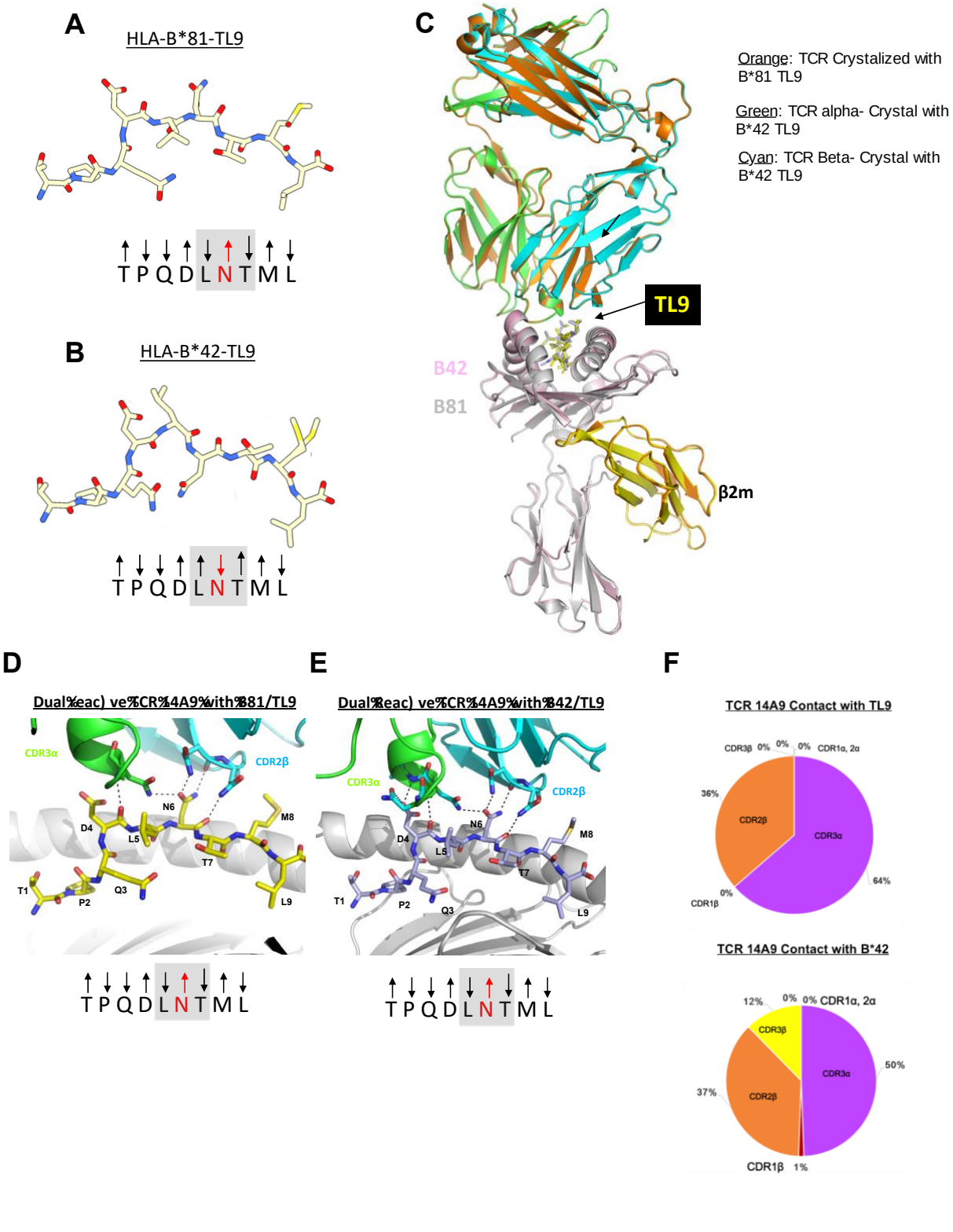
A
HLA-B*81-TL9
T P Q D L N T M L
B
HLA-B*42-TL9
T P Q D L N T M L
C
Orange: TCR Crystalized with B*81 TL9
Green: TCR alpha- Crystal with B*42 TL9
Cyan: TCR Beta- Crystal with B*42 TL9
TL9
B42
B81
β2m
D
Dual%eac) ve%TCR%14A9%with%B81/TL9
CDR3α
CDR2β
N6
D4
L5
M8
T7
T1
P2
Q3
L9
T P Q D L N T M L
E
Dual%eac) ve%TCR%14A9%with%B42/TL9
CDR3α
CDR2β
N6
D4
L5
M8
T7
T1
P2
Q3
L9
T P Q D L N T M L
F
TCR 14A9 Contact with TL9
CDR3β 0%
0%
0% CDR1α, 2α
36%
CDR2β
CDR3α
64%
0%
CDR1β
TCR 14A9 Contact with B*42
12%
0%
0% CDR1α, 2α
CDR3β
CDR3α
50%
37%
CDR2β
CDR1β 1%

Figure 4-7. Structure of B*42 dual reactive TCR bound to B*42-TL9 adopts "B*81-like" confirmation.(A and B)

In the absence of TCR, the TL9 peptide adopts a different orientation when bound to HLA-B*81 (**A**) verses B*42 (**B**) (peptide models based on Kloverpris et al. [6]). The direction of the arrows below each figure indicates that the residue is exposed to TCR (up) or buried in the HLA binding groove (down). Note the orientation of residues L5, N6 and T7; in particular, residue N6 is pointing upwards and is solvent exposed in the B*81 bound structure, while it is buried in the B*42 bound structure. (**C**) Crystal structures were solved for the tripartite complex of TCR clone 14A9 (dual-reactive B*42-derived clone) bound to either B*81/TL9 or B*42-TL9. An overlay of these structures illustrates that the TCR engages both antigens using an identical mechanism. Notably, in the TCR-bound structure TL9 is presented by B*42 in a "B*81-like" conformation, with residue N6 exposed and forming critical interactions with TCR (**D and E**). Interestingly, the TCR beta chain engages the peptide using its CDR2 region (indicated in Cyan) **(D and E)**. (**F**) The pie charts represent the contribution of different TCR domains to the total contact surface for peptide (top) and HLA-B*42 (bottom), illustrating the unusual absence of CDR3 beta interaction with peptide. The structural data and images shown in panels C, D, and E were generated by our collaborators, G Gao and S Li.

4.3.5. The Q3P peptide variant is exclusively recognized by dual-reactive TCR

My data suggest that dual-reactive TCR clonotypes encoding *TRBV12-3* may be beneficial for control of HIV infection in the context of B*42, due to their intrinsic ability to recognize a greater variety of viral escape mutations. If so, it might be advantageous to elicit such CD8+ T-cell responses by vaccination, either to control new infections or as part of a strategy to enhance existing host responses in order to reduce or eliminate latent HIV reservoirs. One potential way to do this is to identify a TL9 variant that is preferentially recognized by dual-reactive TCR clones, which could be used as a novel vaccine antigen to stimulate this subset of the TL9-specific TCR repertoire. My efforts to screen 171 single amino acid TL9 variants pointed to a handful of peptides that could be used to differentiate between mono- and dual-reactive TCR. I selected three promising candidate peptides, Q3P, T7V and T7D, and tested the reactivity of all 13 B*42-derived TCR clones towards these peptides over a range of doses (20μM - 0.08μM). Representative results generated at the 1.33 μM peptide dose are summarized in **Figure 4-8 A**. All of the dual-reactive TCR clones recognized Q3P, whereas none of the mono-reactive clones responded to this variant. In contrast, all of the mono-reactive TCR recognized T7V, but none of the dual-reactive clones responded to this variant. Finally, none of the TCR clones recognized T7D at this peptide dose.

In collaboration with the Gao laboratory, we obtained a crystal structure of the Q3P peptide variant bound to B*42. In contrast to work by Kloverpris et al. using the wildtype TL9 peptide [6], we observed that the Q3P variant adopts a “B*81-like” conformation on B*42, with the variant residue P3 buried in the HLA groove and residue N6 exposed and thereby accessible to the TCR **(Figure 4-8 B)**. This new structure is entirely consistent with my functional data indicating that Q3P is recognized exclusively by dual-reactive TCR clones. Indeed, the Q3P/B*42 structure is remarkably similar to the wildtype TL9/B*42 structure obtained in the presence of dual-reactive TCR (shown in **Figure 4-7**), suggesting that this peptide variant does not require the conformational shift that is otherwise necessary for dual-reactive TCR to engage TL9 when bound to B*42. This result also provides indirect support for the conclusion that mono-reactive TCR clones cannot recognize TL9 when it is in a “B*81-like” conformation, though additional studies will be needed to confirm this model**.** Based on these data, we believe that the Q3P variant could serve as a novel vaccine antigen to selectively stimulate a cross-reactive subset of TL9-specific CD8+ T cells. While the effectiveness of the Q3P variant to elicit such responses remains to be proven, by focusing T cell reactivity at the clonotype level, our work points to a potentially novel strategy for vaccine discovery.

4.4. Discussion

The results presented in this chapter extend and complement my data and analyses shown in **Chapter 3**. Because mono- and dual-reactive TCR showed the greatest functional differences in the setting of B*42, I focused this work on B*42-derived TCR clones. I isolated eight additional clones, resulting in a final panel of 13 TL9-specific TCR (five mono- and eight dual-reactive). Each of these clones was functionally characterized by examining their ability to recognize 171 TL9 peptide variants. My new results using the expanded panel of clones are consistent with those reported in Chapter 3, further supporting the conclusion that dual-reactive TCR clones from B*42 individuals are genetically and functionally similar to TCR from B*81 individuals. In addition, dual-reactive TCR clones demonstrated enhanced recognition of HIV escape mutations and pathway variants, suggesting that they could contribute to HIV control in some B*42 individuals. To improve our ability to isolate paired TCR alpha/beta sequences in the future, I also established an Illumina-based sequencing strategy that demonstrated substantially higher throughput. These efforts identified 22 additional TCR clones that

can be explored in future studies. Next, I examined the potential link between antigen sensitivity and cross-reactivity for these TCR clones. No association was found between these features of our TCR. While both mono- and dual-reactive clones displayed a range of antigen sensitivities, the TCR clone with the highest sensitivity was dual-reactive

A

TCR Name	TL9	T7V	Q3P	T7D
Mono 7A10	+	+	-	-
Mono 7C12	+	+	-	-
Mono 13A10	+	+	-	-
Mono 13D8	+	+	-	-
Mono 13B11	+	+	-	-
Dual 14A4	+	-	+	-
Dual 7A4	+	-	+	-
Dual 14A9	+	-	+	-
Dual 14A10	+	-	+	-
Dual 14D7	+	-	+	-
Dual 16A7	+	-	+	-
Dual 16A11	+	-	+	-
Dual 16A12	+	-	+	-

B

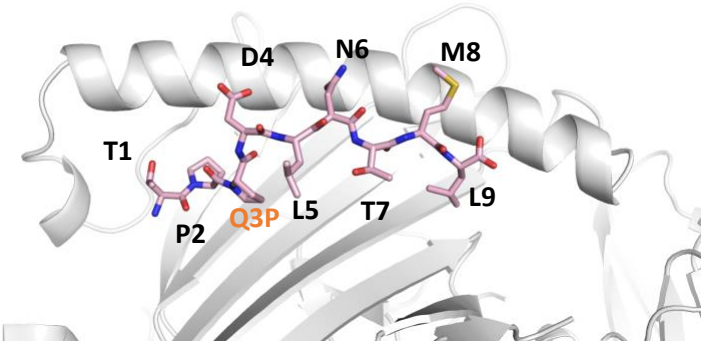

Figure 4-8. Proline variant at position 3 is recognized selectively by dual-reactive TCR.

(A) TCR reactivity towards TL9, T7V, Q3P, and T7D was assessed using peptide titrations to identify variants that can preferentially stimulate dual-reactive TCR. The figure summarizes the results of TCR reactivity assays using 1.33μM peptide. Green boxes indicate normalized signaling values >0.25 of wildtype TL9. Mono-reactive TCR selectively recognized T7V, while dual-reactive TCR specifically recognized Q3P. (B) The crystal structure of Q3P bound to HLA-B*42 shows that this peptide adopts a B*81-like confirmation where N6 is exposed. The structure data and image was generated by our collaborators, G Gao and S Li.

In collaboration with Dr. George Gao's laboratory, we have generated the first crystal structures for TCR bound to TL9/B*42 or TL9/B*81. These data offer important structural information to help define mechanisms that contribute to TCR cross-recognition in the setting of immunodominant responses to TL9. Notably, we observed that TL9 adopted a "HLA-B*81-like" conformation when it was bound to B*42 in the presence of a dual-reactive TCR clone, suggesting that TCR engagement induced a shift in the peptide structure. If so, dual-reactive TCR clones are likely to place different

selective pressures on TL9 compared to mono-reactive clones in B*42 individuals, resulting in the generation of escape variants that are more often associated with HLA-B*81 that may have greater fitness costs to the virus [21]. Previous studies have indicated that TCR binding can influence peptide orientation in the HLA binding groove [22-24], but our data is the first evidence that this happens in the context of TL9. Another important observation from the crystal structures is that the dual-reactive TCR (clones 14A9 and 14A4) used their CDR2 beta domain to make contact with the TL9 peptide, with key residues focused on residue N6. Since the CDR2 domain is determined by the V gene, this result explains why there may be an enrichment in *TRBV12-3* gene usage in dual-reactive B*42-derived TCR as well as B*81-derived TCR. This structure is unusual, since the more variable CDR3 regions are usually the primary sites of contact with peptide [19]. Mono-reactive B*42-derived TCR, such as 7A10, 7C12 and 7A4, also harbor *TRBV12-3*, demonstrating that this TCR beta gene alone is not sufficient to engage TL9 in the "B*81-like" conformation. Other features of the alpha or beta chain are also likely to contribute to this phenotype, but additional structural and mutational studies will be necessary to work out these details. It should be noted that my peptide screening experiments were highly complementary to the structural studies. Indeed, the screening assays indicated that all TCR clones displayed limited recognition of peptide variants at position 6, which was usually confined to only the wildtype residue N6. We hypothesize that mutations at position 6 must either disrupt HLA binding in the "B*42-like" conformation or disrupt TCR binding in the "B*81-like" conformation, but additional structural studies will be needed to address this question.

Since dual-reactive TCR are associated with enhanced cross-reactivity to TL9 escape variants, we believe that eliciting this type of response would be beneficial in an HIV vaccine strategy. We discovered that a proline variant at position 3 of the peptide (Q3P) is recognized selectively by dual-reactive TCR clones, and thus this variant could serve as a novel vaccine antigen. My work describes a strategy to gain a more detailed understanding of how TCR cross-reactivity contributes to the TL9 response, which may serve as a proof of concept in studying other important T cell epitopes. The limitation of our approach is that quantitative measurements of TCR binding affinity are lacking. Using our TCR reporter assay to assess NFAT signaling with limiting doses of peptide, we can generate a reproducible rank order of antigen sensitivity, but more accurate measurements with techniques such as Surface Plasmon Resonance (SPR) will be

needed to quantify these differences. Another limitation of my analysis is the number of the participants who were studied. Experiments are underway to screen more B*42 individuals to test for TL9 reactivity and dual-reactivity by tetramer staining. The goal of future research will thus be to isolate and sequence the repertoire from more HIV-infected individuals in order to study the impact of dual-reactive TCR on viral loads and clinical progression in B*42 individuals.

In summary, I have presented a comprehensive functional and structural analysis of TCR clones from individuals that show enhanced control of HIV. This includes the first reported ternary structures of TCR in combination with Gag TL9 presented on HLA-B*42 (and B*81). My studies identify key elements of a highly effective CD8+ T cell response that can inform the development of vaccines or new therapeutic strategies. Moreover, the methodology I presented here can serve as a foundation for TCR studies against other HIV peptide-HLA combinations.

4.5. Methods

4.5.1. TCR sequencing using Illumina

First round RT-PCR products derived from single TL9 tetramer-labeled CD8+ T cells, described in **Chapter 3**, were used to establish an Illumina-based method. Mono and dual reactive TCR repertoires were re-collected from all six individuals (three B*42 and three B*81). A nested second round PCR reaction, that attached forward and reverse tags to the amplicons, was preformed on these 12 RT-PCR reaction plates. This was followed by an indexing reaction that primed off the tags attached in the second round, to add PCR well specific forward and reverse barcodes. The barcodes were 8-nt in length and the combination of the forward and reverse barcode was used to de-multiplex the amplicons. The PCR amplification strategy is shown in **Figure 4-1**. Using this barcoding strategy, we can index up to 1920 unique TCR PCR reactions. Whether or not we can run all the samples on one MiSeq run needs to be optimized as appropriate read depth, to get reliable sequence analysis, remains to be determined. The PCR reactions, post indexing, were purified using AMPure beads (Beckman), normalized for DNA quantity and the libraries were amplicon sequenced on the MiSeq using a 500 cycle kit (Illumina). This generated reads in both forward and reverse directions spanning the entire length of the TCR.

4.5.2. Illumina sequence analysis

Raw sequences are obtained from the MiSeq output directories and the paired ends are joined. Because the TCR amplicon lengths (~275 bp) are well below twice the read length of the 500 cycle kit, almost all read pairs are expected to be mated successfully. Fragment sizes under 200bp are discarded. To assist with troubleshooting, fragments under 60bp are saved to a separate file for analysis of primer dimer bias. These results will inform future efforts to modify primers to reduce or eliminate frequent sequence artefacts. The remaining fragments are binned together if they have identical nucleotide sequences; for each unique sequence the number of MiSeq read pairs that support it are stored. Bins that have less than 100 read coverage are ignored as likely artefacts. Next, the fragments are organized for TCR classification. Primer sequences are aligned at the ends of the fragments. If the 5' and 3' ends of a fragment do not exactly match any of the 76 primers, the sequence is discarded as a likely artefact. The primer sequences are then removed from the fragment, and the positively identified, deprimered fragments are classified using igblastn. The appropriate TCR sequence and classification information is then extracted to a csv file.

4.5.3. TCR reporter assay

Paired TCR alpha and beta clones that were of interest for functional characterization was re-constructed to full length and cloned into p-SELECT expression vector. These methods and methods for the TCR reporter assay are discussed in detail in **Chapters 2** and **3**. The variant peptides tested here were all resuspended based off of mass, therefore, there may be minor variations in the molar concentrations of the peptides in TCR reporter assay experiments. All peptides are 9mers with single amino acid variations and were ordered at a purity of >80%.

4.5.4. Protein expression and purification (Gao laboratory)

The TCR α and β chains were cloned into pET21a (Invitrogen) and expressed individually in *E. coli* strain BL21(DE3) as inclusion bodies. Resolubilized TCR (30 mg each) were mixed and injected four times per 8 h into 2 L of refolding buffer (5 M urea, 400 mM L-arginine HCl, 100 mM Tris [pH 8.0], 5 mM reduced glutathione, and 0.5 mM oxidized glutathione) at 4°C. The refolded mixture was dialyzed for 24 h in 10 volumes of

ultrapure water (Milli-Q system) and then against 10 volumes of 10 mM Tris (pH 8.0) at 4°C. The refolded TCR protein was first separated using a Source 15Q anion exchange column (GE Healthcare) and further purified by gel filtration on a Superdex 200 10/30 GL column (GE Healthcare) pre-equilibrated in gel filtration buffer (20 mM Tris [pH 8.0] and 50 mM NaCl). Residues 1 to 274 of the HLA-B*42:01 heavy chain or HLA-B*81:01 were cloned into pET21a (Invitrogen), and expressed in BL21(DE3) cells as inclusion bodies. Resolubilized B*42:01 or B*81:01 and human β2m were co-refolded with peptides in a L-arginine refolding buffer (400 mM L-arginine HCl, 100 mM Tris [pH 8.0], 5 mM reduced glutathione, and 0.5 mM oxidized glutathione). The refolded proteins were further purified by gel filtration on a Superdex 200 10/30 GL column (GE Healthcare) preequilibrated in gel filtration buffer (20 mM Tris [pH 8.0] and 50 mM NaCl). To obtain TCR/pMHC complexes, the refolded TCR and pMHC proteins were mixed at a molar ratio of 1:2 incubated for 1 h at 4°C. The protein mixture was then purified on a Superdex 200 10/30 GL column (GE Healthcare) pre-equilibrated in gel filtration buffer (20 mM Tris [pH 8.0] and 50 mM NaCl). The complex proteins were concentrated to a final concentration of 5 mg/ml and 10 mg/ml for crystal screening.

4.5.5. Protein crystallization, data collection, and processing (Gao laboratory)

All crystallization trials were performed by the hanging-drop vapor diffusion technique at 18°C with a protein-to-reservoir drop ratio of 1:1. Crystals grew after 7 to 10 days. Crystals were flash-cooled in liquid nitrogen with cryoprotectant containing precipitant buffer plus 30% glycerol. Diffraction data were collected at the Shanghai Synchrotron Radiation Facility (SSRF) BL17U, and all data were processed with HKL2000. The complex structure was solved by molecular replacement with Phaser using models from PDB codes: 4U1 for MHCs and 5XOT for TCRs. The structure was modeled by iterative cycles of manual building and refinement using Phenix and COOT. The stereochemical qualities of the final model were assessed with MolProbity. The protein interfaces were analyzed using COOT and PISA. All structural figures were generated using Pymol (http://www.pymol.org).

4.6. References

[1] R. S. Ntale *et al.*, "Temporal association of HLA-B*81:01- and HLA-B*39:10-mediated HIV-1 p24 sequence evolution with disease progression," *Journal of virology,* vol. 86, no. 22, pp. 12013-24, Nov 2012, doi: 10.1128/JVI.00539-12.

[2] P. Kiepiela *et al.*, "Dominant influence of HLA-B in mediating the potential co-evolution of HIV and HLA," *Nature,* vol. 432, no. 7018, pp. 769-775, 2004/12/01 2004, doi: 10.1038/nature03113.

[3] F. Bihl *et al.*, "Impact of HLA-B alleles, epitope binding affinity, functional avidity, and viral coinfection on the immunodominance of virus-specific CTL responses," *J Immunol,* vol. 176, no. 7, pp. 4094-101, Apr 1 2006. [Online]. Available: http://www.ncbi.nlm.nih.gov/pubmed/16547245.

[4] J. M. Carlson *et al.*, "Correlates of protective cellular immunity revealed by analysis of population-level immune escape pathways in HIV-1," *Journal of virology,* vol. 86, no. 24, pp. 13202-16, Dec 2012, doi: 10.1128/JVI.01998-12.

[5] P. Kiepiela *et al.*, "CD8+ T-cell responses to different HIV proteins have discordant associations with viral load," (in eng), *Nature medicine,* vol. 13, no. 1, pp. 46-53, Jan 2007, doi: 10.1038/nm1520.

[6] H. N. Kloverpris *et al.*, "A molecular switch in immunodominant HIV-1-specific CD8 T-cell epitopes shapes differential HLA-restricted escape," (in eng), *Retrovirology,* vol. 12, p. 20, Feb 20 2015, doi: 10.1186/s12977-015-0149-5.

[7] C. K. Koofhethile *et al.*, "CD8+ T cell breadth and ex vivo virus inhibition capacity distinguish between viremic controllers with and without protective HLA class I alleles," *Journal of virology,* May 18 2016, doi: 10.1128/JVI.00276-16.

[8] Y. Moosa *et al.*, "Case report: mechanisms of HIV elite control in two African women," *BMC Infect Dis,* vol. 18, no. 1, p. 54, Jan 25 2018, doi: 10.1186/s12879-018-2961-8.

[9] A. Sette and J. Sidney, "Nine major HLA class I supertypes account for the vast preponderance of HLA-A and -B polymorphism," (in eng), *Immunogenetics,* vol. 50, no. 3-4, pp. 201-12, Nov 1999.

[10] J. Sidney, B. Peters, N. Frahm, C. Brander, and A. Sette, "HLA class I supertypes: a revised and updated classification," *BMC Immunol,* vol. 9, p. 1, Jan 22 2008, doi: 10.1186/1471-2172-9-1.

[11] C. Geldmacher *et al.*, "Minor viral and host genetic polymorphisms can dramatically impact the biologic outcome of an epitope-specific CD8 T-cell response," *Blood,* vol. 114, no. 8, pp. 1553-62, Aug 20 2009, doi: 10.1182/blood-2009-02-206193.

[12] H. N. Kloverpris *et al.*, "HIV control through a single nucleotide on the HLA-B locus," *Journal of virology,* vol. 86, no. 21, pp. 11493-500, Nov 2012, doi: 10.1128/JVI.01020-12.

[13] A. Leslie *et al.*, "Differential selection pressure exerted on HIV by CTL targeting identical epitopes but restricted by distinct HLA alleles from the same HLA supertype," (in eng), *J Immunol,* vol. 177, no. 7, pp. 4699-708, Oct 01 2006.

[14] F. Ogunshola *et al.*, "Dual HLA B*42 and B*81-reactive T cell receptors recognize more diverse HIV-1 Gag escape variants," *Nature communications,* vol. 9, no. 1, pp. 5023-5023, 2018, doi: 10.1038/s41467-018-07209-7.

[15] A. Han, J. Glanville, L. Hansmann, and M. M. Davis, "Linking T-cell receptor sequence to functional phenotype at the single-cell level," (in eng), *Nature biotechnology,* vol. 32, no. 7, pp. 684-92, Jul 2014, doi: 10.1038/nbt.2938.
[16] H. R. Lapointe *et al.*, "HIV Drug Resistance Testing by High-Multiplex “Wide” Sequencing on the MiSeq Instrument," *Antimicrobial Agents and Chemotherapy,* vol. 59, no. 11, pp. 6824-6833, 2015, doi: 10.1128/aac.01490-15.
[17] K. Ladell *et al.*, "A molecular basis for the control of preimmune escape variants by HIV-specific CD8+ T cells," (in eng), *Immunity,* vol. 38, no. 3, pp. 425-36, Mar 21 2013, doi: 10.1016/j.immuni.2012.11.021.
[18] H. N. Kloverpris *et al.*, "CD8+ TCR Bias and Immunodominance in HIV-1 Infection," (in eng), *J Immunol,* vol. 194, no. 11, pp. 5329-45, Jun 01 2015, doi: 10.4049/jimmunol.1400854.
[19] N. L. La Gruta, S. Gras, S. R. Daley, P. G. Thomas, and J. Rossjohn, "Understanding the drivers of MHC restriction of T cell receptors," (in eng), *Nature reviews. Immunology,* vol. 18, no. 7, pp. 467-478, Jul 2018, doi: 10.1038/s41577-018-0007-5.
[20] A. Culshaw *et al.*, "Germline bias dictates cross-serotype reactivity in a common dengue-virus-specific CD8(+) T cell response," (in eng), *Nature immunology,* vol. 18, no. 11, pp. 1228-1237, Nov 2017, doi: 10.1038/ni.3850.
[21] J. K. Wright *et al.*, "Impact of HLA-B*81-Associated Mutations in HIV-1 Gag on Viral Replication Capacity," *Journal of virology,* vol. 86, no. 6, pp. 3193-3199, 2012, doi: 10.1128/jvi.06682-11.
[22] F. E. Tynan *et al.*, "A T cell receptor flattens a bulged antigenic peptide presented by a major histocompatibility complex class I molecule," *Nature immunology,* Article vol. 8, p. 268, 01/28/online 2007, doi: 10.1038/ni1432.
[23] F. Madura *et al.*, "TCR-induced alteration of primary MHC peptide anchor residue," (in eng), *Eur J Immunol,* vol. 49, no. 7, pp. 1052-1066, Jul 2019, doi: 10.1002/eji.201948085.
[24] O. Y. Borbulevych *et al.*, "T cell receptor cross-reactivity directed by antigen-dependent tuning of peptide-MHC molecular flexibility," *Immunity,* vol. 31, no. 6, pp. 885-96, Dec 18 2009, doi: 10.1016/j.immuni.2009.11.003.

Chapter 5. Conclusions

5.1. Summary

The presence of CD8+ T cells capable of mounting high avidity and/or cross-reactive responses to HIV epitopes and epitope variants has been associated with viral control [1, 2]. Since the antigen specificity and sensitivity of a T cell is determined by its TCR, the composition of an individual's TCR repertoire may play an important role in modulating clinical outcomes. In support of this hypothesis, prior studies of the B*27-restricted KK10 response and the B*57-restricted TW10 response have implicated TCR clonotype features in HIV control [3, 4]; however, similarly detailed studies have not been conducted for other immunodominant epitopes. More comprehensive efforts to characterize TCR sequence and functional diversity in individuals that control HIV infection may elucidate clonotype-dependent mechanisms that can inform the development of effective vaccines or novel therapeutics.

CD8+ T cell responses targeting the immunodominant Gag TL9 epitope (TPQDLNTML) are associated with control of HIV-1 subtype C infection, particularly in the context of HLA-B*81. TL9 is also presented as an immunodominant epitope by HLA-B*42, but in this case it is not associated with viral control [3-7]. While past studies have observed distinct TCR sequences among the CD8+ T cells that respond to TL9 in the setting of B*81 and B*42 [8, 9], there has been no detailed analysis of potential clonotypic differences in TCR function or intrinsic antiviral activity. My studies were sparked by an observation from collaborators in South Africa, who observed CD8+ T cells in B*81 and B*42 individuals that could recognize TL9 presented on the both HLA alleles. Such, dual-reactive T cells were unexpected, since earlier studies by Kloverpris et al [5] demonstrated that TL9 adopted a different conformation when bound to each of these HLA proteins. A substantial portion of my PhD research has been devoted to solving this riddle.

In this thesis, I have examined the sequence and function of TCR clones isolated from B*81 and B*42 individuals that display the ability to recognize Gag TL9 when it is presented by one or both of these HLA alleles (referred to as mono- or dual-reactive, respectively). I developed and optimized methods to isolate paired TCR alpha/beta

sequences from single T cells, allowing me to examine the clonotypic repertoire of antigen-specific CD8+ T cells that contribute to mono- and dual-reactive responses. In addition, I established methods to reconstruct individual TCR clones and to assess their *in vitro* function, which have supported detailed analyses of TCR cross-reactivity and antigen sensitivity. Finally, working with expert collaborators, I have begun to explore structural determinants of TCR cross-reactivity.

In **chapter 2**, which was published in the *Journal of Immunological Methods* [10], I described a luciferase-based reporter cell assay that I have employed successfully to assess TCR antigen recognition. This assay, which measures TCR-dependent NFAT signaling, provides a rapid and robust measure of TCR function. Our results demonstrated that Nef-mediated downregulation of HLA-A*02 had a substantial impact on T cell recognition. Furthermore, this method could be used to examine the relative immune evasion activity of Nef mutants. A major benefit of this assay is that it can be modified easily to study other TCR clones since these proteins are expressed transiently and independently, in contrast to use of retroviral vectors to stably express TCR, as described by others [11].

In **chapter 3**, which was published in Nature Communications [12], I described a comprehensive analysis of Gag TL9-specific TCR clones isolated from three B*81 and three B*42 individuals. The overall goal of this work was to identify TCR features that were associated with the unexpected dual-reactive population of CD8+ T cells that recognized TL9 bound to both B*42 and B*81. These CD8+ T cells were present in both B*81 and B*42 individuals, despite the fact they only expressed one of these HLA alleles. Individuals that possessed these CD8+ T cell populations displayed lower plasma viral loads compared to those that did not, suggesting that this cross-reactive T cell phenotype was associated with HIV control. I used single-cell methods to isolate paired TCR alpha/beta sequences, and the luciferase reporter cell assay to examine the function of selected mono- and dual-reactive TCR clones. Notably, dual-reactive TCR from B*42 individuals and all clones from B*81 individuals were highly enriched for usage of the *TRBV12-3* gene. In addition, dual-reactive TCR from B*42 individuals were dominated by several public clonotypes. My functional studies demonstrated that dual-reactive TCR from B*42 individuals displayed similar antigen recognition profiles as clones from B*81 individuals, including an enhanced ability to recognize potential HIV escape variants and “escape pathway” mutations. Thus, both the sequence and function

of dual-reactive TCR clones from B*42 individuals resembled that of TCR clones typically found in B*81 individuals, suggesting that these “B*81-like” properties contribute to TL9-mediated control of HIV.

These findings were further validated in **chapter 4**, where I performed additional sequence and functional analyses, focusing on B*42-derived mono- and dual-reactive TCR clones. Results from this expanded panel of TCR clones were consistent with those reported in chapter 3, strengthening my conclusion that dual-reactive TCR clones from B*42 individuals displayed “B*81-like” features. Additional studies using peptide titrations and TL9 variants confirmed that dual-reactive TCR clones displayed greater capacity to recognize TL9 escape mutants compared to mono-reactive clones, and furthermore, that dual-reactive TCR could be selectively stimulated by the Q3P peptide bound to HLA-B*42. Notably, structural analyses of two dual-reactive TCR clones (done in collaboration with the Gao laboratory) illustrated that the TL9 peptide adopted a “B*81-like” conformation on HLA-B*42 when it was engaged by both dual-reactive TCR, providing important visual confirmation of my functional results

In addition to these studies on the Gag TL9 epitope, I have used similar methods to examine other TCR clones and contexts that are not included in the main body of my thesis. The results from these studies demonstrate that the strategies presented in this thesis can be adopted readily to assess the function of TCR clones directed towards other peptide/HLA antigens. Preliminary data for TCR clones recognizing the HIV Gag FK10 epitope (FLGKIWPSYK), restricted by HLA-A*02, and the Gag KK10 epitope (KRWIILGLNK), restricted by HLA-B*27 are included in **Appendix Figure 5-1 and Appendix Figure 5-2**. Future work will use similar methods to extend these analyses and also aim to examine TCR clones targeting additional viral and non-viral epitopes.

5.2. Significance and Impact

My thesis research significantly enhances our understanding of CD8+ T cell responses targeting the Gag TL9 epitope in the context of HIV control. Specifically, my studies have:

(1) isolated public TCR clonotypes that may contribute to viral control in B*42 individuals, which can be used to support larger scale sequence-based

strategies to assess the frequency of dual-reactive T cells in HIV-infected individuals;

(2) defined cross-recognition of Gag TL9 escape variants (and escape pathways) as a functional correlate of viral control for TCR clones from B*81 individuals and dual-reactive TCR clones from B*42 individuals;

(3) provided new structural details of TCR engagement with TL9/B*42 antigen, including discovery of an atypical “germ-line” mediated interaction between the CDR2 domain of TRBV12-3 and TL9 peptide, which likely explains the bias for *TRBV12-3* in TL9-specific CD8+ T cells from B*81 individuals and dual-reactive TCR clones from B*42 individuals.

In addition, my studies highlight the benefits that a more comprehensive strategy to characterize antigen-specific TCR clonotypes may have for vaccine discovery and immune-based therapeutics for HIV cure. Indeed, by determining complex antigen-recognition profiles for mono- and dual-reactive TCR clones, I identified a TL9 variant (Q3P) that is selectively recognized by dual-reactive TCR in the context of B*42. This epitope could be useful as a vaccine antigen to elicit or expand cross-reactive CD8+ T cell responses. Alternatively, it could serve as a reagent to determine the frequency of cross-reactive T cells in B*42 individuals to (i.e. by Elispot). In the realm of immunotherapies, soluble TCR-based products called Immune-mobilizing monoclonal T Cell receptors Against Viruses (or ImmTAVs) are currently being considered as a component of HIV cure strategies [13, 14] or as novel cancer treatments (as ImmTACs) [15, 16]. These products link a soluble, single-chain TCR alpha/beta protein, which serves as the antigen recognition domain of the construct, with an anti-CD3 binding to redirect CD3+ T cells to the target. This approach is appealing because its soluble design allows the product to be administered to individuals transiently, through infusions or slow-release methods, and for the dose to be regulated carefully to avoid toxicity. The methods that I have employed in my thesis may serve as an efficient strategy to quickly screen and prioritize antigen-specific TCR clones.

While a number of studies have indicated that TCR clonotypes can be important factor in CD8+ T cell-mediated control of HIV [17-20], other studies suggest that the contribution of TCR is limited and/or other non-TCR factors play a larger role in determining the avidity of CD8+ T cell responses [11, 21]. My results demonstrate that

TL9-specific TCR clones derived from CD8+ T-cells that are associated with HIV control appear to be more cross-reactive towards TL9 peptide variants, but they display a range of antigen sensitivities. Unfortunately, the methods that I used did not provide a quantitative measure of TCR affinity or avidity. For example, TCR signal did not plateau at high peptide concentrations, so even though the assay could generate a reproducible rank order of TCR activity, it was not possible to calculate half-maximal effective concentration (EC50) values for individual TCR or peptides. Saturation was still not achieved even at four-fold higher peptide doses **(Appendix Figure 5-3)**. While I interpret my data to suggest that TCR cross-reactivity is a more important determinant of HIV control in the setting of TL9, additional biochemical studies will be necessary to confirm this point. Analyses of selected TCR clones is underway using surface plasmon resonance (SPC), in collaboration with the Gao laboratory.

In summary, my thesis research identified sequence, functional, and structural features of Gag TL9-specific TCR clonotypes that may contribute to HIV control in the context of HLA-B*81 and B*42. In addition to providing new data that significantly enhance our understanding of CD8+ T cell responses against the immunodominant Gag TL9 epitope, my studies lay a methodological foundation for a strategy to comprehensively examine any TCR-peptide-HLA combination.

5.3. References

[1] W. L. Dinges *et al.*, "Virus-specific CD8+ T-cell responses better define HIV disease progression than HLA genotype," (in eng), *Journal of virology,* vol. 84, no. 9, pp. 4461-8, May 2010, doi: 10.1128/jvi.02438-09.

[2] S. A. Migueles *et al.*, "CD8(+) T-cell Cytotoxic Capacity Associated with Human Immunodeficiency Virus-1 Control Can Be Mediated through Various Epitopes and Human Leukocyte Antigen Types," (in eng), *EBioMedicine,* vol. 2, no. 1, pp. 46-58, Jan 2015, doi: 10.1016/j.ebiom.2014.12.009.

[3] H. Chen *et al.*, "TCR clonotypes modulate the protective effect of HLA class I molecules in HIV-1 infection," *Nature immunology,* vol. 13, no. 7, pp. 691-700, Jul 2012, doi: 10.1038/ni.2342.

[4] K. Ladell *et al.*, "A molecular basis for the control of preimmune escape variants by HIV-specific CD8+ T cells," (in eng), *Immunity,* vol. 38, no. 3, pp. 425-36, Mar 21 2013, doi: 10.1016/j.immuni.2012.11.021.

[5] H. N. Kloverpris *et al.*, "A molecular switch in immunodominant HIV-1-specific CD8 T-cell epitopes shapes differential HLA-restricted escape," (in eng), *Retrovirology,* vol. 12, p. 20, Feb 20 2015, doi: 10.1186/s12977-015-0149-5.

[6] H. N. Kloverpris *et al.*, "HIV control through a single nucleotide on the HLA-B locus," *Journal of virology,* vol. 86, no. 21, pp. 11493-500, Nov 2012, doi: 10.1128/JVI.01020-12.

[7] H. N. Kloverpris *et al.*, "CD8+ TCR Bias and Immunodominance in HIV-1 Infection," (in eng), *J Immunol,* vol. 194, no. 11, pp. 5329-45, Jun 01 2015, doi: 10.4049/jimmunol.1400854.

[8] C. Geldmacher *et al.*, "Minor viral and host genetic polymorphisms can dramatically impact the biologic outcome of an epitope-specific CD8 T-cell response," *Blood,* vol. 114, no. 8, pp. 1553-62, Aug 20 2009, doi: 10.1182/blood-2009-02-206193.

[9] A. Leslie *et al.*, "Differential selection pressure exerted on HIV by CTL targeting identical epitopes but restricted by distinct HLA alleles from the same HLA supertype," (in eng), *J Immunol,* vol. 177, no. 7, pp. 4699-708, Oct 01 2006.

[10] G. Anmole *et al.*, "A robust and scalable TCR-based reporter cell assay to measure HIV-1 Nef-mediated T cell immune evasion," (in eng), *J Immunol Methods,* vol. 426, pp. 104-13, Nov 2015, doi: 10.1016/j.jim.2015.08.010.

[11] N. C. Flerin *et al.*, "T-Cell Receptor (TCR) Clonotype-Specific Differences in Inhibitory Activity of HIV-1 Cytotoxic T-Cell Clones Is Not Mediated by TCR Alone," (in eng), *Journal of virology,* vol. 91, no. 6, Mar 15 2017, doi: 10.1128/jvi.02412-16.

[12] F. Ogunshola *et al.*, "Dual HLA B*42 and B*81-reactive T cell receptors recognize more diverse HIV-1 Gag escape variants," *Nature communications,* vol. 9, no. 1, pp. 5023-5023, 2018, doi: 10.1038/s41467-018-07209-7.

[13] H. Yang, Z. Wallace, and L. Dorrell, "Therapeutic Targeting of HIV Reservoirs: How to Give T Cells a New Direction," (in eng), *Frontiers in immunology,* vol. 9, pp. 2861-2861, 2018, doi: 10.3389/fimmu.2018.02861.

[14] H. Yang *et al.*, "Elimination of Latently HIV-infected Cells from Antiretroviral Therapy-suppressed Subjects by Engineered Immune-mobilizing T-cell Receptors," (in eng), *Mol Ther,* vol. 24, no. 11, pp. 1913-1925, 2016, doi: 10.1038/mt.2016.114.

[15] C. Boudousquie, G. Bossi, J. M. Hurst, K. A. Rygiel, B. K. Jakobsen, and N. J. Hassan, "Polyfunctional response by ImmTAC (IMCgp100) redirected CD8(+) and CD4(+) T cells," (in eng), *Immunology,* vol. 152, no. 3, pp. 425-438, 2017, doi: 10.1111/imm.12779.

[16] E. McCormack *et al.*, "Bi-specific TCR-anti CD3 redirected T-cell targeting of NY-ESO-1- and LAGE-1-positive tumors," (in eng), *Cancer Immunol Immunother,* vol. 62, no. 4, pp. 773-785, 2013, doi: 10.1007/s00262-012-1384-4.

[17] J. R. Almeida *et al.*, "Superior control of HIV-1 replication by CD8+ T cells is reflected by their avidity, polyfunctionality, and clonal turnover," (in eng), *The Journal of experimental medicine,* vol. 204, no. 10, pp. 2473-85, Oct 1 2007, doi: 10.1084/jem.20070784.

[18] J. R. Almeida *et al.*, "Antigen sensitivity is a major determinant of CD8+ T-cell polyfunctionality and HIV-suppressive activity," *Blood,* vol. 113, no. 25, pp. 6351-60, Jun 18 2009, doi: 10.1182/blood-2009-02-206557.

[19] C. T. Berger *et al.*, "High-Functional-Avidity Cytotoxic T Lymphocyte Responses to HLA-B-Restricted Gag-Derived Epitopes Associated with Relative HIV Control," *Journal of virology,* vol. 85, no. 18, pp. 9334-9345, 2011, doi: 10.1128/jvi.00460-11.

[20] B. Mothe *et al.*, "CTL Responses of High Functional Avidity and Broad Variant Cross-Reactivity Are Associated with HIV Control," *PloS one,* vol. 7, no. 1, p. e29717, 2012, doi: 10.1371/journal.pone.0029717.

[21] A. V. Joglekar *et al.*, "T cell receptors for the HIV KK10 epitope from patients with differential immunologic control are functionally indistinguishable," (in eng), *Proceedings of the National Academy of Sciences of the United States of America,* vol. 115, no. 8, pp. 1877-1882, Feb 20 2018, doi: 10.1073/pnas.1718659115.

Appendix.

HIV Subtype-C p24 Gag codons 133-363

HLA-B*81/
HLA-B*42

PIVQNLQGQMVHQAISPRTL NAWVKVIEEKAFSPEVIPMF TALSEGATPQDLNTMLNTVG 192

HLA-B*57

GHQAAMQMLKDTINEEAAEW DRLHPVHAGPIAPGQMREPR GSDIAGTTSTLQEQIAWMTS 253

HLA-B*27

NPPIPVGDIYKRWIILGLNK IVRMYSPVSILDIKQGPKEP FRDYVDRFFKTLRAEQATQD 312

VKNWMTDTLLVQNANPDCKT ILRALGPGATLEEMMTACQG VGGPSHKARVL 363

Appendix Figure 1-1. HIV Gag Subtype C p24 sequence map

HIV Subtype C Gag p24 consensus sequence was obtained from the HIV Los Alamos National Library sequence database. The p24 protein spans amino acid HIV Gag codons 133-363 (HXB2 aligned nucleotide codons: 1186-1878). The HLA-B*81 and HLA-B*42 restricted TL9 epitope is highlighted in red. HLA-B*57 restricted TW10 is shown in green and HLA-B*27 restricted KK10 is shown in blue.

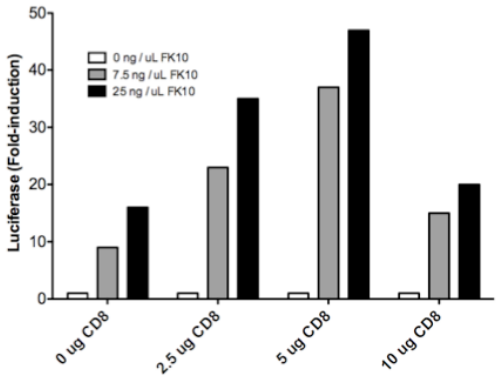

Appendix Figure 2-1. CD8 enhanced TCR mediated signalling in Jurkat cells.

Jurkat T cells were transfected with TCR alpha and beta with differing amounts of pORF9-CD8a plasmid and co-cultured with FK10 peptide pulsed CEM-A*02 cells. In all cases, FK10 peptide was recognized by TCR transfected Jurkat cells. The signalling was most robust when 5ug of CD8a plasmid was included, therefore, this quantity was used in subsequent experiments.

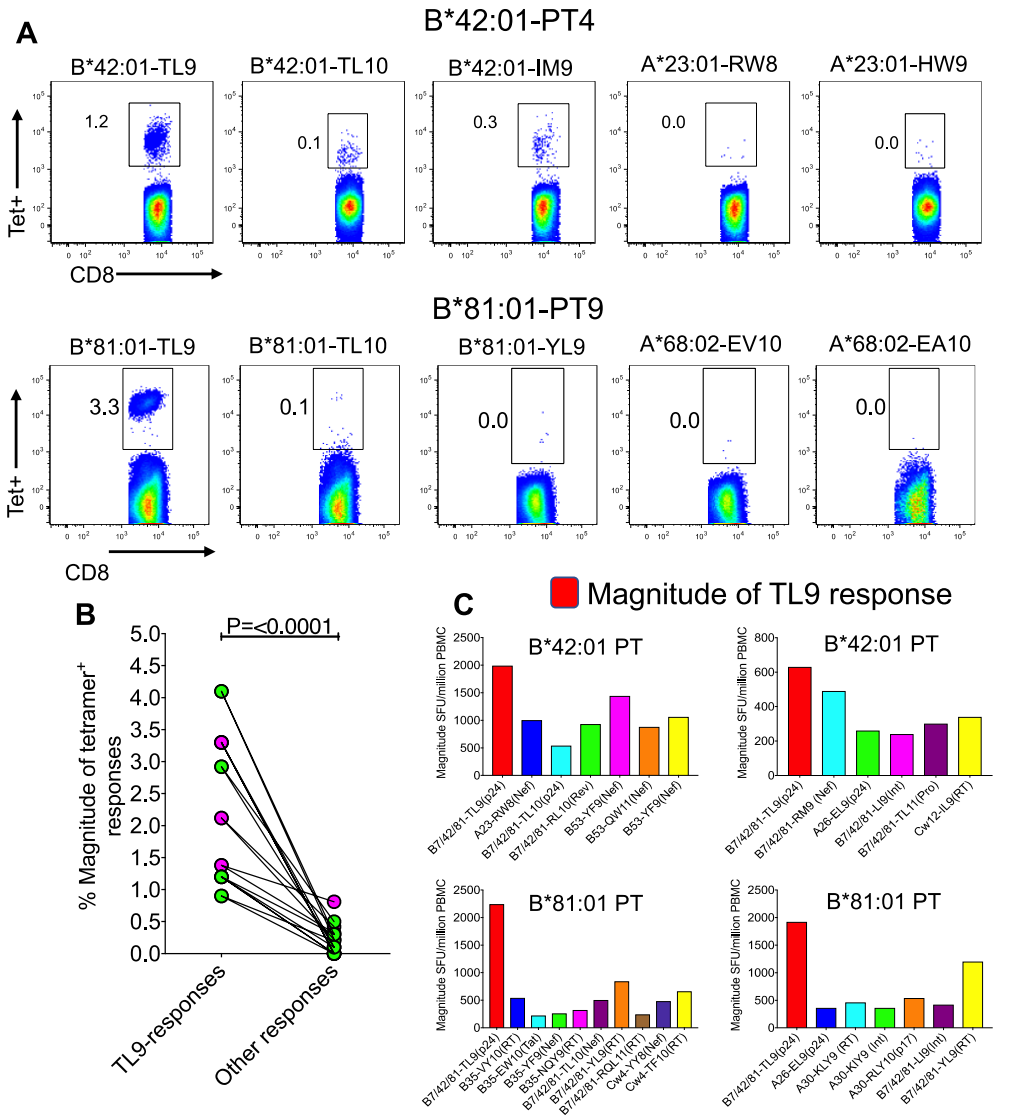

Appendix Figure 3-1. Intra-patient comparison of TL9 response with responses restricted by other alleles. Flow plot showing HIV-specific responses in a B*81:01 and B*42:01 representative donors (A), and aggregate data of TL9 responses compared to other responses (B) showing that TL9 responses are maintained at significantly higher frequencies than other responses, where green is B*42 and purple is B*81. ELISPOT data showing the magnitude of TL9 responses compared to other responses in B*81:01 and B*42:01 participants (C).

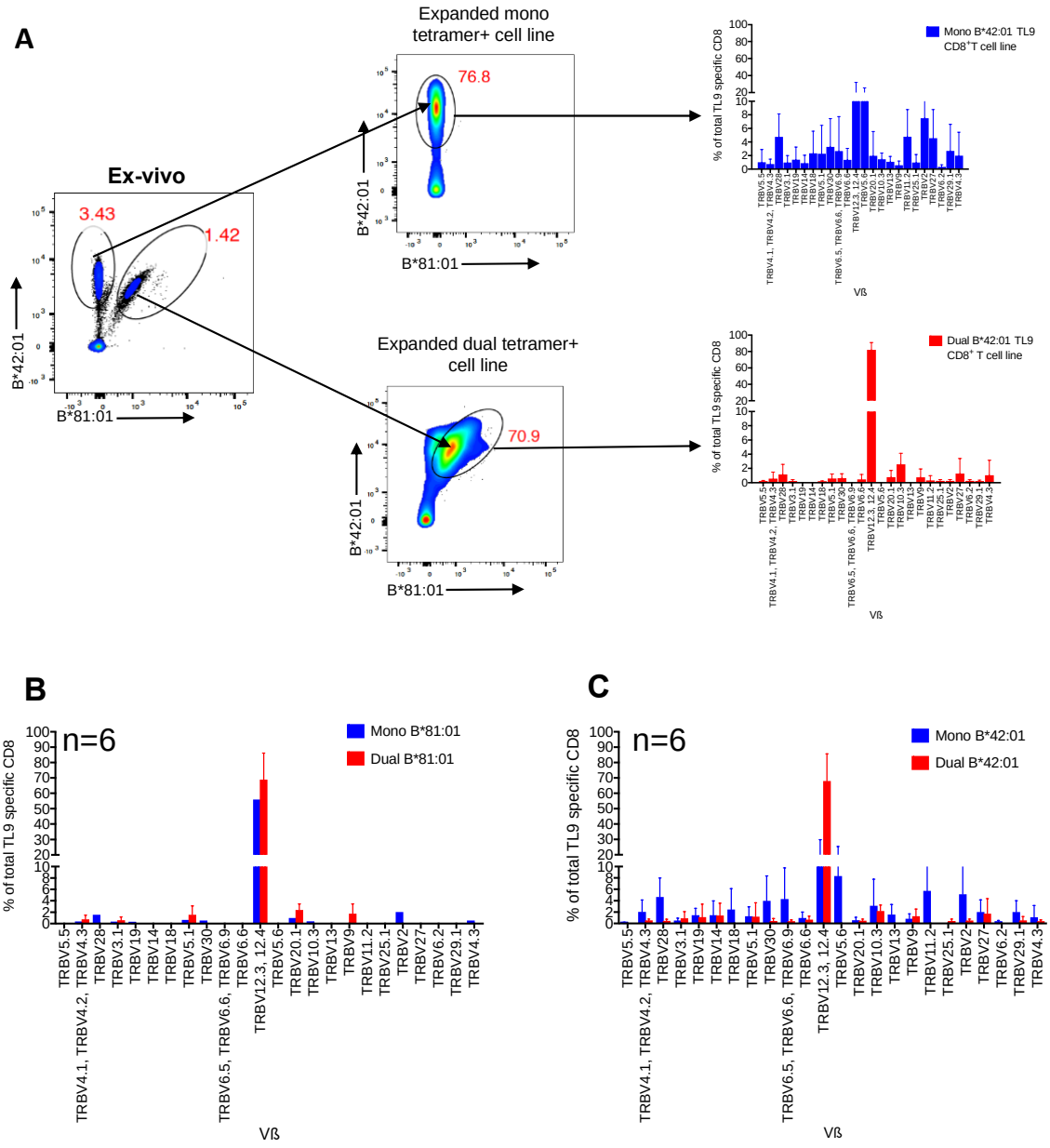

Appendix Figure 3-2. TCR-Vβ is conserved in dual TL9 tetramer$^+$ CD8 T cell lines. Representative flow plot and TCR-Vβ family usage is shown for mono- and dual-reactive TL9 tetramer+ T cells isolated from a B*42:01 donor after expansion for 2 weeks (A). Aggregate data on TCR-Vβ family usage by mono-reactive compared to dual-reactive TL9 tetramer+ T cells in six B*81:01 donors (B) and six B*42:01 donors (C).

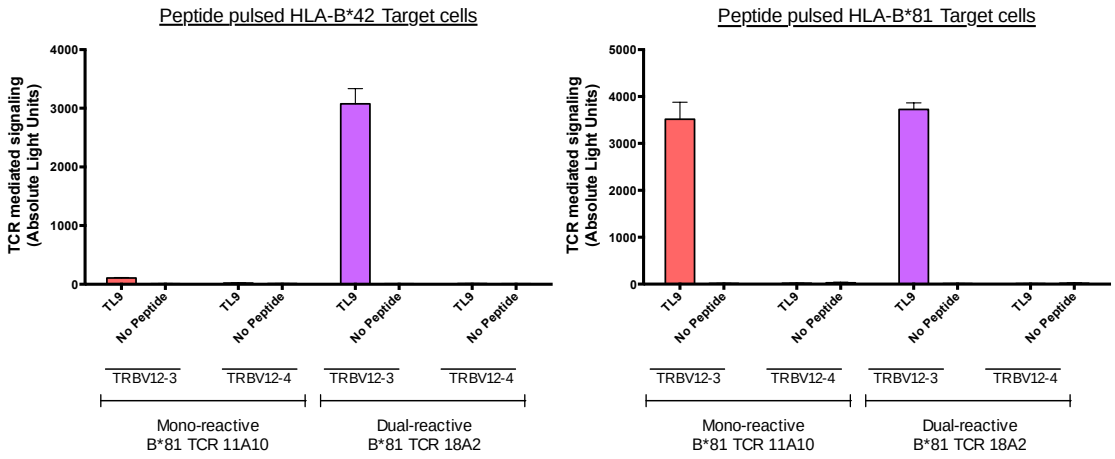

Appendix Figure 3-3. TRBV12-3 vs. TRBV12-4 signalling capacity. TCR were synthesized with TCR V beta genes 12- 3 and 12-4 to assess functionality of the genes in the TCR reporter assay. Representative image indicated TRBV12-4 was non-functional for the B*81 derived TCR 11A10 (red) and 18A2 (purple) at 20uM peptide concentration. Representative image where error bars indicate mean of 3 co- culture reactions, plus standard deviation. The experiment was conducted once to validate whether 12-3 or 12-4 are functional. As both TCR with 12-4 were non-functional, we proceeded to order all TCR constructs with 12-3 for further experimentation.

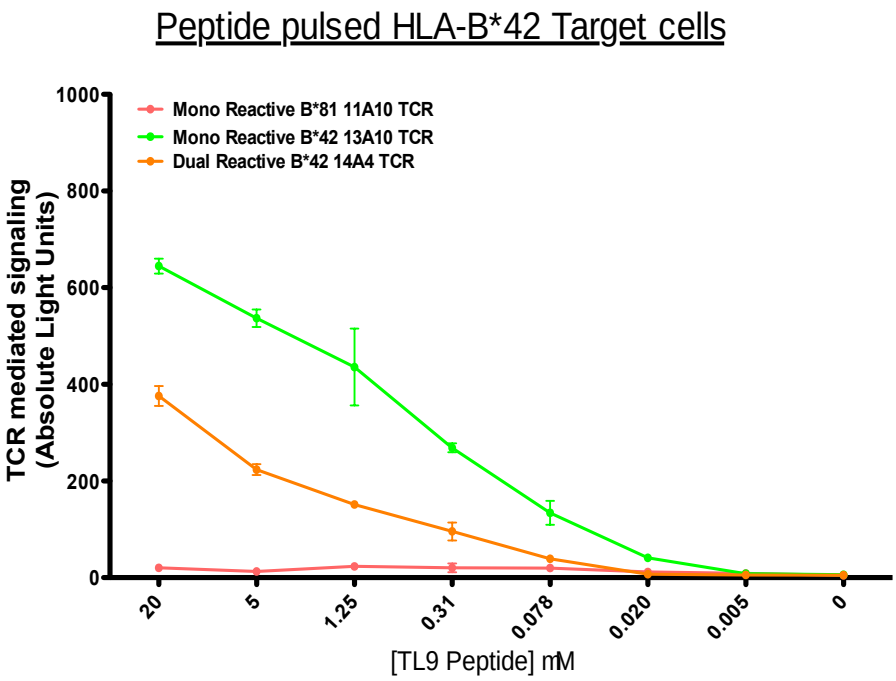

Appendix Figure 3-4. TCR signalling in response to TL9 peptide dilutions. Mono-reactive TCR clones 11A10 (B*81; red) and 13A10 (B*42; green) and dual reactive TCR clone 14A4 (B*42; orange) were tested using target cells expressing HLA-B*42:01. Similar mono- or dual-reactive phenotypes were observed over a range of TL9 peptide doses (5 nM to 20 µM). The mono-reactive B*42:01-derived clone 13A10 displayed greater signalling activity compared to the dual-reactive clone 14A4 at all peptide doses tested. In addition, the mono reactive B*81:01-derived clone 11A10 was unable to recognize TL9 bound to HLA-B*42:01 at all peptide doses tested. Combined with data shown in Figure 4, these results confirm the mono- and dual-reactive phenotypes of these TCR clones and also suggest that antigen sensitivity is independent of dual-reactivity for the B*42:01-derived public TCR clones examined in this study. Representative image where error bars indicate mean of 3 co- culture reactions, plus standard error mean. The experiment was conducted 3 times.

PID	Class I HLA	Epitope tested	Tetramer response
PT4	A*23:01, A*29:02, B*53:01, B*42:01, C*03:04, C*17:00	**HLA-B*42:01 TL9**	**1.20**
		HLA-B*42:01 TL10	0.10
		HLA-B*42:01 IM9	0.30
		HLA-A*23:01 RW8	0.00
		HLA-A*23:01 HW9	0.00
PT5	A*30:01, A*34:02, B*35:01, B*42:01, C*02:10, C*17:01	**HLA-B*42:01 TL9**	**2.12**
		HLA-B*42:01 TL10	0.00
		HLA-B*42:01 IM9	0.00
		HLA-B*35:01 DL9	0.05
PT6	A*43:01, A*74:01, B*57:01, B*81:01, C*04:01, C*07:01	**HLA-B*81:01 TL9**	**2.08**
		HLA-B*81:01 TL10	0.00
		HLA-B*81:01 YL9	0.01
		HLA*C*07:01 KY11	0.53
PT9	A*23:01, A*68:02, B*14:02, B*81:01, C*08:02, C*18:00	**HLA-B*81:01 TL9**	**3.30**
		HLA-B*81:01 TL10	0.10
		HLA-B*81:01 YL9	0.00
		HLA-A*68:02 EV10	0.00
		HLA-A*68:02 EA10	0.00
PT10	A*02:05, A*33:01, B*42:01, B*15:03, C*07:01, B*17:01	**HLA-B*42:01 TL9**	**1.48**
		HLA-B*42:01 TL10	0.00
		HLA-B*15:03 FY10	0.81
		HLA-C*07:01 KY11	0.32
PT13	A*30:01, A*32:01, B*42:01, B*58:02, C*06:02, B*17:01	**HLA-B*42:01 TL9**	**4.70**
		HLA-B*42:01 TL10	0.00
		HLA-B*58:02 LF11	0.42
		HLA-B*58:02 QL11	0.30
PT14	A*02:01, A*30:01, B*42:01, B*45:07, C*16:01, B*17:01	**HLA-B*42:01 TL9**	**0.90**
		HLA-A*02:01 SL9	0.00
		HLA-B*42:01 TL10	0.20
		HLA-A*02:01 SV10	0.00
PT15	A*01:01, A*74:01, B*35:01, B*81:01, C*04:01, B*18:01	**HLA-B*81:01 TL9**	**1.38**
		HLA-B*42:01 TL10	0.10
		HLA-B*35:01 DL9	0.76
PT18	A*30:01, A*68:02, B*14:02, B*42:01, C*08:02, B*17:01	**HLA-B*42:01 TL9**	**4.60**
		HLA-B*42:01 TL10	0.10
		HLA-A*68:02 EA10	0.00
		HLA-A*68:02 EV10	0.20
PT19	A*23:01, A*30:01, B*42:01, B*57:02, C*07:01, B*17:00	**HLA-B*42:01 TL9**	**2.92**
		HLA-B*42:01 TL10	0.20
		HLA-B*57:02 TW10	0.10
		HLA-A*23:01 RW8	0.90
		HLA-C*07:01 KY11	0.50

Appendix Table 3-1. Frequencies of HIV specific $CD8^+$ T cell tetramer responses tested. All values are displayed as percent tetramer positive $CD8^+$ T cells. Tetramer responses tested were based on published epitopes restricted by HLA alleles of the study participants and tetramer availability.

Forward

1st Round	Sequence
TRAV1-R1	CTGCACGTACCAGACATCTGGGTT
TRAV2,-R1	GGCTCAAAGCCTTCTCAGCAGG
TRAV3,-R1	GGATAACCTGGTTAAAGGCAGCTA
TRAV4,-R1	GGATACAAGACAAAAGTTACAAACGA
TRAV5,-R1	GCTGACGTATATTTTTTCAAATATGGA
TRAV6,-R1	GGAAGAGGCCCTGTTTTCTTGCT
TRAV7,-R1	GCTGGATATGAGAAGCAGAAAGGA
TRAV8,-R1	AGGACTCCAGCTTCTCCTGAAGTA
TRAV9,-R1	GTATGTCCAATATCCTGGAGAAGGT
TRAV10-R1	CAGTGAGAACACAAAGTCGAACGG
TRAV12.1,-R1	CCTAAGTTGCTGATGTCCGTATAC
TRAV12.2,-R1	GGGAAAAGCCCTGAGTTGATAATGT
TRAV12.3,-R1	GCTGATGTACACATACTCCAGTGG
TRAV13.1,-R1	CCCTTGGTATAAGCAAGAACTTGG
TRAV13.2,-R1	CCTCAATTCATTATAGACATTCGTTC
TRAV14,-R1	GCAAAATGCAACAGAAGGTCGCTA
TRAV16,-R1	TAGAGAGAGCATCAAAGGCTTCAC
TRAV17,-R1	CGTTCAAATGAAAGAGAGAAACACAG
TRAV18,-R1	CCTGAAAAGTTCAGAAAACCAGGAG
TRAV19,-R1	GGTCGGTATTCTTGGAACTTCCAG
TRAV20,-R1	GCTGGGGAAGAAAAGGAGAAAGAAA
TRAV21,-R1	GTCAGAGAGAGCAAACAAGTGGAA
TRAV22,-R1	GGACAAAACAGAATGGAAGATTAAGC
TRAV23,-R1	CCAGATGTGAGTGAAAAGAAAGAAG
TRAV24,-R1	GACTTTAAATGGGGATGAAAAGAAGA
TRAV25,-R1	GGAGAAGTGAAGAAGCAGAAAAGAC
TRAV26.1,-R1	CCAATGAAATGGCCTCTCTGATCA
TRAV26.2,-R1	GCAATGTGAACAACAGAATGGCCT
TRAV27,-R1	GGTGGAGAAGTGAAGAAGCTGAAG
TRAV29,-R1	GGATAAAAATGAAGATGGAAGATTCAC
TRAV30,-R1	CCTGATGATATTACTGAAGGGTGGA
TRAV34,-R1	GGTGGGGAAGAGAAAAGTCATGAA
TRAV35,-R1	GGTGAATTGACCTCAAATGGAAGAC
TRAV36,-R1	GCTAACTTCAAGTGGAATTGAAAAGA
TRAV38,-R1	GAAGCTTATAAGCAACAGAATGCAAC
TRAV39,-R1	GGAGCAGTGAAGCAGGAGGGAC
TRAV40,-R1	GAGAGACAATGGAAAACAGCAAAAAC
TRAV41,-R1	GCTGAGCTCAGGGAAGAAGAAGC

TRBV2,-R1	CTGAAATATTCGATGATCAATTCTCAG
TRBV3-1,-R1	TCATTATAAATGAAACAGTTCCAAATCG
TRBV4,-R1	AGTGTGCCAAGTCGCTTCTCAC
TRBV5-4,8,-R1	CAGAGGAAACTYCCCTCCTAGATT
TRBVS-1,-R1	GAGACACAGAGAAACAAAGGAAACTTC
TRBV6-1,-R1	GGTACCACTGACAAAGGAGAAGTCC
TRBV6-2,3,-R1	GAGGGTACAACTGCCAAAGGAGAGGT
TRBV6-4,-R1	GGCAAAGGAGAAGTCCCTGATGGTT
TRBV6-5,6,-R1	AAGGAGAAGTCCCSAATGGCTACAA
TRBV6-8,-R1	CTGACAAAGAAGTCCCCAATGGCTAC
TRBV6-9,-R1	CACTGACAAAGGAGAAGTCCCCGAT
TRBV7-2,-R1	AGACAAATCAGGGCTGCCCAGTGA
TRBV7-3,-R1	GACTCAGGGCTGCCCAACGAT
TRBV7-8,-R1	CCAGAATGAAGCTCAACTAGACAA
TRBV7-4,6,-R1	GGTTCTCTGCAGAGAGGCCTGAG
TRBV7-7,-R1	GGCTGCCCAGTGATCGGTTCTC
TRBV7-9,-R1	GACTTACTTCCAGAATGAAGCTCAACT
TRBV9,-R1	GAGCAAAAGGAAACATTCTTGAACGATT
TRBV10-1,3-R1	GGCTRATCCATTACTCATATGGTGTT
TRBV10-2,-R1	GATAAAGGAGAAGTCCCCGATGGCT
TRBV11,-R1	GATTCACAGTTGCCTAAGGATCGAT
TRBV12-3,4,-R1	GATTCAGGGATGCCCGAGGATCG
TRBV12-5,-R1	GATTCGGGGATGCCGAAGGATCG
TRBV13'-R1	GCAGAGCGATAAAGGAAGCATCCCT
TRBV14,-R1	TCCGGTATGCCCAACAATCGATTCT
TRBV15,-R1	GATTTTAACAATGAAGCAGACACCCCT
TRBV16,-R1	GATGAAACAGGTATGCCCAAGGAAAG
TRBV18,-R1	TATCATAGATGAGTCAGGAATGCCAAAG
TRBV19,-R1	GACTTTCAGAAAGGAGATATAGCTGAA
TRBV20-1,-R1	CAAGGCCACATACGAGCAAGGCGTC
TRBV24-1,-R1	CAAAGATATAAACAAAGGAGAGATCTCT
TRBV25-1,-R1	AGAGAAGGGAGATCTTTCCTCTGAGT
TRBV27-1,-R1	GACTGATAAGGGAGATGTTCCTGAAG
TRBV28,-R1	GGCTGATCTATTTCTCATATGATGTTAA
TRBV29,-R1	GCCACATATGAGAGTGGATTTGTCATT
TRBV30,-R1	GGTGCCCCAGAATCTCTCAGCCT

Reverse

1st Round	Sequence
TRAC,-R1	CGGTGAATAGGCAGACAGACTTGT
TRBC,-R1	ACCAGTGTGGCCTTTTGGGTGTG

Appendix Table 3-2. 1st round RT-PCR conducted with cocktail of forward and reverse primers. Primers have ability to encompass both TCR alpha and beta sequences. The concentration of each forward primer in the PCR reaction was 0.06 μM and the concentration of each reverse primer was 0.3 μM.

Forward

1st Round	Sequence
TRAV1,R2_TAG	CCAGGGTTTTCCCAGTCACGACAGGTCGTTTTTCTTCATTCCTTAGTC
TRAV2,R2_TAG	CCAGGGTTTTCCCAGTCACGACACGATACAACATGACCTATGAACGG
TRAV3.1,R2_TAG	CCAGGGTTTTCCCAGTCACGACCTTTGAAGCTGAATTTAACAAGAGCC
TRAV4.1,R2_TAG	CCAGGGTTTTCCCAGTCACGACCTCCCTGTTTATCCCTGCCGAC
TRAV5.1,R2_TAG	CCAGGGTTTTCCCAGTCACGACAAACAAGACCAAAGACTCACTGTTC
TRAV6,R2_TAG	CCAGGGTTTTCCCAGTCACGACAAGACTGAAGGTCACCTTTGATACC
TRAV7,R2_TAG	CCAGGGTTTTCCCAGTCACGACACTAAATGCTACATTACTGAAGAATGG
TRAV8,R2_TAG	CCAGGGTTTTCCCAGTCACGACGCATCAACGGTTTTGAGGCTGAATTTAA
TRAV9,R2_TAG	CCAGGGTTTTCCCAGTCACGACGAAACCACTTCTTTCCACTTGGAGAA
TRAV10,R2_TAG	CCAGGGTTTTCCCAGTCACGACTACAGCAACTCTGGATGCAGACAC
TRAV12,R2_TAG	CCAGGGTTTTCCCAGTCACGACGAAGATGGAAGGTTTACAGCACA
TRAV13.1,R2_TAG	CCAGGGTTTTCCCAGTCACGACGACATTCGTTCAAATGTGGGCGAA
TRAV13.2,R2_TAG	CCAGGGTTTTCCCAGTCACGACGGCAAGGCCAAAGAGTCACCGT
TRAV14,R2_TAG	CCAGGGTTTTCCCAGTCACGACTCCAGAAGGCAAGAAAATCCGCCA
TRAV16,R2_TAG	CCAGGGTTTTCCCAGTCACGACGCTGACCTTAACAAAGGCGAGACA
TRAV17,R2_TAG	CCAGGGTTTTCCCAGTCACGACTTAAGAGTCACGCTTGACACTTCCA
TRAV18,R2_TAG	CCAGGGTTTTCCCAGTCACGACGCAGAGGTTTTCAGGCCAGTCCT
TRAV19,R2_TAG	CCAGGGTTTTCCCAGTCACGACTCCACCAGTTCCTTCAACTTCACC
TRAV20,R2_TAG	CCAGGGTTTTCCCAGTCACGACGCCACATTAACAAAGAAGGAAAGCT
TRAV21,R2_TAG	CCAGGGTTTTCCCAGTCACGACGCCTCGCTGGATAAATCATCAGGA
TRAV22,R2_TAG	CCAGGGTTTTCCCAGTCACGACACGACTGTCGCTACGGAACGCTA
TRAV23,R2_TAG	CCAGGGTTTTCCCAGTCACGACCACAATCTCCTTCAATAAAAGTGCCA
TRAV24,R2_TAG	CCAGGGTTTTCCCAGTCACGACACGAATAAGTGCCACTCTTAATACCA
TRAV25,R2_TAG	CCAGGGTTTTCCCAGTCACGACGTTTGGAGAAGCAAAAAAGAACAGCT
TRAV26.1,R2_TAG	CCAGGGTTTTCCCAGTCACGACCAGAAGACAGAAAGTCCAGCACCT
TRAV26.2,R2_TAG	CCAGGGTTTTCCCAGTCACGACATCGCTGAAGACAGAAAGTCCAGT
TRAV27,R2_TAG	CCAGGGTTTTCCCAGTCACGACACTAACCTTTCAGTTTGGTGATGCAA
TRAV29,R2_TAG	CCAGGGTTTTCCCAGTCACGACCTTAAACAAAAGTGCCAAGCACCTC
TRAV30,R2_TAG	CCAGGGTTTTCCCAGTCACGACAATATCTGCTTCATTTAATGAAAAAAAGC
TRAV34,R2_TAG	CCAGGGTTTTCCCAGTCACGACCCAAGTTGGATGAGAAAAAGCAGCA
TRAV35,R2_TAG	CCAGGGTTTTCCCAGTCACGACCTCAGTTTGGTATAACCAGAAAGGA
TRAV36,R2_TAG	CCAGGGTTTTCCCAGTCACGACGGAAGACTAAGTAGCATATTAGATAAG
TRAV38,R2_TAG	CCAGGGTTTTCCCAGTCACGACCTGTGAACTTCCAGAAAGCAGCCA
TRAV39,R2_TAG	CCAGGGTTTTCCCAGTCACGACCCTCACTTGATACCAAAGCCCGT
TRAV40,R2_TAG	CCAGGGTTTTCCCAGTCACGACAGGCGGAAATATTAAAGACAAAAACTC
TRAV41,R2_TAG	CCAGGGTTTTCCCAGTCACGACGATTAATTGCCACAATAAACATACAGG
TRBV2,R2_TAG	CCAGGGTTTTCCCAGTCACGACGCCTGATGGATCAAATTTCACTCTG
TRBV3-1,R2_TAG	CCAGGGTTTTCCCAGTCACGACTCTCACCTAAATCTCCAGACAAAGCT
TRBV4,R2_TAG	CCAGGGTTTTCCCAGTCACGACCCTGAATGCCCCAACAGCTCTC
TRBV5-4,8,R2_TAG	CCAGGGTTTTCCCAGTCACGACCTCTGAGCTGAATGTGAACGCCT
TRBV5-1,R2_TAG	CCAGGGTTTTCCCAGTCACGACCGATTCTCAGGGCGCCAGTTCTCT
TRBV6-1,R2_TAG	CCAGGGTTTTCCCAGTCACGACTGGCTACAATGTCTCCAGATTAAACAA
TRBV6-2,3,R2_TAG	CCAGGGTTTTCCCAGTCACGACCCCTGATGGCTACAATGTCTCCAGA
TRBV6-4,R2_TAG	CCAGGGTTTTCCCAGTCACGACGTGTCTCCAGAGCAAACACAGATGATT
TRBV6-5,6,R2_TAG	CCAGGGTTTTCCCAGTCACGACGTCTCCAGATCAACCACAGAGGAT
TRBV6-8,R2_TAG	CCAGGGTTTTCCCAGTCACGACGTCTCTAGATTAAACACAGAGGATTTC
TRBV6-9,R2_TAG	CCAGGGTTTTCCCAGTCACGACGGCTACAATGTATCCAGATCAAACA
TRBV7-2,R2_TAG	CCAGGGTTTTCCCAGTCACGACTCGCTTCTCTGCAGAGAGGACTGG
TRBV7-3,R2_TAG	CCAGGGTTTTCCCAGTCACGACCGGTTCTTTGCAGTCAGGCCTGA
TRBV7-8,R2_TAG	CCAGGGTTTTCCCAGTCACGACCCAGTGATCGCTTCTTTGCAGAAA
TRBV7-4,6,R2_TAG	CCAGGGTTTTCCCAGTCACGACTCTCCACTCTGAMGATCCAGCGCA
TRBV7-7,R2_TAG	CCAGGGTTTTCCCAGTCACGACGCAGAGAGGCCTGAGGGATCCAT
TRBV7-9,R2_TAG	CCAGGGTTTTCCCAGTCACGACCTGCAGAGAGGCCTAAGGGATCT
TRBV9,R2_TAG	CCAGGGTTTTCCCAGTCACGACCTCCGCACAACAGTTCCCTGACTT
TRBV10-1,3,R2_TAG	CCAGGGTTTTCCCAGTCACGACCAGATGGCTAYAGTGTCTCTAGATCAAA
TRBV10-2,R2_TAG	CCAGGGTTTTCCCAGTCACGACGTTGTCTCCAGATCCAAGACAGAGAA
TRBV11,R2_TAG	CCAGGGTTTTCCCAGTCACGACGCAGAGAGGCTCAAAGGAGTAGACT
TRBV12-3,4,R2_TAG	CCAGGGTTTTCCCAGTCACGACGCTAAGATGCCTAATGCATCATTCTC
TRBV12-5,R2_TAG	CCAGGGTTTTCCCAGTCACGACCTCAGCAGAGATGCCTGATGCAACT
TRBV13,R2_TAG	CCAGGGTTTTCCCAGTCACGACTCTCAGCTCAACAGTTCAGTGACTA
TRBV14,R2_TAG	CCAGGGTTTTCCCAGTCACGACGCTGAAAGGACTGGAGGGACGTAT
TRBV15,R2_TAG	CCAGGGTTTTCCCAGTCACGACGATAACTTCCAATCCAGGAGGCCG
TRBV16,R2_TAG	CCAGGGTTTTCCCAGTCACGACGCTAAGTGCCTCCCAAATTCACCC
TRBV18,R2_TAG	CCAGGGTTTTCCCAGTCACGACGGAACGATTTTCTGCTGAATTTCCCA
TRBV19,R2_TAG	CCAGGGTTTTCCCAGTCACGACGGTACAGCGTCTCTCGGGAGAAGA
TRBV20-1,R2_TAG	CCAGGGTTTTCCCAGTCACGACGGACAAGTTTCTCATCAACCATGCAA
TRBV24-1,R2_TAG	CCAGGGTTTTCCCAGTCACGACTGGATACAGTGTCTCTCGACAGGC
TRBV25-1,R2_TAG	CCAGGGTTTTCCCAGTCACGACCAACAGTCTCCAGAATAAGGACGGA
TRBV27-1,R2_TAG	CCAGGGTTTTCCCAGTCACGACTACAAAGTCTCTCGAAAAGAGAAGAGGA
TRBV28,R2_TAG	CCAGGGTTTTCCCAGTCACGACGGGGTACAGTGTCTCTAGAGAGA
TRBV29,R2_TAG	CCAGGGTTTTCCCAGTCACGACGTTTCCCATCAGCCGCCCAAACCTA
TRBV30,R2_TAG	CCAGGGTTTTCCCAGTCACGACCAGACCCCAGGACCGGCAGTTCAT

Reverse

2nd Round	Sequence
TRAC,R2_TAG	AAGCAGTGGTATCAACGCAGAGTCAGACAGACTTGTCACTGGATTTAG
TRBC,R2_TAG	AAGCAGTGGTATCAACGCAGAGTCTTTTGGGTGTGGGAGATCTCTG

3rd Round Alpha reaction	Sequence
TCR_UNI_F	CCAGGGTTTTCCCAGTCACGAC
TRAC,-R2	CAGACAGACTTGTCACTGGATTTAG

3rd Round Alpha reaction	Sequence
TCR_UNI_F	CCAGGGTTTTCCCAGTCACGAC
TRBC,-R2	CTTTTGGGTGTGGGAGATCTCTG

Appendix Table 3-3. 2nd round PCR was conducted on 1 µL of RT-PCR product with cocktail of forward and reverse primers. Primers have ability to encompass both TCR alpha and beta sequences. The concentration of each forward primer in the second round PCR reaction was 0.06uM and the concentration of each reverse primer was 0.3uM. The second round PCR was diluted and 1uL was transferred into a 3rd round PCR, which was either TCR alpha or beta specific. With the respective 3rd round forward and reverse primers at a final concentration of 0.2 µM.

Appendix Figure 4-1. TL9 Variant screen heat maps for all B*42 and B*81 TCR

TRAV1R2	**TCGTCGGCAGCGTCAGATGTGTATAAGAGACAGAGGTCGTTTTTCTTCATTCCTTAGTC**
TRAV2R2	**TCGTCGGCAGCGTCAGATGTGTATAAGAGACAGACGATACAACATGACCTATGAACGG**
TRAV3.1R2	**TCGTCGGCAGCGTCAGATGTGTATAAGAGACAGCTTTGAAGCTGAATTTAACAAGAGCC**
TRAV4.1R2	**TCGTCGGCAGCGTCAGATGTGTATAAGAGACAGCTCCCTGTTTATCCCTGCCGAC**
TRAV5.1R2	**TCGTCGGCAGCGTCAGATGTGTATAAGAGACAGAAACAAGACCAAAGACTCACTGTTC**
TRAV6R2	**TCGTCGGCAGCGTCAGATGTGTATAAGAGACAGAAGACTGAAGGTCACCTTTGATACC**
TRAV7R2	**TCGTCGGCAGCGTCAGATGTGTATAAGAGACAGACTAAATGCTACATTACTGAAGAATGG**
TRAV8R2	**TCGTCGGCAGCGTCAGATGTGTATAAGAGACAGGCATCAACGGTTTTGAGGCTGAATTTAA**
TRAV9R2	**TCGTCGGCAGCGTCAGATGTGTATAAGAGACAGGAAACCACTTCTTTCCACTTGGAGAA**
TRAV10R2	**TCGTCGGCAGCGTCAGATGTGTATAAGAGACAGTACAGCAACTCTGGATGCAGACAC**
TRAV12R2	**TCGTCGGCAGCGTCAGATGTGTATAAGAGACAGGAAGATGGAAGGTTTACAGCACA**
TRAV13.1R2	**TCGTCGGCAGCGTCAGATGTGTATAAGAGACAGGACATTCGTTCAAATGTGGGCGAA**
TRAV13.2R2	**TCGTCGGCAGCGTCAGATGTGTATAAGAGACAGGGCAAGGCCAAAGAGTCACCGT**
TRAV14R2	**TCGTCGGCAGCGTCAGATGTGTATAAGAGACAGTCCAGAAGGCAAGAAAATCCGCCA**
TRAV16R2	**TCGTCGGCAGCGTCAGATGTGTATAAGAGACAGGCTGACCTTAACAAAGGCGAGACA**
TRAV17R2	**TCGTCGGCAGCGTCAGATGTGTATAAGAGACAGTTAAGAGTCACGCTTGACACTTCCA**
TRAV18R2	**TCGTCGGCAGCGTCAGATGTGTATAAGAGACAGGCAGAGGTTTTCAGGCCAGTCCT**
TRAV19R2	**TCGTCGGCAGCGTCAGATGTGTATAAGAGACAGTCCACCAGTTCCTTCAACTTCACC**
TRAV20R2	**TCGTCGGCAGCGTCAGATGTGTATAAGAGACAGGCCACATTAACAAAGAAGGAAAGCT**
TRAV21R2	**TCGTCGGCAGCGTCAGATGTGTATAAGAGACAGGCCTCGCTGGATAAATCATCAGGA**
TRAV22R2	**TCGTCGGCAGCGTCAGATGTGTATAAGAGACAGACGACTGTCGCTACGGAACGCTA**
TRAV23R2	**TCGTCGGCAGCGTCAGATGTGTATAAGAGACAGCACAATCTCCTTCAATAAAAGTGCCA**
TRAV24R2	**TCGTCGGCAGCGTCAGATGTGTATAAGAGACAGACGAATAAGTGCCACTCTTAATACCA**
TRAV25R2	**TCGTCGGCAGCGTCAGATGTGTATAAGAGACAGGTTTGGAGAAGCAAAAAAGAACAGCT**
TRAV26.1R2	**TCGTCGGCAGCGTCAGATGTGTATAAGAGACAGCAGAAGACAGAAAGTCCAGCACCT**
TRAV26.2R2	**TCGTCGGCAGCGTCAGATGTGTATAAGAGACAGATCGCTGAAGACAGAAAGTCCAGT**
TRAV27R2	**TCGTCGGCAGCGTCAGATGTGTATAAGAGACAGACTAACCTTTCAGTTTGGTGATGCAA**
TRAV29R2	**TCGTCGGCAGCGTCAGATGTGTATAAGAGACAGCTTAAACAAAAGTGCCAAGCACCTC**

TRAV30R2	**TCGTCGGCAGCGTCAGATGTGTATAAGAGACAGAATATCTGCTTCATTTAATGAAAAAAAGC**
TRAV34R2	**TCGTCGGCAGCGTCAGATGTGTATAAGAGACAGCCAAGTTGGATGAGAAAAAGCAGCA**
TRAV35R2	**TCGTCGGCAGCGTCAGATGTGTATAAGAGACAGCTCAGTTTGGTATAACCAGAAAGGA**
TRAV36R2	**TCGTCGGCAGCGTCAGATGTGTATAAGAGACAGGGAAGACTAAGTAGCATATTAGATAAG**
TRAV38R2	**TCGTCGGCAGCGTCAGATGTGTATAAGAGACAGCTGTGAACTTCCAGAAAGCAGCCA**
TRAV39R2	**TCGTCGGCAGCGTCAGATGTGTATAAGAGACAGCCTCACTTGATACCAAAGCCCGT**
TRAV40R2	**TCGTCGGCAGCGTCAGATGTGTATAAGAGACAGAGGCGGAAATATTAAAGACAAAAACTC**
TRAV41R2	**TCGTCGGCAGCGTCAGATGTGTATAAGAGACAGGATTAATTGCCACAATAAACATACAGG**
TRBV2R2	**TCGTCGGCAGCGTCAGATGTGTATAAGAGACAGGCCTGATGGATCAAATTTCACTCTG**
TRBV3.1R2	**TCGTCGGCAGCGTCAGATGTGTATAAGAGACAGTCTCACCTAAATCTCCAGACAAAGCT**
TRBV4R2	**TCGTCGGCAGCGTCAGATGTGTATAAGAGACAGCCTGAATGCCCCAACAGCTCTC**
TRBV5.4.8R2	**TCGTCGGCAGCGTCAGATGTGTATAAGAGACAGCTCTGAGCTGAATGTGAACGCCT**
TRBV5.1R2	**TCGTCGGCAGCGTCAGATGTGTATAAGAGACAGCGATTCTCAGGGCGCCAGTTCTCT**
TRBV6.1R2	**TCGTCGGCAGCGTCAGATGTGTATAAGAGACAGTGGCTACAATGTCTCCAGATTAAACAA**
TRBV6.2.3R2	**TCGTCGGCAGCGTCAGATGTGTATAAGAGACAGCCCTGATGGCTACAATGTCTCCAGA**
TRBV6.4R2	**TCGTCGGCAGCGTCAGATGTGTATAAGAGACAGGTGTCTCCAGAGCAAACACAGATGATT**
TRBV6.5.6R2	**TCGTCGGCAGCGTCAGATGTGTATAAGAGACAGGTCTCCAGATCAACCACAGAGGAT**
TRBV6.8R2	**TCGTCGGCAGCGTCAGATGTGTATAAGAGACAGGTCTCTAGATTAAACACAGAGGATTTC**
TRBV6.9R2	**TCGTCGGCAGCGTCAGATGTGTATAAGAGACAGGGCTACAATGTATCCAGATCAAACA**
TRBV7.2R2	**TCGTCGGCAGCGTCAGATGTGTATAAGAGACAGTCGCTTCTCTGCAGAGAGGACTGG**
TRBV7.3R2	**TCGTCGGCAGCGTCAGATGTGTATAAGAGACAGCGGTTCTTTGCAGTCAGGCCTGA**
TRBV7.8R2	**TCGTCGGCAGCGTCAGATGTGTATAAGAGACAGCCAGTGATCGCTTCTTTGCAGAAA**
TRBV7.4.6R2	**TCGTCGGCAGCGTCAGATGTGTATAAGAGACAGTCTCCACTCTGAMGATCCAGCGCA**
TRBV7.7R2	**TCGTCGGCAGCGTCAGATGTGTATAAGAGACAGGCAGAGAGGCCTGAGGGATCCAT**
TRBV7.9R2	**TCGTCGGCAGCGTCAGATGTGTATAAGAGACAGCTGCAGAGAGGCCTAAGGGATCT**
TRBV9R2	**TCGTCGGCAGCGTCAGATGTGTATAAGAGACAGCTCCGCACAACAGTTCCCTGACTT**
TRBV10.1.3R2	**TCGTCGGCAGCGTCAGATGTGTATAAGAGACAGCAGATGGCTAYAGTGTCTCTAGATCAAA**
TRBV10.2R2	**TCGTCGGCAGCGTCAGATGTGTATAAGAGACAGGTTGTCTCCAGATCCAAGACAGAGAA**

TRBV11R2	**TCGTCGGCAGCGTCAGATGTGTATAAGAGACAGGCAGAGAGGCTCAAAGGAGTAGACT**
TRBV12.3.4R2	**TCGTCGGCAGCGTCAGATGTGTATAAGAGACAGGCTAAGATGCCTAATGCATCATTCTC**
TRBV12.5.R2	**TCGTCGGCAGCGTCAGATGTGTATAAGAGACAGCTCAGCAGAGATGCCTGATGCAACT**
TRBV13R2	**TCGTCGGCAGCGTCAGATGTGTATAAGAGACAGTCTCAGCTCAACAGTTCAGTGACTA**
TRBV14R2	**TCGTCGGCAGCGTCAGATGTGTATAAGAGACAGGCTGAAAGGACTGGAGGGACGTAT**
TRBV15R2	**TCGTCGGCAGCGTCAGATGTGTATAAGAGACAGGATAACTTCCAATCCAGGAGGCCG**
TRBV16R2	**TCGTCGGCAGCGTCAGATGTGTATAAGAGACAGGCTAAGTGCCTCCCAAATTCACCC**
TRBV18R2	**TCGTCGGCAGCGTCAGATGTGTATAAGAGACAGGGAACGATTTTCTGCTGAATTTCCCA**
TRBV19R2	**TCGTCGGCAGCGTCAGATGTGTATAAGAGACAGGGTACAGCGTCTCTCGGGAGAAGA**
TRBV20.1R2	**TCGTCGGCAGCGTCAGATGTGTATAAGAGACAGGGACAAGTTTCTCATCAACCATGCAA**
TRBV24.1R2	**TCGTCGGCAGCGTCAGATGTGTATAAGAGACAGTGGATACAGTGTCTCTCGACAGGC**
TRBV25.1R2	**TCGTCGGCAGCGTCAGATGTGTATAAGAGACAGCAACAGTCTCCAGAATAAGGACGGA**
TRBV27.1R2	**TCGTCGGCAGCGTCAGATGTGTATAAGAGACAGTACAAAGTCTCTCGAAAAGAGAAGAGGA**
TRBV28R2	**TCGTCGGCAGCGTCAGATGTGTATAAGAGACAGGGGGTACAGTGTCTCTAGAGAGA**
TRBV29R2	**TCGTCGGCAGCGTCAGATGTGTATAAGAGACAGGTTTCCCATCAGCCGCCCAAACCTA**
TRBV30R2	**TCGTCGGCAGCGTCAGATGTGTATAAGAGACAGCAGACCCCAGGACCGGCAGTTCAT**
TRACR2	**GTCTCGTGGGCTCGGAGATGTGTATAAGAGACAGTCAGACAGACTTGTCACTGGATTTAG**
TRBCR2	**GTCTCGTGGGCTCGGAGATGTGTATAAGAGACAGTCTTTTGGGTGTGGGAGATCTCTG**

Appendix table 4-1. 2nd round primers for TCR MiSeq.

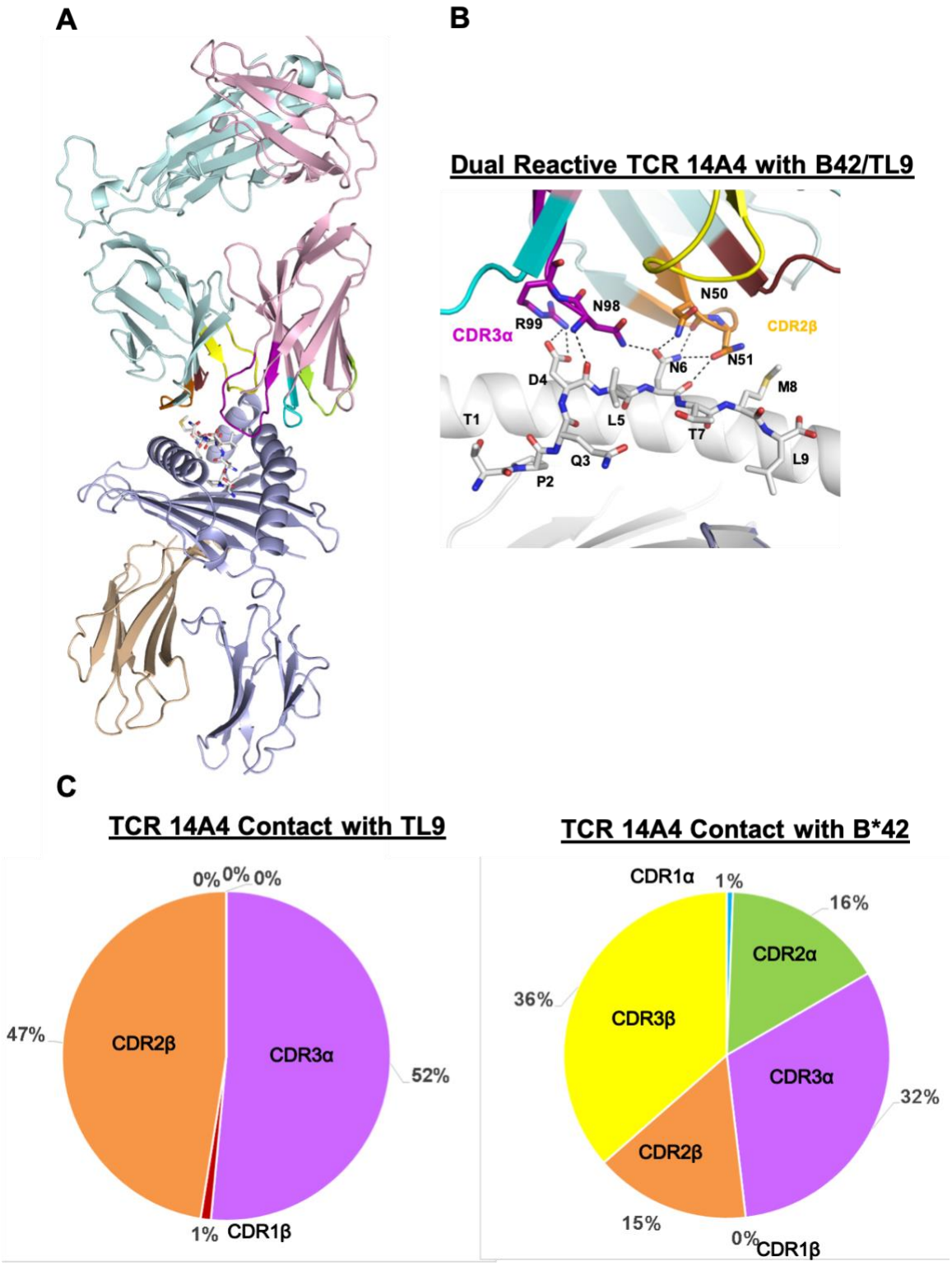

Appendix Figure 4-2. TCR 14A4 interaction with HLA-B*42 and HLA-B*81

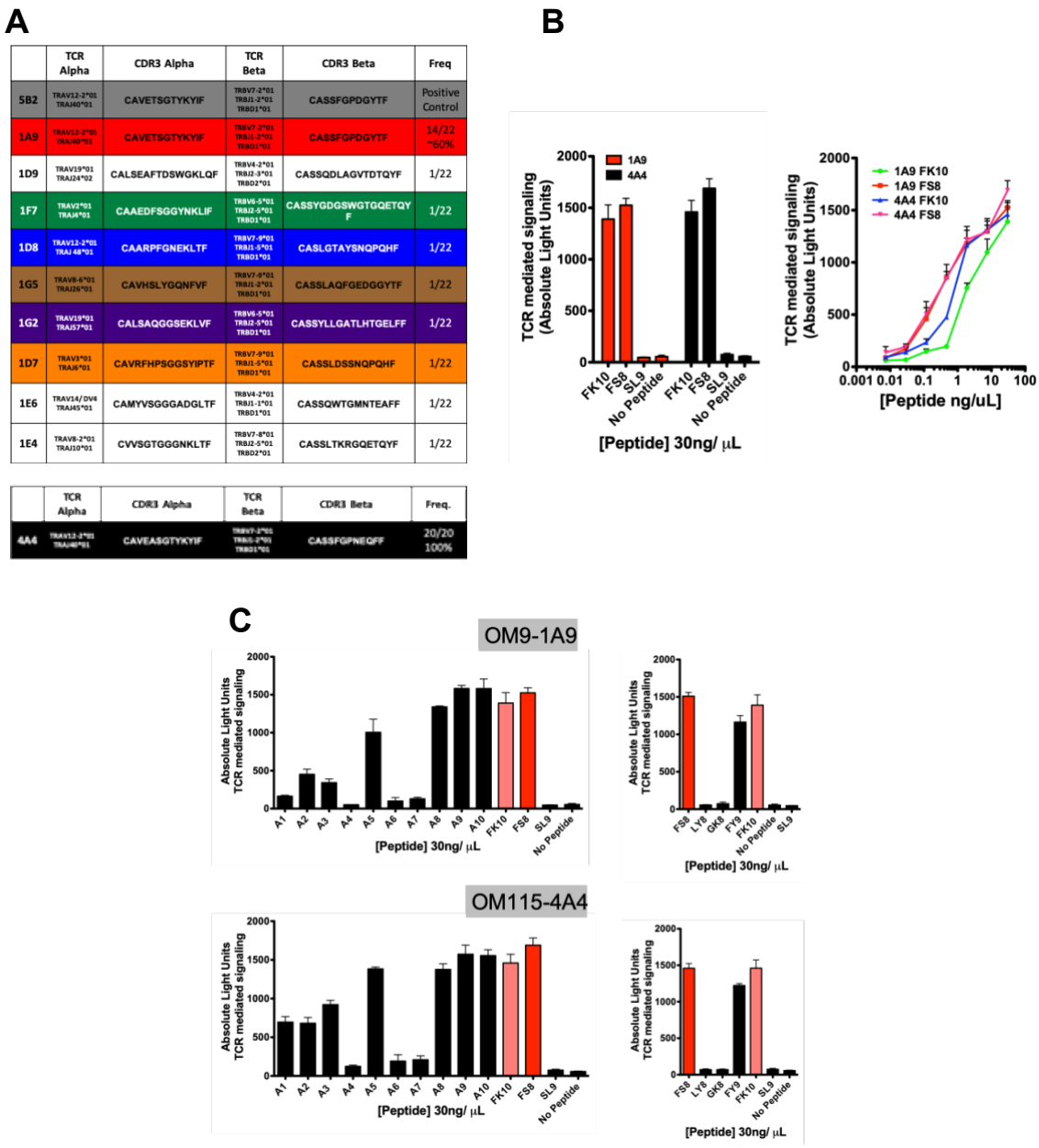

Appendix Figure 5-1. Characterization of TCR towards HLA-A*02 FK10

The TCR Gag FK10 (FLGKIWPS) specific TCR repertoire was single cell sequenced in 2 HLA-A*02+ HIV infected individuals **(A)** that showed the most dominant TCR to be public across the 2 individuals. The TCR are functional in the NFAT reporter assay and display dose dependant signalling in response to peptide **(B)**. The known FK10 (FLGKIWPSYK) epitope is a 10-mer, but through mutational studies we determined that FS8 (FLGKIWPS) is the minimal epitope and through alanine scanning, mutations at position 4, 6 and 7 disrupt signaling.

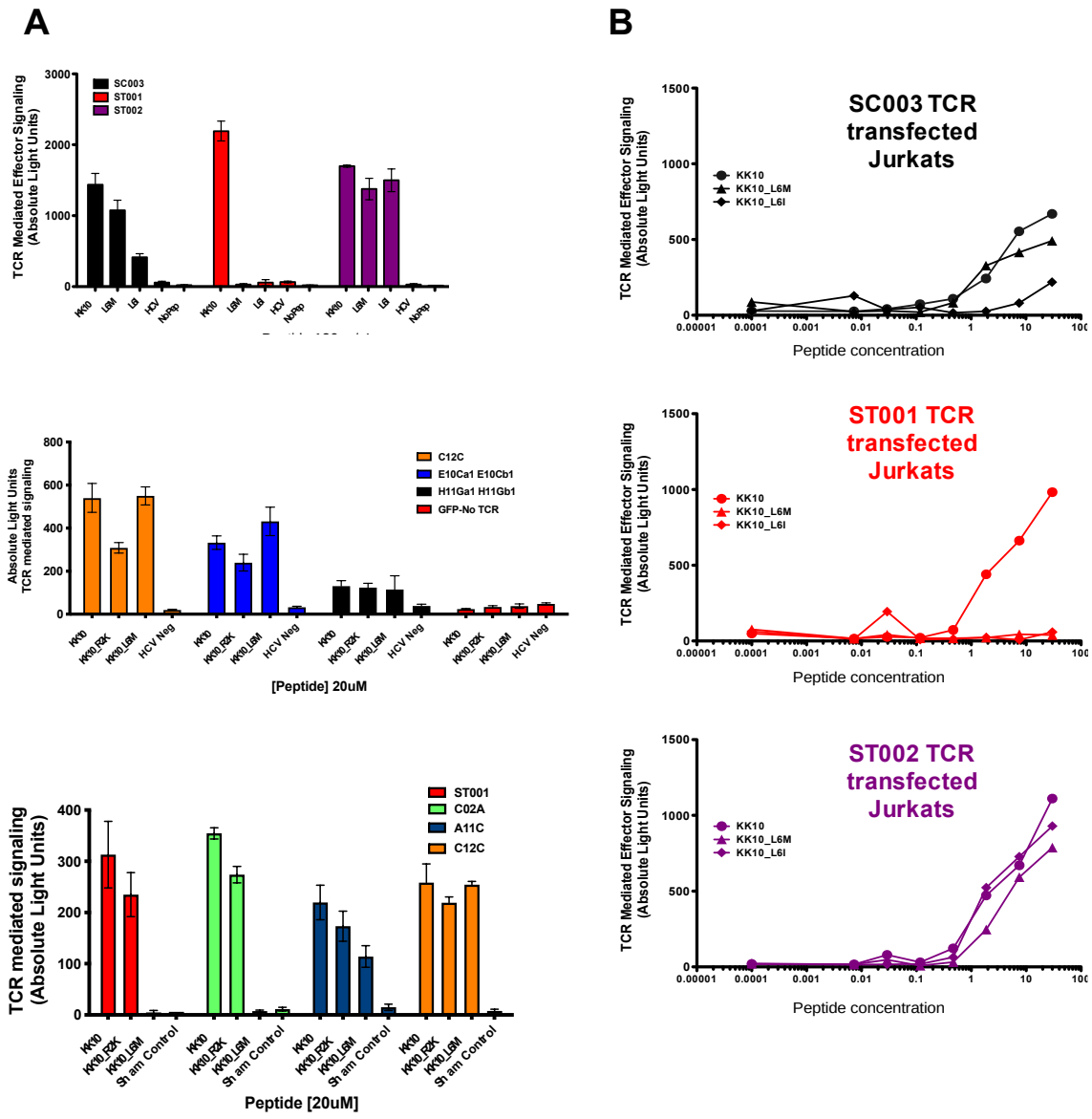

Appendix Figure 5-2. Panel of HLA-B*27 KK10 restricted TCR studied in reporter assay.

The NFAT reporter assay is can be used to study HLA-B*27 KK10 (KRWIILGLNK) specific TCR. We have a total of 8 TCR against KK10 (A). Their reactivity has been tested against wildtype KK10, R264K and L268M.

A

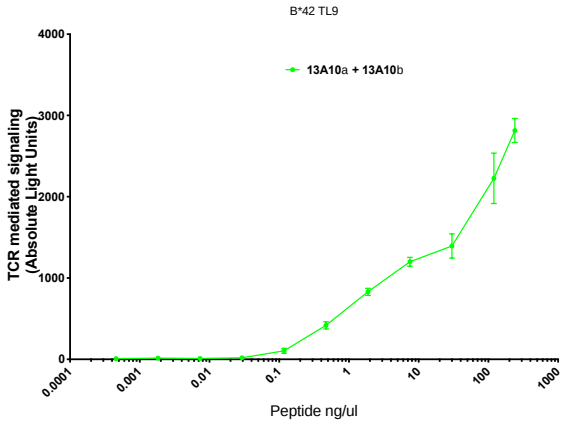

B

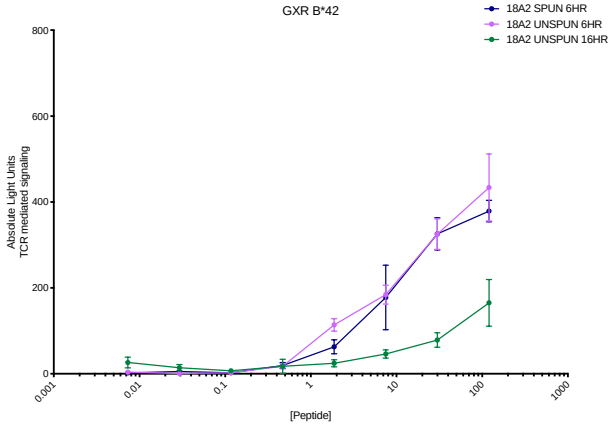

Appendix Figure 5-3. Higher peptide dose and peptide wash in TCR reporter assay. Increasing the peptide dose 4x higher than previous experiments did not cause the TCR signaling to plateau, nor did washing the peptide off after peptide pulse, prior to target cell co-culture with TCR expressing Jurkat cells.